In compliance with the
Canadian Privacy Legislation
some supporting forms
may have been removed from
this dissertation.

While these forms may be included
in the document page count,
their removal does not represent
any loss of content from the dissertation.

University of Alberta

Pharmacokinetic and Biochemical Evaluations of Novel Synthetic Pyrimidine Nucleoside Analogues

by

Panteha Khalili ©

A thesis submitted to the Faculty of Graduate Studies and Research in partial fulfillment of the requirements for the degree of Doctor of Philosophy

in

Pharmaceutical Sciences

Faculty of Pharmacy and Pharmaceutical Sciences

Edmonton, Alberta

Fall 2003

National Library
of Canada

Acquisitions and
Bibliographic Services

395 Wellington Street
Ottawa ON K1A 0N4
Canada

Bibliothèque nationale
du Canada

Acquisisitons et
services bibliographiques

395, rue Wellington
Ottawa ON K1A 0N4
Canada

Your file Votre référence
ISBN: 0-612-88004-4
Our file Notre référence
ISBN: 0-612-88004-4

The author has granted a non-exclusive licence allowing the National Library of Canada to reproduce, loan, distribute or sell copies of this thesis in microform, paper or electronic formats.

The author retains ownership of the copyright in this thesis. Neither the thesis nor substantial extracts from it may be printed or otherwise reproduced without the author's permission.

L'auteur a accordé une licence non exclusive permettant à la Bibliothèque nationale du Canada de reproduire, prêter, distribuer ou vendre des copies de cette thèse sous la forme de microfiche/film, de reproduction sur papier ou sur format électronique.

L'auteur conserve la propriété du droit d'auteur qui protège cette thèse. Ni la thèse ni des extraits substantiels de celle-ci ne doivent être imprimés ou aturement reproduits sans son autorisation.

Canadä

University of Alberta

Library Release Form

Name of Author: Panteha Khalili

Title of Thesis: Pharmacokinetic and Biochemical Evaluations of Novel Synthetic Pyrimidine Nucleoside Analogues

Degree: **Doctor of Philosophy**

Year this Degree Granted: 2003

Permission is hereby granted to The University of Alberta Library to reproduce single copies of this thesis and to lend or sell such copies for private, scholarly or scientific research purposes only.

The author reserves other publication rights and other rights in association with the copyright in the thesis, and except as hereinbefore provided, neither the thesis nor any substantial portion thereof may be printed or otherwise reproduced in any material form whatever without the author's prior written permission.

July 07, 2003

University of Alberta

Faculty of Graduate Studies and Research

The undersigned certify that they have read, and recommend to the Faculty of Graduate Studies and Research for acceptance, a thesis entitled **Pharmacokinetic and Biochemical Evaluations of Novel Synthetic Pyrimidine Nucleoside Analogues** submitted by Panteha Khalili in partial fulfillment of the requirements for the degree of Doctor of Philosophy in Pharmaceutical Sciences.

Date: July 07, 2003

Dedication

This thesis is dedicated to:

my parents, ***Maharam*** and ***Mohsen***, and my brother ***Reza***,

for their enormous support and kindness throughout my life,

my husband ***Siamak***, for his patience, encouragement and help.

Abstract

The purpose of this project was to investigate the pharmacokinetics and biochemical properties of 1-(2-deoxy-β-D-ribofuranosyl)-2,4-difluoro-5-iodobenzene (5-IDFPdR) and 1-(2,3-dideoxy-3-nitrooxy-β-D-ribofuranosyl)uracil (INUdR) as representative members of two novel classes of pyrimidine nucleoside analogues with potential anticancer/antiviral activity.

The physiochemical evaluation of 5-IDFPdR showed high lipophilicity (log $P = 2.8$), 69 to 75% binding to bovine serum albumin, and stability towards phosphorolysis since there was no evidence of metabolic deglycosylation by thymidine phosphorylase. 5-IDFPdR exhibited negligible cytotoxicity ($IC_{50} = 10^{-4}$ M range) against various murine and human cancer cell lines. The pharmacokinetics of 5-IDFPdR was studied in male Sprague-Dawley rats following intravenous bolus (iv) and oral administration (po) of 5-IDFPdR at different doses. The total body clearance (Cl_T) of 5-IDFPdR was decreased with increasing oral doses, as well as, at highest iv dose. Since renal clearance appears to play a minor role in elimination of 5-IDFPdR, the dose-dependent pharmacokinetics of 5-IDFPdR could be partially due to saturable hepatic and/or non-renal metabolism. Both glucuronide and sulfate conjugates of 5-IDFPdR were present in urine and bile.

The physiochemical evaluation of INUdR showed high lipophilicity (log $P = 1.12$), good chemical stability (except in serum or plasma), and also stability towards phosphorolysis by thymidine phosphorylase enzyme. In vitro binding of INUdR to bovine serum albumin (BSA) was estimated to be 65 to 77 %, depending on the INUdR concentration. There was no spontaneous release of NO by INUdR in PBS, in the absence of sulfhydryl groups. On the other hand, both L-cysteine (Cys) and glutathione (GSH) accelerated release of NO by INUdR in a concentration and time dependent manner. INUdR exhibited only a moderate cytotoxicty in the studied cancer cell lines but exhibited some selectivity against herpes simplex virus type 1 (KOS), herpes simplex virus type 2 (G), and vaccinia virus (IC_{50} = 48 μg/mL). The pharmacokinetics of INUdR following single intravenous bolus and oral doses of INUdR (40 mg/kg) to male Sprague-Dawley (SD) rats were characterized by a short elimination half-life ($T_{1/2} = 0.27$ h), a large steady-state volume of distribution ($V_{ss} = 0.89$ L/kg) and high oral bioavailability (Fa = 0.95). Glucuronide metabolites of INUdR were recovered in both urine and bile samples.

Acknowledgements

My most sincere gratitudes are extended to my supervisor Dr. Leonard I. Wiebe and my co-supervisor Dr. Edward E. Knaus for their supervision, guidance and support during my graduate program.

I wish to thank Dr. Yun K. Tam, Dr. John Samuel, Dr. James D. Young, and Dr. Pollen Yeung for their contributions in editing my thesis and for their critical comments and suggestions.

I wish to extend special thanks to Dr. Ebrahim Naimi for the skillful synthesis of all the compounds used in my studies.

I am also much grateful to Dr. Dr. Reza Khosravan, Dr. Kevin Morin, Dr. Tahereh Khazaenia, Dr. Keykavoos Parang, and Dr. Pyush Kumar for many helpful discussions during this work and for their kind guidance and suggestions.

I wish to thank Mr. Don Whyte for his enormous technical assistance throughout my graduate program and special thanks to Mrs. Weilie Duan and Mrs. Aihua Zhou for their kind help and technical assistance throughout my studies.

Finally, I would like to thank Canadian Institutes of Health Research for financial support of the research projects.

Table of Contents

1. INTRODUCTION 1

1.1. Applications of Pyrimidine Nucleosides in Medicine 1

1.2. Nucleoside Transport Processes 1

1.3. Pyrimidine Nucleosides and Cancer Chemotherapy 3

1.3.1. The Cell Cycle 4

1.3.2. Modes of Cell Death 6

1.3.3. Antineoplastic Pyrimidine Nucleosides 9

1.3.3.1. Fluoropyrimidines 11

1.3.3.2. Cytidine Analogues 15

1.4. Pyrimidine Nucleosides and Treatment of Viral Diseases 20

1.4.1. Overview of Antiviral Therapy 21

1.4.2. Nonretroviral Antiviral Pyrimidine Nucleosides 23

1.4.2.1. Idoxuridine 24

1.4.2.2. Trifluridine 24

1.4.2.3. Cidofovir 25

1.4.3. Antiretroviral Pyrimidine Nucleosides 26

1.4.3.1. Zidovudine 28

1.4.3.2. Stavudine 30

1.4.3.3. Zalcitabine 31

1.4.3.4. Lamivudine 33

1.5. Pharmacokinetic Optimization of Treatments with Nucleoside Analogues 34

1.5.1. Dose-Dependent Pharmacokinetics and Nucleoside Therapy 37

1.6. References 41

2. OBJECTIVES..55

2.1. Evaluation of the novel synthetic *C*-nucleoside, 1-(2-Deoxy-β-D-ribofuranosyl)-2,4-difluoro-5-iodobenzene (5-IDFPdR) 55

2.2. Evaluation of 5-iodo-3'-*O*-nitro-2'-deoxyuridine (INUdR), a novel nitric oxide (NO)-releasing 5-iodo-2'-deoxyuridine (IUdR) prodrug 56

3. *C*-NUCLEOSIDES AND THEIR VERSATILE APPLICATIONS.......................59

3.1. Introduction 59

3.2. Experimental 65

3.2.1. Materials 65

3.2.2. Cell lines, cell culture media and materials 67

3.2.3. High performance liquid chromatography 68

3.2.4. Stability of 5-IDFPdR in solution (water and PBS) and upon incubation with rat plasma 69

3.2.5. Enzymatic stability of 5-IDFPdR toward phosphorolysis by *E. coli* thymidine phosphorylase 69

3.2.6. In vitro incubation of 5-IDFPdR with rat liver microsomes 70

3.2.7. Determination of partition coefficients (log P).. 71

3.2.8. Protein binding of 5-IDFPdR 72

3.2.9. In vitro cytotoxicity assay 73

3.2.10. Flow cytometry study... 74

3.2.11. Animal pharmacokinetic studies.. 75

3.2.11.1. Enzymatic hydrolysis assays.. 77

3.2.11.2. Quantitative analyses of biological samples... 78

3.2.11.3. Quantitation limits and analytical recovery 78

3.2.11.4. Pharmacokinetic analyses.. 79

3.2.12. Blood-to-plasma ratio.. 80

3.3. Results... 81

3.3.1. Stability of 5-IDFPdR in solution (water and PBS), and in rat plasma 81

3.3.2. Stability of 5-IDFPdR toward phosphorolysis by *E. coli* thymidine phosphorylase.. 81

3.3.3. In vitro incubation of 5-IDFPdR with rat liver microsomes 82

3.3.4. Partition coefficients 82

3.3.5. Protein binding of 5-IDFPdR 83

3.3.6. In vitro cytotoxicity and flow cytometry studies... 84

3.3.7. Animal pharmacokinetic studies.. 89

3.3.8. Blood-to-plasma ratio of 5-IDFPdR 94

3.4. Discussion 95

3.5. References 108

4. NITRIC OXIDE AND NITRIC OXIDE DONORS 115

4.1. Introduction 115

4.1.1. An Overview of Some Nitric Oxide Functions within the Immune System. 116

4.1.2. Current Approaches to the Development of Nitric Oxide Donors 118

4.1.3. Novel Pyrimidine Nucleoside Nitric Oxide Donor Agents As Potential Anticancer/Antiviral Agents 120

4.1.4. Detection and Quantification of Nitric Oxide (NO) in Stock Solutions of NO Donors and in Biological Matrices 121

4.2. Experimental 124

4.2.1. Materials 124

4.2.2. High Performance Liquid Chromatography 125

4.2.3. Stability of INUdR in solution (water, PBS, and in an acidic environment), and in incubates of rat plasma 125

4.2.4. Enzymatic stability of INUdR and NTdR toward phosphorolysis by *E. coli* thymidine phosphorylase 127

4.2.5. Determination of partition coefficients (log P) 127

4.2.6. Protein binding of INUdR and NTdR 128

4.2.7. In vitro nitric oxide release assays 128

4.2.8. Animal pharmacokinetic studies 130

4.2.8.1. Enzymatic hydrolysis assays 133

4.2.9. Blood-to-plasma ratio 134

4.2.10. Pharmacokinetic Analysis 135

4.3. Results 136

4.3.1. Stability of INUdR in solution (water, PBS, and in an acidic environment), and in rat plasma 136

4.3.2. Enzymatic stability of INUdR and NTdR toward phosphorolysis by *E. coli* thymidine phosphorylase 137

4.3.3. Partition coefficients (log P) 138

4.3.4. Protein binding of INUdR and NTdR 139

4.3.5. In vitro nitric oxide release of INUdR 140

4.3.6. Pharmacokinetic Studies of INUdR 144

4.3.7. Blood-to-plasma ratio of INUdR 148

4.4. Discussion 149

4.4. References 155

5. GENERAL DISCUSSIONS AND CONCLUSIONS 162

5.1. References 165

6. APPENDIX 166

List of Tables

Table 3.1. Experimental and calculated log P values of 5-IDFPdR, 5-MeDFPdR and dThd ... 82

Table 3.2. Percent bovine serum albumin binding of 5-IDFPdR at various 5-IDFPdR concentrations. ... 83

Table 3.3. Mean IC_{50} values of 5-IDFPdR and reference compounds FUdR, IUdR, and thymidine in various cell lines ... 86

Table 3.4. Pharmacokinetic parameters of 5-IDFPdR in iv dosed male SD rats. ... 89

Table 3.5. Pharmacokinetic parameters of 5-IDFPdR in po dosed male SD rats. ... 89

Table 3.6. Percent of the 5-IDFPdR dose recovered as unchanged and unchanged plus metabolites in the urine, and mean renal clearance after iv and po administration of 5-IDFPdR to rats. ... 92

Table 3.7. Mean percent of the 5-IDFPdR dose recovered as sulfates and glucuronides in the urine after iv and po administration of 5-IDFPdR to rats. ... 92

Table 3.8. Mean percent of the 5-IDFPdR dose recovered as unchanged, and unchanged plus metabolites in the bile following iv administration of 5-IDFPdR to rats ... 93

Table 3.9. Mean absolute amounts of 5-IDFPdR glucuronides and sulfate conjugates recovered in the bile following iv administration of 5, 15 and 54 mg/kg doses ... 93

Table 3.8. In vitro blood-to-plasma ratio of 5-IDFPdR (rat blood) ... 94

Table 4.1. Experimental and calculated log P values for INUdR, IUdR, NTdR and dThd ... 138

Table 4.2. Percent binding of INUdR to bovine plasma albumin at various INUdR concentrations. 139

Table 4.3. Percent binding of NTdR to bovine plasma albumin at various NTdR concentrations. 140

Table 4.4. Nitric oxide release from INUdR and ISDN in PBS, upon incubation with increasing cysteine concentrations, as % NO per molecule of INUdR or ISDN 141

Table 4.5. Nitric oxide release from INUdR and ISDN in PBS, upon incubation with increasing glutathione concentrations, as % NO per molecule of INUdR or ISDN 141

Table 4.6. Nitric oxide release from INUdR and ISDN in incubates of rat plasma, as % NO per molecule of INUdR or ISDN 144

Table 4.7. Pharmacokinetic parameters for INUdR in male SD rats following single intravenous and oral doses of INUdR (40 mg/kg). 145

Table 4.8. Percent of the INUdR dose recovered as unchanged, and as glucuronides and sulfates in the 24h urine specimens of each rat (n = 3) following intravenous administration of INUdR (40 mg/kg). 147

Table 4.9. Percent of the INUdR dose recovered as unchanged, and as glucuronides and sulfates in the bile specimens of each rat (n = 3) following intravenous administration of INUdR (40 mg/kg). 147

Table 4.10. In vitro blood-to-plasma ratio of INUdR (rat blood). 148

List of Figures

Figure 1.1. The phases of cell cycle 4

Figure 1.2. Antineoplastic pyrimidine nucleoside analogues 10

Figure 1.3. Anabolism and catabolism of 5-fluorouracil 14

Figure 1.4. Synthesis of deoxythymidine monophosphate 14

Figure 1.5. Structures of selected antiherpesvirus pyrimidine analogues 23

Figure 1.6. Structures of antiretroviral pyrimidine nucleosides 27

Figure 3.1. Structures of thymidine, 1-(2-deoxy-β-D-ribofuranosyl)-2,4-difluoro-5-methylbenzene (5-MeDFPdR), and 1-(2-deoxy-β-D-ribofuranosyl)-2,4-difluoro-5-iodobenzene (5-IDFPdR) 61

Figure 3.2. Percent of cells surviving following 72h exposure to various concentrations (M) of 5-IDFPdR 84

Figure 3.4. Mean (+S.D.) concentrations of 5-IDFPdR in rat blood following intravanous bolus administration at 5, 15 and 54 mg/kg 90

Figure 3.5. Mean (+S.D.) concentrations of 5-IDFPdR in rat blood following oral administration at 20, 40 and 54 mg/kg 91

Figure 4.1. Structures of selected 3'-O-nitro-2'-deoxyuridines 121

Figure 4.2. Proposed reaction pathway for the Griess reaction 123

Figure 4.3. Formation of NUdR from INUdR as a function of incubation time (at 37 °C) in rat plasma 137

Figure 4.4. Mean nitrite generation from ISDN and INUdR in PBS as a function of increasing L-cysteine/glutathione concentrations following 1 h incubation at 37 °C 142

Figure 4.5. Mean percent NO release of INUdR/ISDN in PBS with increasing cysteine concentrations (0 to 25 mM) and for various incubation times. 143

Figure 4.6. Concentration-time curves for INUdR in plasma following iv bolus and oral administration of INUdR (40 mg/kg) to rats. 146

Glossary of Symbols and Abbreviations

α	Distribution phase associated rate constant in two-compartment model
A	Zero time intercept associated with the distribution phase in two-compartment model
A	Adenine, Adenosine
ADP	Adenosine 5'-diphosphate
AIDS	Acquired Immunodeficiency Syndrome
AML	Acute Myelogenous Leukemia
AM1	Austin Model 1
Ara-A	1-(β-D-arabinofuranosyl)adenine
Ara-C	1-(β-D-arabinofuranosyl)cytosine
Ara-CMP	1-(β-D-arabinofuranosyl)cytosine 5'-monophosphate
Ara-CTP	1-(β-D-arabinofuranosyl)cytosine 5'-triphosphate
Ara-UMP	1-(β-D-arabinofuranosyl)uridine 5'-monophosphate
ATCC	American Type Culture Collection
AUC	Area under the concentration-time curve
$AUC_{0\to\infty}$	Area under the concentration-time curve from the time of dose administration to time infinity
$AUMC_{0\to\infty}$	Area under the first moment curve from the time of dose administration to time infinity
AZT	3'-Azido-2',3'-dideoxythymidine

B	Zero time intercept associated with the elimination phase in two-compartment model
β	Elimination phase associated rate constant in two-compartment model
BBB	Blood-brain-barrier
° C	Degrees Celsius
C	Cytosine, Cytidine
CD4	Cluster of differentiation 4
cib	Concentrative, insensitive to NBMPR, accepts a broad range of permeants
cif	Concentrative, insensitive to NBMPR and accepts formycin B as a permeant
cit	Concentrative, insensitive to NBMPR and accepts thymidine as a permeant
Cl_{nr}	Nonrenal clearance
Cl_r	Renal clearance
CL_T	Total body clearance
CMP	Cytidine 5'-monophosphate
CMV	Cytomegalovirus
CNT	Concentrative nucleoside transporter
C_o	Concentration at time zero in one compartment model
CTP	Cytidine 5'-triphosphate
*cyclo*Sal	Cyclosaligenyl

d4T	2',3'-Didehydro-2',3'-dideoxythymidine
dATP	2'-Deoxyadenosine 5'-triphosphate
dCMP	2'-Deoxycytidine- 5'-monophosphate
dCTP	2'-Deoxycytidine 5'-triphosphate
ddC	2',3'-Dideoxycytidine
dFdCDP	2',2'-Difluorodeoxycytidine diphosphate
dFdCTP	2',2'-Difluorodeoxycytidine triphosphate
dF'TP	1-(2-deoxy-β-D-ribofuranosyl)-2,4-difluoro-5-methylbenzene 5'-triphosphate
dGTP	2'-Deoxyguanosine 5'-triphosphate
DHFU	5'-6'-Dihydrofluorouracil
DMEM	Dulbecco's Modified Eagle Medium
DMSO	Dimethylsulfoxide
DNA	Deoxyribonucleic acid
DNIC	Dinitrosyl-iron-di-L-cysteine complex
DPD	Dihydropyrimidine dehydrogenase
dThd	Thymidine
dTMP	Deoxythymidine-5'-monophosphate
dTTP	Deoxythymidine-5'-triphosphate
dUMP	Deoxyuridine 5'-monophosphate
E. coli	*Escherichia coli*
EBV	Epstein-Barr Virus
EDTA	Ethylenediaminetetraacetic acid

ei	Equilibrative insensitive
eNOS	Endothelial nitric oxide synthase
ENT	Equilibrative nucleoside transporter
EPR	Electron spin resonance
es	Equilibrative sensitive
5-EtDFPdR	1-(2-deoxy-β-D-ribofuranosyl)-2,4-difluoro-5-ethylbenzene
Fa	Bioavailability
F	Fluorine
FAD	Flavin adenine dinucleotide
FBAL	Fluoro-β-alanine
FBS	Fetal bovine serum
FDA	Food and Drug Administration
FdUDP	5-Fluoro-2'-deoxyuridine 5'-diphosphate
FdUMP	5-Fluoro-2'-deoxyuridine 5'-monophosphate
FdUrd	5-Fluoro-2'-deoxyuridine
FdUTP	5-Fluoro-2'-deoxyuridine 5'-triphosphate
fe	Fraction excreted unchanged (in the urine)
f_t	Fraction of unbound drug in the tissue
f_u	Fraction of unbound drug in the plasma
FIAU	1-(2-Deoxy-2-fluoro-β-D-arabinosyl)-5-iodouracil
5-FU	5-Fluorouracil
FUDP	5-Fluorouridine 5'-diphosphate
FUDR	5-Fluoro-2'-deoxyuridine

FUPA	α-Fluoroureido-propionic acid
FUrd	5-Fluorouridine
FUTP	5-Fluorouridine 5'-triphosphate
G	Guanine, Guanosine
G_1	Gap 1
G-418	Geneticine
GSH	Glutathione (reduced)
h	Hour
h	Human (e.g. hCNT1, hENT1, etc.)
HBV	Hepatitis B Virus
HEPES	*N*-2-Hydroxyethylpiperazine-*N'*-2-ethanesulfonic acid
HIV	Human Immunodeficiency Virus
HL-60	Human Leukemia-60 (cell line)
HPLC	High Performance Liquid Chromatography
HSLAS	Health Sciences Laboratory Animal Services
HSV	Herpes Simplex Virus
IC_{50}	Median inhibitory concentration
5-IDFPdR	1-(2-deoxy-β-D-ribofuranosyl)-2,4-difluoro-5-iodobenzene
i.e.	That is
iNOS	Inducible nitric oxide synthase
INUdR	5-Iodo-3'-*O*-nitro-2'-deoxyuridine
ISDN	Isosorbide dinitrate
IUdR	5-Iodo-2'-deoxyuridine

iv	Intravenous (bolus)
k	Elimination rate constant from the central compartment in one compartment model
KF	Klenow Fragment
K_m	Michaelis constant
L	Liter
Lambda$_{(max)}$ (λ_{max})	Maximum absorption wavelength
Lambda$_z$ (λ_z)	Terminal slope
L-cys	L-Cysteine
LDH	Lactate dehydrogenase
μ	Micro
μg	Microgram(s)
μL	Microliter(s)
M	Molar concentration
MAT	Mean absorption time
5-MeDFPdR	1-(2-deoxy-β-D-ribofuranosyl)-2,4-difluoro-5-methylbenzene
mg	Milligram(s)
mg/kg	Milligram per kilogram
min	Minute(s)
mL	Milliliter(s)
mM	Millimolar concentration
mmol	Millimole(s)
mRNA	Messenger RNA

MRT	Mean residence time
MTT	3-(4,5-dimethylthiazol-2-yl)-2,5-diphenyltetrazolium bromide
NADP	Nicotinamide adenine dinucleotide phosphate
NADPH	Nicotinamide adenine dinucleotide phosphate, reduced form
NBMPR	6-[(4-Nitrobenzyl)thio]-9-β-D-ribofuranosylpurine
ND	Not determined
NMR	Nuclear magnetic resonance spectroscopy
nNOS	Neuronal nitric oxide synthase
NO	Nitric oxide
NOS	Nitric oxide synthase
NR	Not recovered
NSAID	Nonsteroidal anti-inflammatory drugs
NTdR	3'-*O*-Nitro-2'-deoxythymidine
NUdR	3'-*O*-Nitro-2'-deoxyuridine
PAPS	3'-Phosphoadenosine-5'-phosphosulfate
PBS	Phosphate-buffered saline
PEG	Polyethylene glycol
PI	Propidium iodide
po	per oral
pol I	*Escherichia coli* DNA polymerase I
PRPP	5-Phosphoribosyl-1-pyrophosphate
RNA	Ribonucleic acid
RNase	Ribonuclease

SD	Sprague-Dawley
S.D.	Standard deviation
S.E.	Standard error
T	Thymine, Thymidine
3TC	2',3'-Dideoxy-3'-thiacytidine
$T_{½}$	Elimination half-life
TK	Thymidine kinase
T_M	Maximum transport rate
TMP	Thymidine 5'-monophosphate
TS	Thymidylate synthase
U	Uracil, Uridine
UDPGA	Uridine diphosphate glucuronic acid
UMP	Uridine 5'-monophosphate
UTP	Uridine triphosphate
UV	Ultraviolet
V_d	Volume of distribution
VEGF	Vascular Endothelial Growth Factor
V_{max}	Maximum velocity
V_p	Volume of plasma
V_{ss}	Volume of distribution at steady-state
V_t	Volume of tissues
VZV	Varicella Zoster Virus
X_U^{∞}	Total amount of compound excreted unchanged in the urine

1. Introduction

1.1. Applications of Pyrimidine Nucleosides in Medicine

The pyrimidine analogues form a major group of antimetabolite cytotoxic drugs in current clinical use for the treatment of various neoplastic and viral diseases. The term antimetabolite refers to their extensive structural similarities to endogenous nucleic acid precursors, as this group of agents consists of base and nucleoside analogues of the naturally occurring pyrimidine bases uracil, thymine and cytosine. Structural differences between the pyrimidine antimetabolites and naturally occurring pyrimidines usually involve substituents at one of the carbons in the pyrimidine ring or substitution of a hydrogen atom attached to the ring of the pyrimidine or sugar (ribose or deoxyribose). Despite these small structural differences, pyrimidine analogues still undergo uptake into cells and are metabolized via the same pathways used by endogenous pyrimidines. A cytotoxic effect results when the pyrimidine antimetabolite is incorporated in place of a naturally occurring pyrimidine metabolite into a key molecule, such as DNA or RNA, and/or when metabolic pathways are inhibited as a result of competition between the antimetabolite and naturally occurring pyrimidine metabolite for the same enzyme (Daher et al., 1990).

1.2. Nucleoside Transport Processes

Since most nucleosides, including those with anticancer and/or antiviral activities are hydrophilic, specialized plasma membrane nucleoside transporter (NT) proteins are often required for their uptake into the cells. There are however, some pharmacologically active nucleoside analogues, such as 3'-azido-2',3'-dideoxythymidine (AZT) and troxacitabine, which seem to enter some cell types largely by diffusion (Zimmerman et al., 1987; Gourdeau et al., 2001). In human and other mammalian cells, seven distinct nucleoside transport processes have been observed. Molecular cloning studies have led to the identification of proteins responsible for the five major nucleoside transport processes. These transport processes differ in their permeant selectivities, inhibition by diagnostic agents, and mechanisms of transport (Griffith and Jarvis, 1996). Three of these five processes are concentrative (Na^+ dependent) (systems *cit*, *cif*, and *cib*) and the other two are equilibrative (Na^+ independent) (systems *es* and *ei*). The *cit* (concentrative, insensitive to nitrobenzylthioinosine (NBMPR) and accepts thymidine as a permeant) system transports pyrimidine nucleosides and adenosine. The *cif* (concentrative, insensitive to NBMPR and accepts formycin B as a permeant) system transports purine nucleosides and uridine. The *cib* (concentrative, insensitive to NBMPR and accepts a broad range of permeants), *es* (equilibrative sensitive), and *ei* (equilibrative insensitive) systems are broadly selective for both pyrimidine and purine nucleosides (Baldwin et al., 1999).

In human cells, the equilibrative transport processes *es* and *ei* are mediated by equilibrative nucleoside transporters hENT1 and hENT2, respectively (Cass et al., 1999; Yao et al., 2002). Equilibrative nucleoside transporters (ENTs) act as bi-directional facilitated diffusion systems that mediate a much faster flux of nucleoside molecules across biomembranes than simple diffusion (Baldwin et al., 1999).

The concentrative transport processes *cit*, *cif*, and *cib* are mediated in human cells by human concentrative nucleoside transporters hCNT1, hCNT2, and hCNT3, respectively (Cass et al., 1999; Yao et al., 2002). Concentrative nucleoside transporters (CNTs) catalyze the inwardly-directed co-transport of a nucleoside and a sodium ion, across the cell membrane. By using energy derived from Na^+ ion gradient across the plasma membrane, CNTs allow for the transport of nucleosides into the cell against their concentration gradients (Baldwin et al., 1999). Due to the differences in their substrate specificities, hCNT1 and hCNT2 have a complementary role in the transport of pyrimidine and purine anticancer and antiviral nucleoside analogues. On the other hand, hCNT3 transporter that exhibits *cib*-type Na^+ dependent nucleoside transport activity transports both pyrimidine and purine anticancer and antiviral nucleoside drugs (Ritzel et al., 2001 and references therein).

1.3. Pyrimidine Nucleosides and Cancer Chemotherapy

Cytokinetic assessment of antineoplastic drugs is an important consideration in oncologic chemotherapy, since the objective of cancer chemotherapy is the destruction of neoplastic cells with minimal effects on nonneoplastic or normal tissues. Cycles of intensive therapy are often employed and repeated as frequently as allowed by the tolerance of dose-limiting tissues such as the bone marrow or gastrointestinal tract, in an attempt to destroy as many tumor cells as possible, through the multiplicative effect of successive fractional cell kills (Kaufman and Chabner, 1996). An understanding of cell-cycle kinetics is essential for the proper use of current antineoplastic agents (Calabresi and Chabner, 2001). Therefore, an introduction to the cell cycle process will precede the introduction pertaining to the metabolism and mechanisms of action of individual pyrimidine antimetabolites used in the treatment of neoplastic diseases.

1.3.1. The Cell Cycle

Despite differences in duration of the cell cycle among various cell types, all cells display a similar pattern during the division process (Figure 1.1):

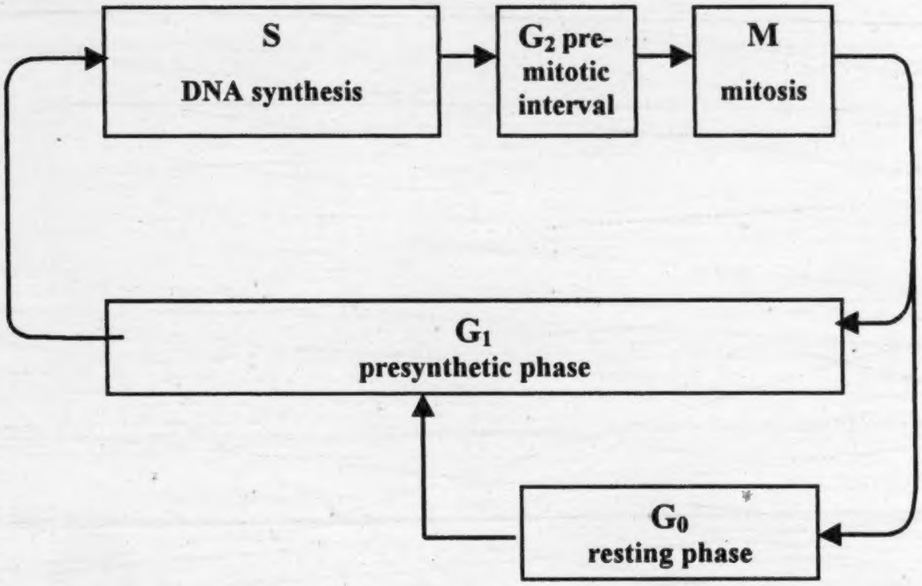
S
DNA synthesis
G2 pre-mitotic interval
M
mitosis
G1
presynthetic phase
G0
resting phase

Figure 1.1. The phases of cell cycle (modified from Calabresi and Chabner, 2001)

The cell cycle is comprised of a "G_1 or presynthetic phase" where precursors for DNA are formed; a "S or synthetic phase" in which the synthesis of DNA occurs; the "G_2 premitotic or postsynthetic phase"; and the "mitosis or M-phase" where the G_2 cell, containing a double complement of DNA, divides into two daughter G_1 cells. Each one of these daughter cells may reenter the cell cycle or pass into the so called "resting or G_0 phase", where cells are in a nonproliferative stage. While the G_0 cells of certain specialized tissues may differentiate into functional cells that can no longer divide, many other G_0 cells, especially those of slow-growing tumors, remain dormant for longer periods of time and reenter the cell cycle at a later time (Calabresi and Chabner, 2001).

The effectiveness of most antineoplastic drugs, including some important antimetabolites, is greater on cells that are progressing through the cell cycle, compared to cells that are resting in the G_0 phase. Accordingly, faster growing hematological (nonsolid) malignancies (leukemias and lymphomas) are more responsive to treatment with cytotoxic drugs than are slower growing solid tumors (carcinomas and sarcomas) [Wingard et al., 1991(a)].

Poor drug access to the non-vascularized areas of solid tumors is another important factor contributing to the lower responsiveness of such tumors to cytotoxic agents. While the outer or most recently synthesized parts of many solid tumors are highly vascularized and have good access to drugs, the inner and older areas are usually hypoxic, often necrotic, and not readily accessible by the drugs. The necrotic inner cells may be dead or merely dormant such that they are capable of reentering the cycle of cell division [Wingard et al., 1991(a)]. The delivery of drugs to the non-vascularized regions of tumors has been a major challenge for clinical oncologists.

1.3.2. Modes of Cell Death

In contrast to "cell quiescence or dormancy", which is characterized by decreased rates of biological activity, the process of "cell death" culminates with cessation of all biological activities within the dying cell (Darzynkiewicz et al., 1997). "Apoptosis" and "necrosis" have generally been accepted as two distinct, mutually exclusive, modes of cell death (Majno and Joris, 1995; Vaux, 1993). Apoptosis is an actively regulated mode of cell death, which occurs physiologically, and also as a result of certain pathologies, or exposure to cytotoxic agents. In the process of apoptosis, sometimes referred to as "cell death by suicide", the cell itself designs and executes the program of its own demise and subsequent disposal (Darzynkiewicz et al., 1997).

At least two distinct checkpoints within the cell cycle, one controlled by the bcl-2/bax family of proteins, and another by the cysteine- and possibly serine proteases, are thought to be involved in the complex, multistep mechanism that regulates the cell's propensity to respond by apoptosis to various stimuli (Reed, 1994; Fernandes-Alnembri et al., 1995; Lazebnik et al., 1994; Weaver et al., 1993). This complex system, in turn, interacts with the regulatory mechanisms associated with cell proliferation and DNA repair, through the action of several oncogenes and tumor suppressor genes such as p53 (Vaux, 1993).

In cells that are undergoing apoptosis, a number of important morphological and biochemical changes have been identified. Many of the changes occurring during the apoptotic process, which are very characteristic of this mode of cell death, have become markers used to identify apoptotic events biochemically, as well as, by microscopy or cytometry (Darzynkiewicz et al., 1997).

During early stage of apoptosis, cells become dehydrated due to the loss of their intracellular water. As cell cytoplasm shrinks, the originally round cells become elongated or convoluted in shape and diminished in size. Chromatin condensation, followed by nuclear disintegration and formation of membrane-enclosed apoptotic bodies are other important features of apoptosis. The apoptotic bodies contain nuclear fragments, formed as a result of nuclear disintegration, and constituents of the cytoplasm that are enveloped by fragments of the plasma membrane. The apoptotic bodies shed from the dying cells are rapidly phagocytized in vivo by neighboring cells, without triggering an inflammatory response (Darzynkiewicz et al., 1995).

The most prominent biochemical event during apoptosis is the activation of specific endonucleases that cleave DNA at specific sites between nucleosomes (internucleosomal regions), leading to formation of DNA fragments whose molecular sizes are multiples of about 180 base pairs. These fragments generate a characteristic DNA "laddering" during agarose gel electrophoresis (Wyllie et al., 1980). Some other important features of apoptosis include loss of microtubules (Endersen et al., 1995) and loss of asymmetry of the phospholipids on the plasma membrane leading to exposure of phosphatidylserine on the outer surface (Fadok et al., 1992).

In contrast to apoptosis, necrosis is a passive and degenerative mode of cell death. Necrosis tends to occur as a result of a marked toxic or physical insult. The early events include mitochondrial swelling followed by the rupture of the plasma membrane and release of cytoplasmic contents (including many proteolytic enzymes) into the intercellular space. Necrosis, in contrast to apoptosis, elicits an inflammatory reaction in the tissue. During necrosis, DNA degradation is not as extensive as in the case of apoptosis, and the resulting DNA fragments that are heterogenous in size do not form any discrete bands on electrophoretic gels (Darzynkiewicz et al., 1995).

There has been a long-standing interest in apoptosis in disciplines such as embryology and immunology, as this mode of cell death plays a pivotal role in tissue and organ development, and in various normal and pathological immune responses (Darzynkiewicz et al., 1997). The interest in apoptosis in oncology is more recent and derives from several findings in various fields (Darzynkiewicz et al., 1995). It has been suggested that apoptosis plays an important role in deletion of pre-neoplastic cells and, therefore, in preventing the progression of disease (Kerr et al., 1994). Accordingly, an inability to delete pre-neoplastic cells by apoptosis is thought to play an important role in the fixation of genetic mutations that eventually lead to development of tumors (Clarke et al., 2000). The importance of apoptosis in cancer therapy is based on the observation that many anticancer agents, as well as, radiation, induce cell death by apoptosis (Hickman, 1992; Potten et al., 1994). With apoptosis being an active and regulated mode of cell death, a possibility exists to modulate the propensity of cells to respond to the intrinsic or exogenous signals by this mode of death, via interaction with apoptotic regulatory machinery. To exploit such a possibility in oncological research, scientists are currently exploring strategies to modulate the sensitivity of cancerous and/or normal cells to anticancer agents (Darzynkiewicz, 1995; Dive and Hickmann, 1991; Fisher, 1994).

It is known that tumor progression and increased malignancy may be associated with a change in the propensity of tumor cells to undergo spontaneous apoptosis (Hercbergs and Leith, 1993; Laidlaw and Potten, 1992), and the efficacy of many anticancer drugs has been associated with their ability to induce apoptosis (Horber et al., 1995). The rate of apoptosis, whether it is a spontaneous apoptosis in tumors or an induced apoptosis by anticancer drugs, has gained prognostic value in oncology (Darzynkiewicz et al., 1997). Analysis of cell death in various tissue systems and assessment of the cell cycle specificity of anticancer agents will, therefore, provide crucial information regarding the efficiency of the anticancer treatments (in terms of induction of apoptosis in the course of therapy), and will also allow for screening of apoptosis-modulating drugs.

1.3.3. Antineoplastic Pyrimidine Nucleosides

The most useful clinical and best-characterized antineoplastic pyrimidine nucleosides belong to the families of fluoropyrimidine and cytidine analogues (Figure 1.2). These include agents such as 5-fluorouracil, 5-fluoro-2'-deoxyuridine, cytarabine, 5-azacytidine, and gemcitabine.

The pathways for their metabolic activation and degradation will be explained to better understand the concept of the requirement for metabolic activation by these compounds, while providing an overview of normal pyrimidine nucleotide metabolism.

Fluoropyrimidine Analogues

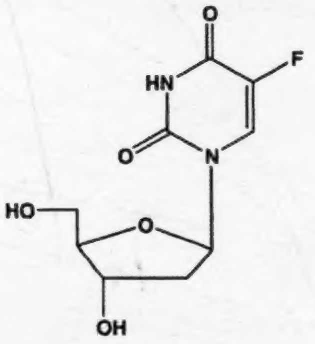

5-Fluoro-2'-deoxyuridine (FUdR)

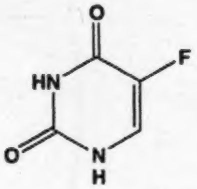

5-Fluorouracil (5-FU)

Cytidine Analogues

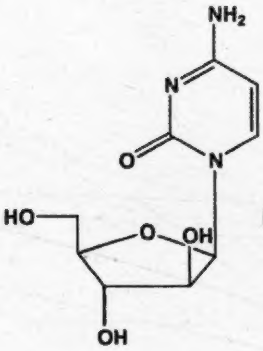

Cytarabine (Ara C)

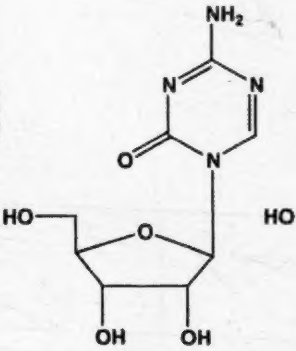

5-Azacytidine

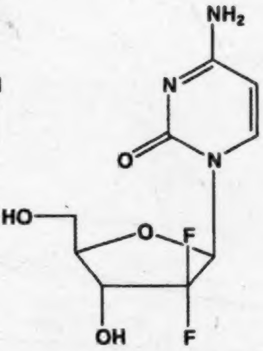

Gemcitabine

Figure 1.2. Antineoplastic pyrimidine nucleoside analogues

1.3.3.1. Fluoropyrimidines

5-Fluorouracil (5-FU) was first synthesized in 1957 (Dushinsky et al, 1957). 5-FU is used in the treatment of metastatic breast and gastrointestinal tract carcinomas, producing partial responses in 10 to 20 % of the patients. There have also been some beneficial effects reported in the treatment of hepatomas, and carcinomas of the ovary, cervix, urinary bladder, prostate, pancreas, and oropharyngeal areas (Calabresi and Chabner, 2001). Transport studies with 5-FU in cultured cells, tissues, tumors, or intestinal preparations have reported that 5-FU enters cells by nonfacilitated diffusion, facilitated diffusion, active and concentrative mechanisms, or combinations of these (Wohlhueter et al., 1980; Domin et al., 1993; Yuasa et al., 1996). Following administration, 5-FU undergoes a series of anabolic and catabolic reactions (Figure 1.3). Anabolic reactions lead to the formation of the cytotoxic metabolites 5-fluorouridine 5'-triphosphate (FUTP) and 5-fluoro-2'-deoxyuridine 5'-monophosphate (FdUMP). FUTP can be incorporated into RNA by the action of RNA polymerase, in place of the normal nucleotide uridine triphosphate (UTP). This leads to inhibition of the nuclear processing of ribosomal and messenger RNA and may also cause other errors in base pairing during transcription of RNA (Moore and Erlichman, 1998). FdUMP exerts its cyotoxic action by tight binding to the enzyme thymidylate synthase (TS) and thereby, preventing formation of thymidylate (thymidine 5'-monophosphate, dTMP). As thymidylate is the precursor of thymidine 5'-triphosphate (dTTP), one of four deoxyribonucleotides required for DNA synthesis and repair, its depletion due to the interaction of FdUMP and TS enzyme, leads to an inhibition of both DNA synthesis and repair (Grem, 2001).

Figure 1.4 depicts the involvement of thymidylate synthase in the synthesis of deoxythymidine nucleotide dTMP.

In addition to the direct cytotoxic effects, there are also indirect mechanisms of cytotoxicity, associated with 5-FU treatment. For instance, it has been noted that in 5-FU treated cells, both dUTP (accumulates due to the inhibition of thymidylate synthase) and FdUTP are incorporated into DNA in place of the depleted physiologic TTP. The incorporation of FdUTP into DNA is thought to evoke the excision-repair process, which in these cells, however, may result in DNA strand breakage and no repair. This is due to the fact that TTP, which is required for DNA repair, is lacking in these cells as a result of inhibition of the thymidylate synthase enzyme (Mauro et al., 1993).

As illustrated in Figure 1.3, there are several routes for the anabolic formation of the 5'-monophosphate nucleotide (FUMP), which is the precursor to the active triphosphate form (FUTP). 5-FU may be converted to fluorouridine by uridine phosphorylase and then phosphorylated to FUMP by uridine kinase. 5-FU may also react directly with 5-phosphoribosyl-1-pyrophsphate (PRPP) to form FUMP, in a reaction catalyzed by the enzyme orotate phosphoribosyl transferase (Daher et al., 1990). FUMP can then be phosphorylated to the 5'-diphosphate (FUDP) and triphosphate (FUTP) nucleotides by the corresponding kinases. FdUMP, the other cytotoxic anabolite of 5-FU, can be formed via a two-step reaction, involving reduction of FUDP by the enzyme ribonucleotide diphosphate reductase to FdUDP and dephosphorylation of the latter to FdUMP. FdUMP may also be formed directly from 5-FU, following its conversion to the deoxyriboside 5-FUdR by thymidine phosphorylase and phosphorylation of 5-FUdR by thymidine kinase (Daher et al., 1990; Hartmann and Heidelberger, 1961).

The catabolic degradation of 5-FU is an important factor in regulating the amount of available drug for anabolic reactions, and in determining the toxicity to normal tissue. About 90% of a dose of 5-FU is cleared by catabolism in liver and extrahepatic tissues, whereas less than 10% undergoes renal excretion (Diasio and Harris, 1989; Heggie et al., 1987). The initial rate-limiting step in catabolism of 5-FU involves reduction of the pyrimidine ring by the enzyme dihydropyrimidine dehydrogenase (DPD) to 5,6-dihydro-5-fluorouracil (DHFU). α-Fluoroureido-propionic acid (FUPA) is then formed as a result of opening of the DHFU ring by the action of the dihydropyrimidinase enzyme. FUPA is then irreversibly converted to fluoro-β-alanine (FBAL), with the release of ammonia (NH_3) and CO_2 (Grem, 2001, Lyer and Ratain, 1999).

5-Fluoro-2'-deoxyuridine (floxuridine, FUDR) has been primarily used for treatment of metastatic carcinoma of the colon (Calabresi and Chabner, 2001). FUDR, a deoxyribonucleoside of 5-FU, bypasses some of the complex metabolic pathways required for activation of 5-FU. FUDR can be directly converted to FdUMP by thymidine kinase, which will inhibit thymidylate synthase and thus block DNA synthesis. The cellular anabolism of FUDR to FdUMP by pyrimidine nucleoside kinase, is, however, offset by the catabolic effects of pyrimidine phosphorylases such as thymidine phosphorylase, which cleaves the glycosidic bond and yields 5-FU (Birnie et al, 1963; Chaudhuri et al, 1959; Uchida et al., 1990).

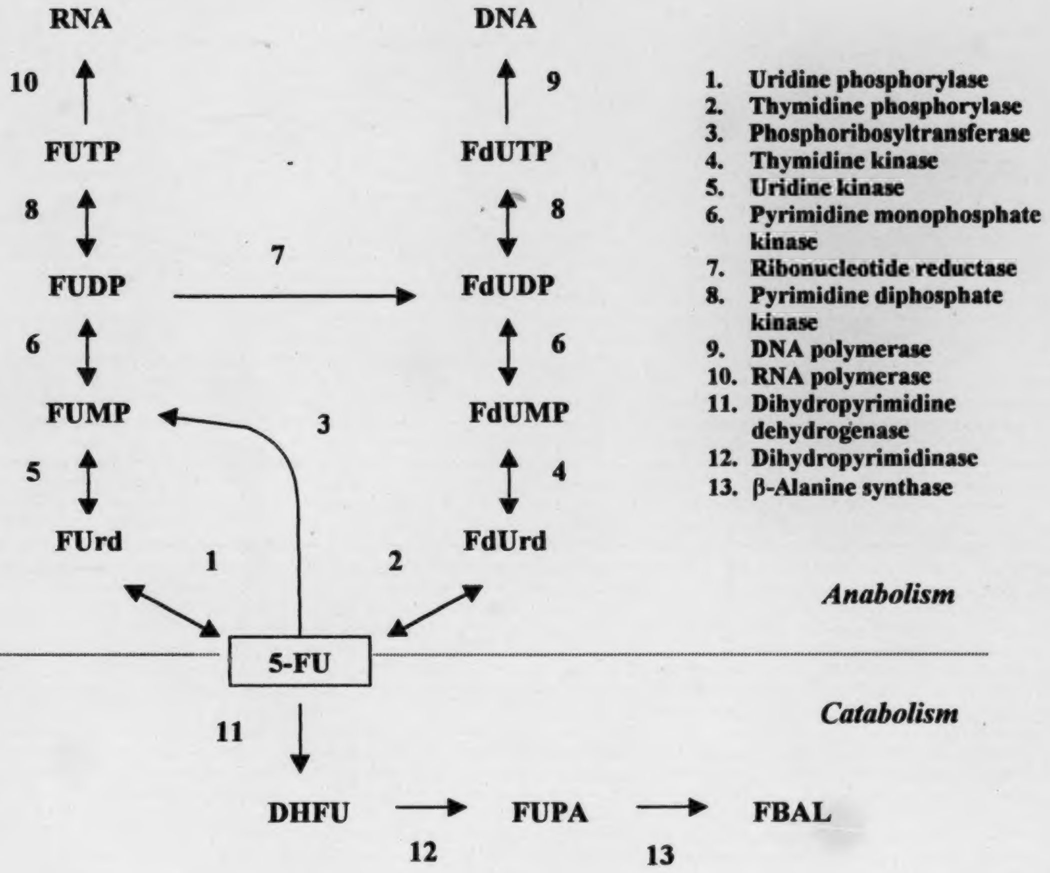
RNA
DNA
10
9
FUTP
FdUTP
8
8
7
FUDP
FdUDP
6
6
FUMP
3
FdUMP
5
4
FUrd
FdUrd
1
2
5-FU
11
DHFU
FUPA
FBAL
12
13
1. Uridine phosphorylase
2. Thymidine phosphorylase
3. Phosphoribosyltransferase
4. Thymidine kinase
5. Uridine kinase
6. Pyrimidine monophosphate kinase
7. Ribonucleotide reductase
8. Pyrimidine diphosphate kinase
9. DNA polymerase
10. RNA polymerase
11. Dihydropyrimidine dehydrogenase
12. Dihydropyrimidinase
13. β-Alanine synthase
Anabolism
Catabolism

Figure 1.3. Anabolism and catabolism of 5-fluorouracil (Lyer and Ratain, 1999)

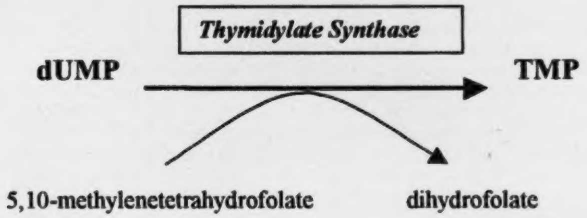
Thymidylate Synthase
dUMP
TMP
5,10-methylenetetrahydrofolate
dihydrofolate

Figure 1.4. Synthesis of deoxythymidine monophosphate

1.3.3.2. Cytidine Analogues

Cytarabine (ara-C) is an effective chemotherapeutic cytidine analogue used in the treatment of many hematological malignancies. Ara-C is one of the most useful agents used in the treatment of acute myelogenous leukemia (AML) and is highly effective in induction of remission in this disease (Ellison et al., 1968; Johnson, 2001). Ara-C contains an arabinose sugar in place of the natural ribose sugar of cytidine (Figure 1.2). Unlike the natural ribose sugar of nucleotides, in which a hydroxyl group is attached to the 2'-carbon in a downward or α configuration, in an arabinose sugar, the hydroxyl group attached to the 2'-carbon is in the β or upward configuration. Ara-C penetrates cells by a carrier-mediated process shared with deoxycytidine (Moore and Erlichman, 1998). Ara-C is recognized enzymatically as a 2'-deoxyriboside and is converted by a series of kinases to the active metabolite araCTP. AraCTP competes with dCTP for incorporation into DNA, where it effectively terminates DNA template function and chain elongation upon misincorporation at the terminal position of a growing DNA strand (Mikita and Beardsley, 1988; Major et al., 1982). The inhibitory effects of ara-C on DNA polymerases extend not only to DNA chain elongation during semiconservative DNA replication, but also to DNA repair (Calabresi and Chabner, 2001). As an inhibitor of DNA synthesis, ara-C has its greatest cytotoxic effects during the S-phase of the cell cycle. In addition to being cell-cycle phase dependent, the cytotoxic action of ara-C is also dependent on the rate of DNA synthesis. For instance, in cell culture studies, exposure to ara-C of cells in periods of active DNA synthesis, such as those recovering from exposure to a cytotoxic agent, produces the greatest cell kill (Karon and Shirakawa, 1970).

Ara-C and its 5'-monophosphate are susceptible to catabolic degradation by cytidine deaminase and deoxycytidylate deaminase enzymes, respectively (Daher et al., 1990). Cytidine deaminase is widely distributed in mammalian tissues including liver, kidney, heart, intestinal mucosa, and granulocytes (Camiener and Smith, 1965; Chabner et al., 1974) as well as in various tumors (Camiener and Smith, 1965, Chabner et al., 1973, Hart et al., 1972). Cytidine deaminase catalyzes the deamination of naturally occurring cytidine and deoxycytidine. It also acts as the primary catabolic enzyme responsible for the inactivation of ara-C, through its deamination to a nontoxic metabolite, arauridine (ara-U). Following oral administration of ara-C, only about 20% of the drug reaches the circulation, as much of the drug is deaminated by the cytidine deaminase enzyme, which is present in high concentrations in the gastrointestinal mucosa and the liver. Thus, ara-C is either administered by rapid intravenous injection or intravenous infusion, rather than the oral route. Less than 10% of the injected ara-C dose is excreted unchanged in the urine within 12 to 24 hours following intravenous dosing; most of the drug appears as the inactive, deaminated product, uracil arabinoside (ara-U) [Calabresi and Chabner, 2001]. Deoxycytidylate deaminase enzyme is responsible for the deamination of CMP to UMP, and it also provides an additional route for the catabolism of ara-C by deaminating its monophosphate metabolite ara-CMP to the inactive metabolite ara-UMP (Daher et al., 1990). Therapeutic response to ara-C is, therefore, influenced by the relative activities of anabolic and catabolic enzymes that determine the proportion of ara-C converted to the active metabolite, ara-CTP (Calabresi and Chabner, 2001).

In ara-C resistant tumors, deoxycytidine kinase, the rate-limiting enzyme responsible for phosphorylation of ara-C to ara-CMP, is often absent (Tattersall et al., 1974). Therefore, attempts were made to develop other cytidine analogues by modifying the basic pyrimidine ring of ribonucleosides, and by making cytidine analogues that will likely be activated by uridine-cytidine kinase, rather than deoxycytidine kinase. 5-Azacytidine, synthesized by Sorm and colleagues in 1963 (Sorm et al, 1964) was, therefore, introduced with great enthusiasm. Although 5-azacytidine was toxic in both bacterial and mammalian cell cultures, in clinical trials, it has only exhibited cytostatic action against acute myelogenous leukemia (AML) [Vogler at al., 1976], and AML is the only malignant disease for which it has been occasionally used (Von Hoff et al., 1976). There has been a longstanding dispute regarding the mechanism of cytotoxicity induced by 5-azacytidine, although both DNA and RNA metabolism are likely targets of this antimetabolite (Murakami et al., 1995). Mechanistically, the triphosphate form of 5-azacytidine appears to compete with CTP for incorporation into RNA (Vesely and Cihak, 1978), where it exerts numerous deleterious effects on RNA processing and function (Glazer et al., 1980). 5-Azacytidine is also, to a lesser extent, incorporated into DNA (Li et al., 1970). The DNA in which 5-azacytidine is substituted for cytidine remains hypomethylated, because the nitrogen atom in this antimetabolite cannot be methylated (Friedman, 1981). By preventing the methylation of DNA, 5-azacytidine has been found to induce the synthesis of various proteins, including hepatic enzymes (Cihak et al., 1973), metallothionein (Stallings et al., 1986), histocompatibility proteins (Carlow et al., 1985), and T-cell surface markers (Richardson et al., 1986). Furthermore, reactivation of various repressed genes encoding for thymidine kinase (Liteplo et al., 1985), hypoxanthine-guanine phosphoribosyl transferase (Jones et al., 1982), or DNA repair (Jeggo and Holliday, 1986) has been attributed to the drug's inhibitory effect on DNA methylation. The latter effects may in turn convert drug-resistant cells to drug-sensitive cells or vice versa.

In in vitro studies of HL-60 cell lines exposed to low concentrations (2-8 μM) of 5-azacytidine, predominantly G_1 cells, *i. e.* cells that have not replicated DNA, are reported to undergo apoptosis. Thus, there appears to be a preference for RNA as the target, at lower 5-azacytidine concentrations (Murakami et al., 1995). In contrast to the effects seen at lower 5-azacytidine concentrations, in cultures treated with higher concentrations (8-16 μM) of 5-azacytidine, an increase in the proportion of S-phase cells undergoing apoptosis were reported (Murakami et al., 1995). The authors concluded that cell cycle-specific effects of 5-azacytidine vary depending on drug concentrations.

Among the therapeutically useful cytidine analogues, 2',2'-difluorodeoxycytidine (gemcitabine) appears to be the most promising antimetabolite to enter the clinic in recent years. Gemcitabine was originally selected for development on the basis of its impressive activity against murine solid tumors and human xenografts in nude mice (Hertel et al., 1990). Gemcitabine is now part of the first-line treatment regimen for patients with metastatic pancreatic cancer (Burris et al., 1997), non-small cell lung cancer (Castellano et al., 1998, Lippe et al., 1999), and transitional cell carcinoma of the bladder (Stadler et al., 1997). Structurally, gemcitabine is an antimetabolite of deoxycytidine, in which two hydrogen atoms at the 2' position of the deoxyribose sugar have been replaced by two fluorine atoms (Hertel et al., 1988). Gemcitabine retains many of the features of cytarabine: it has the same activation pathway (phosphorylation by deoxycytidine kinase) [Bouffard et al, 1993], inhibits DNA synthesis, and appears to exert its cytotoxicity through incorporation into DNA (Huang et al., 1991). However, there are also some important differences between the mechanisms of action and biological activities of gemcitabine and cytarabine.

Gemcitabine, which enters the cells via active nucleoside transporters (Mackey et al., 1998), is a better permeant than cytarabine. It is also a more favorable substrate for deoxycytidine kinase. Both of these factors contribute to the accumulation of greater amounts of gemcitabine nucleotide in cells compared to ara-C. Despite the similar susceptibilities of gemcitabine and ara-C to deamination by cytidine deaminase, and the superior substrate properties of gemcitabine monophosphate for cellular dCMP deaminase, as compared to ara-C monophosphate, gemcitabine triphosphate is able to directly inhibit dCMP deaminase. This inhibitory effect on dCMP deaminase is thought to slow down the elimination of active nucleotide forms of gemcitabine. The slowed clearance, combined with the efficient phosphorylation of gemcitabine, leads to intracellular accumulation of high concentrations of gemcitabine active nucleotides (Plunkett et al., 1996). Gemcitabine has numerous effects on DNA synthesis, which could account for its cytotoxicity. Gemcitabine diphosphate (dFdCDP) is a potent inhibitor of ribonucleotide reductase and exposure to the drug has been shown to block incorporation of labeled cytidine into the cellular pool of dCTP (Heinemann et al., 1990). The decreased cellular concentration of dCTP may indirectly reduce the metabolic clearance of gemcitabine, as dCTP is a requisite activator of dCMP deaminase. Furthermore, since dCTP inhibits the activity of deoxycytidine kinase, lowered dCTP levels should result in more effective activation of gemcitabine. The elevation in the ratio of the cellular concentrations of gemcitabine triphosphate (dFdCTP) to dCTP would favor incorporation of the cytidine analogue into DNA (Plunkett et al., 1996), which in turn leads to perturbation of cellular DNA replication (Huang et al., 1991).

Cytotoxicity induced by gemcitabine, unlike that of ara-C, is not confined to the S phase of the cell cycle, since the drug is equally effective against confluent cells and cells in log-phase growth (Rockwell et al., 1992). Apoptosis appears to be an important mechanism by which gemcitabine exerts its antitumor effects (Huang et al., 1995), although differentiation has also been observed with selected cell lines in culture (Ban et al., 1992).

In summary, the self-potentiation mechanisms responsible for effective accumulation and prolonged retention of gemcitabine nucleotides do not exist in the case of ara-C metabolism. The different metabolic properties of gemcitabine and ara-C may at least partially account for their different spectra of therapeutic activities, with the former being active in solid tumors, and the latter only useful in the treatment of hematological malignancies (Plunkett et al., 1996).

1.4. Pyrimidine Nucleosides and Treatment of Viral Diseases

In addition to their activity as antineoplastic agents, many nucleoside analogues have antibiotic properties with activity directed against bacteria, viruses, fungi or yeast, depending on their biochemical mode of action (Balimane et al., 1999). Among therapeutically active antiviral nucleoside analogues are several pyrimidine analogues that have been clinically used to treat herpes infections as well as retroviral infections such as AIDS (Hayden, 2001).

The pharmacology and mode of action of selected antiherpes and antiretroviral pyrimidine nucleosides are summarized in sections 1.1.2.2 and 1.1.2.3 following a general overview of viruses, their replication cycles and strategies in antiviral therapy.

1.4.1. Overview of Antiviral Therapy

Viruses consist of a core genome of nucleic acid (double- or single-stranded DNA or RNA) contained in a protein shell (capsid) that is sometimes surrounded by a lipoprotein membrane (envelop). In order to replicate, viruses must enter host cells and use cellular energy-generating, DNA- or RNA-replicating, and protein-synthesizing pathways of the host, as they cannot replicate independently [Wingard et al., 1991(b)].

The majority of DNA viruses enter the host cell nucleus, where their (viral) DNA is transcribed into mRNA by host cell mRNA polymerase; this mRNA is then translated in the usual way, however, into virus-specific proteins. DNA viruses (and the diseases they cause) include poxviruses (smallpox), herpes viruses (chickenpox, shingles, herpes), adenoviruses (conjunctivitis, sore throat), hepadnaviruses (hepatitis B), and papillomaviruses (warts) [Hayden, 2001].

The replication of RNA viruses in the host cell relies either on enzymes within the infective viral particle to synthesize its mRNA or on the viral RNA serving as its own mRNA. The mRNA is then translated into various viral proteins, including RNA polymerase, which directs the synthesis of more viral mRNA. Some RNA viruses, such as influenza virus, require active transcription within the host cell nucleus (Hayden, 2001). RNA viruses (and the diseases they cause) include rubella virus (German measles), rhabdoviruses (rabies), picornaviruses (poliomyelitis, meningitis, colds), arenaviruses (meningitis, Lassa fever), arboviruses (yellow fever, arthropod-borne encephalitis), orthomyxoviruses (influenza), and paramyxoviruses (measles, mumps) [Hayden, 2001].

In a special group of RNA viruses, called retroviruses, viral RNA serves as a template from which complementary DNA strands are transcribed. This reverse transcription, which is the distinguishing feature of retroviruses, is catalyzed by the action of a "RNA-dependent DNA polymerase" enzyme, also referred to as, "reverse transcriptase". This DNA copy of viral RNA is then integrated into the host cell genome and is transcribed into both genomic RNA and mRNA, which will translate into viral proteins and give rise to the generation of new viral particles (Raffanti and Haas, 2001). Retroviruses are the causative agents for diseases such as AIDS and T-cell leukemias (Hayden, 2001).

For an antiviral agent to be effective, it must preferentially inhibit viral rather than host cell nucleic acid or protein synthesis and, therefore, inhibit only the virus-specific replicative events. Many of the available antiviral agents interfere with one of the many steps involved in the viral infection and replication cycle (Hayden, 2001).

Many viruses contain unique enzymes or metabolic pathways that make them more susceptible to certain antiviral agents:

Herpes simplex virus (HSV) for instance, encodes a viral thymidine kinase that phosphorylates the antiviral nucleoside analogue acyclovir far more efficiently than the host cell thymidine kinase does. As a result, acyclovir, which upon phosphorylation becomes entrapped within the cell, accumulates in infected cells, leading to greater inhibition of viral growth and fewer side effects in uninfected cells. Similarly, inhibitors of reverse transcriptase enzyme, which is used only by retroviruses to transcribe RNA to DNA early in their replication cycle, have been developed and successfully used in the treatment of retroviral infections, such as human immunodeficiency virus (HIV) infections [Wingard et al., 1991(b)].

1.4.2. Nonretroviral Antiviral Pyrimidine Nucleosides

This group of nucleoside analogues includes antiherpesvirus agents such as idoxuridine, trifluridine, and cidofovir (Figure 1.5).

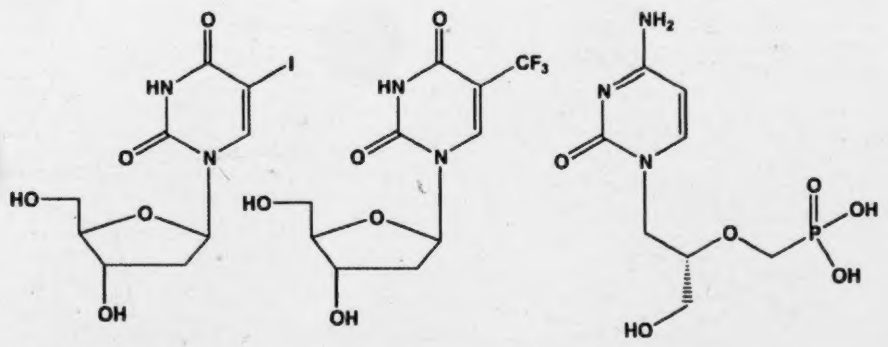

Idoxuridine (IUdR) **Trifluridine** **Cidofovir**

Figure 1.5. Structures of selected antiherpesvirus pyrimidine analogues

1.4.2.1. Idoxuridine

Idoxuridine (5-iodo-2'-deoxyuridine) is an iodinated thymidine analogue that was first synthesized in the late 1950's (Prusoff, 1959) and was used as an antitumor agent and a radiosensitizer in the early 1960's (Calabresi, 1962; Calabresi et al., 1961). Idoxuridine inhibits the *in vitro* replication of various DNA viruses, including herpesviruses and poxviruses (Prusoff, 1988). Like other nucleoside analogues, idoxuridine requires anabolic phosphorylation in order to be activated, and this is accomplished by cellular kinases. Idoxuridine triphosphate inhibits viral DNA synthesis and is incorporated into both viral and cellular DNA (Hayden, 2001).

A topical preparation of idoxuridine in dimethyl sulfoxide (DMSO) is available in Europe for the treatment of herpes labialis, herpes genitalis and localized herpes zoster with only marginal benefits (Silvestri et al., 1982; Spruance et al., 1990; Inouye et al., 2002). In the United States idoxuridine is presently approved only for the topical treatment of HSV keratitis.

1.4.2.2. Trifluridine

Trifluridine (5-trifluoromethyl-2'-deoxyuridine) is a fluorinated pyrimidine nucleoside analogue that has *in vitro* inhibitory activity against HSV-1 and -2, CMV, and vaccinia virus; it also appears to have some inhibitory activity against certain adenoviruses (Carmine et al., 1982, Spector et al., 1983).

In its monophosphate form, trifluridine inhibits thymidylate synthetase irreversibly, while as a triphosphate, it competes with thymidine triphosphate for incorporation into DNA by DNA polymerases. Trifluridine is incorporated into both viral and cellular DNA. The antiviral mechanism of action of trifluridine involves inhibition of viral DNA synthesis by trifluridine triphosphate, which acts as a competitive inhibitor of viral DNA polymerase (Carmine et al., 1982).

The main clinical indication for trifluridine is in the treatment of primary and recurrent HSV infections of the cornea and conjunctiva (Kaufman 1988; Carmine et al., 1982). Topical trifluridine also appears to be clinically useful in the treatment of persistent cutaneous ulcers due to acyclovir-resistant HSV infections in patients with AIDS (Rossi et al., 1995).

1.4.2.3. Cidofovir

Cidofovir (1-[(S)-3-hydroxy-2-(phosphonomethoxy)-propyl]cytosine dihydrate) is a cytidine nucleotide analogue which belongs to a family of phosphonylmethoxyalkyl derivatives of purines and pyrimidines (Inouye et al., 2002). Cidofovir is active against a broad spectrum of herpes viruses, including important human pathogens such as cytomegalovirus (CMV), herpes simplex virus type 1 and 2 (HSV-1, HSV-2), varicella zoster virus (VZV), and Epstein-Barr Virus (EBV) [Lalezari JP et al., 1996].

Cidofivir is taken up by both virally infected and uninfected cells and does not require the action of a virus-induced kinase to be converted to its active moiety (Ho et al., 1996). Cidofovir is metabolized to its active diphosphate form by cellular enzymes, which acts as both a competitive inhibitor with respect to dCTP, and as a competitive inhibitor of the viral DNA polymerases. The diphosphate metabolite has been shown to competitively inhibit CMV and HSV DNA polymerases at concentrations 8- to 600-fold lower than that required for inhibiting human DNA polymerases (Hitchcock, 1996). The prolonged intracellular half-life (>48 h) of cidofovir diphosphate has permitted intermittent dosing regimens not previously possible for other anti-CMV agents (Inouye et al., 2002). Cidofovir can be administered intravenously, topically, and via ocular implant. Intravenous cidofovir is approved for the treatment of CMV retinitis in HIV-infected patients. It also holds promise for the treatment of acyclovir-resistant HSV infections, either by the intravenous route or topically (Lalezari et al., 1997), for the topical treatment of human papillomavirus infections in immunosuppressed and immunocompetent subjects, and for the systemic treatment of progressive multifocal leukoencephalopathy in HIV-infected patients receiving potent antiretroviral therapy (Snoeck et al., 1995).

1.4.3. Antiretroviral Pyrimidine Nucleosides

The design of nucleoside analogues that could combat DNA viruses such as herpes simplex virus type 1 or type 2, and RNA viruses such as those responsible for major respiratory diseases in humans, was the primary focus of antiviral drug development up to the early 1980's (Dolin, 1985). In the mid-1980's, a turning point in the design of effective antiviral agents occurred as a result of an epidemic of acquired immunodeficiency syndrome (AIDS), and the discovery of the human immunodeficiency virus (HIV) as its etiologic cause (Balimane and Sinko, 1999). To date, anti-AIDS drug development has lead to the availability of a number of drugs that act as inhibitors of viral protein processing and reverse transcription. Both nucleoside and non-nucleoside inhibitors of reverse transcriptase have been developed. The pyrimidine class of reverse transcriptase inhibitors includes several FDA approved drugs such as, zidovudine, stavudine, zalcitabine, and lamivudine (Figure 1.6) [Balimane and Sinko, 1999].

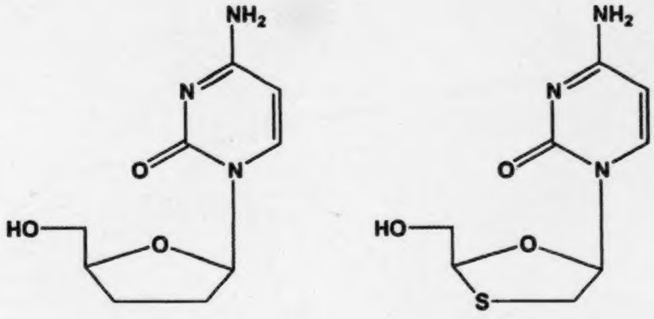

Zalcitabine (ddC) **Lamivudine (3TC)**

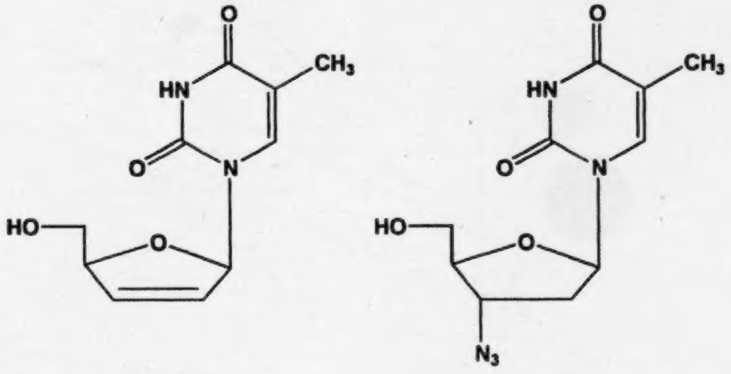

Stavudine (d4T) **Zidovudine (AZT)**

Figure 1.6. Structures of antiretroviral pyrimidine nucleosides

1.4.3.1. Zidovudine

The thymidine analogue, zidovudine (3'-azido-2',3'-dideoxythymidine; AZT) was the first drug approved for the treatment of acquired immunodeficiency syndrome (AIDS). Zidovudine passively diffuses into host lymphocytes, where it is phosphorylated to zidovudine mono- and diphosphate forms by cellular thymidine and thymidylate kinases, respectively. Zidovudine diphosphate is subsequently phosphorylated by a cellular nucleoside diphosphate kinase to the active zidovudine-5-triphosphate (Furman et al., 1986). The diphosphorylation of zidovudine appears to be the rate-limiting step, as reflected by intracellular accumulation of zidovudine monophosphate due to inhibition of thymidylate kinase. Zidovudine triphosphate acts as a competitive substrate for the HIV reverse transcriptase and is incorporated into the elongating 3' end of the yet-unintegrated proviral DNA, resulting in the premature termination of chain elongation. The antiviral specificity of zidovudine stems from its 100-fold greater selectivity for HIV-1 reverse transcriptase than for cellular polymerases such as DNA polymerase α. However, zidovudine triphosphate is known to weakly inhibit cellular DNA polymerase α and mitochondrial polymerase-γ, while its monophosphate form competitively inhibits cellular thymidylate kinase, an effect that reduces the levels of intracellular thymidine triphosphate. These latter effects may at least partially account for AZT's cytotoxicity and adverse effects (Furman et al., 1986).

As a S-phase specific enzyme, thymidine kinase required for zidovudine phosphorylation has increased activity in stimulated rather than resting cells.

Consequently, zidovudine has been found to be more potent in activated cells than in nonactivated cells (Chu et al., 1989).

Following intravenous administration (1 h infusion), zidovudine exhibits a rapid serum clearance with a β-phase $t_{1/2}$ of 0.9 to 1.4 h, which presumably reflects its rapid distribution into vascular and extravascular sites (Blum et al., 1988; Klecker et al., 1987). The plasma/serum half-life of the prodrug (zidovudine) is considerably shorter than the intracellular half-life of the active zidovudine 5-triphosphate (~3 h) [Blum et al., 1988]. Following oral administration, zidovudine is absorbed rapidly from the gastrointestinal tract and undergoes rapid first pass metabolism. Zidovudine is predominantly metabolized hepatically by a uridine diphosphoglucuronosyltransferse to its 5'-*O*-glucuronide, 3'-azido-3'-deoxy-5'-*O*-β-D-glucopyranuronosylthymidine (GAZT) [Good et al., 1986], which is subsequently excreted renally. Following an oral dose of zidovudine, approximately 75% of the dose is recovered in urine as GAZT and 14% as unchanged drug (Blum et al., 1988). The oral bioavailability of zidovudine (60 to 70%) is at least partially determined by the ability of individuals to perform first-pass glucuronidation to zidovudine-5'-*O*-glucuronide (Blum et al., 1988). The hepatic metabolism of zidovudine also leads to the formation of a minor but cytotoxic metabolite, 3'-amino-3'-deoxythymidine, which may be partially responsible for the adverse effects of zidovudine (Dudley, 1995).

As the first antiretroviral agent to show clinical efficacy in treating HIV infection, zidovudine has been intensively studied in numerous clinical trials and extensively used in clinical practice for treating adults and children with HIV infection. Its use is also approved for preventing prenatal transmission of virus in HIV-infected pregnant women (Connor et al., 1994) and is recommended for postexposure prophylaxis in HIV-exposed health-care workers (Cardo et al., 1997). Although its use as monotherapy is approved and has been shown to delay the progression of the disease (Kinloch-De loes et al., 1995), today zidovudine is most commonly used in combination with a second nucleoside reverse transcriptase inhibitor (lamivudine, stavudine, or didanosine) and either a protease inhibitor or a nonnucleoside reverse transcriptase inhibitor. Such triple drug combinations have shown greater and more durable clinical benefits compared to two-drug combinations or monotherapy (Hammer et al., 1997; Staszewski et al., 1999).

1.4.3.2. Stavudine

Stavudine (2',3'-didehydro-2',3'-dideoxythymidine; d4T) is a thymidine analogue that is active in vitro against both HIV type 1 and type 2 viruses (Sommadossi, 1995). The mechanism of action of stavudine is similar to that of zidovudine. Following passive diffusion into cells, stavudine is first phosphorylated by thymidine kinase to stavudine monophosphate. The latter is subsequently phosphorylated by thymidylate kinase and pyrimidine diphosphate kinase. Unlike zidovudine monophosphate, stavudine monophosphate does not accumulate in the cell and phosphorylation of stavudine to its monophosphate is the rate-limiting step of the sequential conversions of stavudine to its active triphosphate anabolite. Stavudine triphosphate competes with the natural substrate of HIV reverse transcriptase, 2'-deoxythymidine-5'-triphosphate. Since stavudine triphosphate lacks a 3'-OH group, formation of the 3'-5' phosphodiester bond that is essential for nucleotide elongation cannot occur and DNA chain elongation is stopped

(Ho and Hitchcock, 1989). As with zidovudine, stavudine is less active against HIV in quiescent cells due to its decreased phosphorylation by the cell-cycle-dependent thymidine kinase (Sommadossi, 1995).

Upon oral administration, stavudine exhibits a high oral bioavailability (82 to 86%) [Dudley et al., 1992]. The mean elimination half-life of stavudine is 1.6 h, with an intracellular half-life of 3 to 4 h. Renal excretion of unchanged drug accounts for 40% of stavudine elimination. Stavudine is also converted to thymine, which then enters the pyrimidine pool. Other miscellaneous metabolites of stavudine may also account for a small proportion of the eliminated drug (Cretton et al., 1993).

Stavudine is FDA-approved for treating patients with HIV infection, in combination with other antiretroviral agents. In patients with more than 6 months of zidovudine experience, a change to stavudine was found to be superior to continued zidovudine therapy, as it delayed clinical progression of the disease (Spruance et al., 1997). In three- and four-drug combination regimens that include stavudine plus other nucleoside reverse transcriptase inhibitors in combination with nonnucleoside reverse transcriptase inhibitors or protease inhibitors, durable suppression of viremia has been reported (Roca et al., 2000).

1.4.3.3. Zalcitabine

The cytidine analogue, zalcitabine (2',3'-dideoxycytidine; ddC) was the third nucleoside analogue to be approved for the treatment of HIV-1 infection in the United States and the first antiretroviral agent to be licensed through FDA's accelerated approval process. Zalcitabine is active against HIV-1, HIV-2, and hepatitis B viruses (Mitsuya et al., 1986; Dahlberg et al., 1987).

Zalcitabine enters cells via both carrier-mediated and non-carrier-mediated mechanisms (Cooney et al., 1986; Plageman et al., 1989), and is activated through a series of three phosphorylations by cellular kinases to the active triphosphate metabolite, dideoxycytidine-5'-triphosphate (Broder, 1990). Zalcitabine decreases the intracellular pools of deoxycytidine triphosphate, and its triphosphate terminates viral DNA elongation (Chen et al., 1991). Unlike zidovudine and stavudine, which are activated through the action of the S-phase specific enzyme, thymidine kinase, the enzymes responsible for zalcitabine activation are cell cycle independent, and phosphorylation is most efficient in resting cells (Gao et al., 1993).

Zalcitabine has a short plasma half-life of 0.34 h and its active triphosphate anabolite has an intracellular half-life of 2.6 h (Shelton et al., 1993). Zalcitabine exhibits a high oral bioavailability (> 80%) and is recovered mostly unchanged in urine (Gustavson et al., 1990).

When used as an initial drug therapy for AIDS, zalcitabine monotherapy has been shown to be inferior to zidovudine monotherapy (Bozzette et al., 1995). When used in combination with zidovudine, zalcitabine has been found to delay disease progression and to improve survival in zidovudine-naive subjects compared to zidovudine alone (Hammer et al., 1996). Overall, zalcitabine has played only a minor role in antiretroviral treatments, due to its limited in vivo potency, its toxicity profile, and its vulnerability to nucleoside cross-resistance (Inouye et al., 2002).

1.4.3.4. Lamivudine

Lamivudine is the (–) enantiomer of 2',3'-dideoxy-3'-thiacytidine, also referred to as 3TC. This cytidine analogue inhibits HBV DNA polymerase, and it also has antiretroviral activity against HIV viruses, as it inhibits HIV reverse transcriptase (Coates et al., 1992). Lamivudine enters cells by passive diffusion and is phosphorylated to its active metabolite, lamivudine triphosphate by cellular kinases. In HBV infected cells, lamivudine triphosphate competitively inhibits HBV DNA polymerase and causes chain termination. Similarly, in HIV infected cells, lamivudine triphosphate competitively inhibits viral reverse transcriptase, and interrupts proviral DNA chain elongation (Raffanti and Haas, 2001; Hayden et al., 2001).

Lamivudine is rapidly absorbed following oral administration, and has a high oral bioavailability (~80%) in adults (Johnson et al., 1999). The plasma half-life of lamivudine is approximately 2 to 4 hours, but the long intracellular half-life of its triphosphate (~17 h) has provided the basis for consideration of once-daily dosing regimens. Lamivudine is excreted primarily unchanged in the urine (~70%)[Gao et al., 1994; Heald et al., 1996, Yuen et al., 1995].

Lamivudine was initially used in humans for the treatment of HIV (Leeuwen et al., 1992). Clinical trials that employed lamivudine to treat patients with chronic HBV infections were carried out after completion of the HIV studies (Tyrrell et al., 1993; Dienstag et al., 1994). Lamivudine is FDA-approved for treating HIV infection in adults and children, in combination with other antiretroviral agents, to overcome the rapidly developing resistance to lamivudine monotherapy in treated patients (Inouye et al., 2002).

1.5. Pharmacokinetic Optimization of Treatments with Nucleoside Analogues

Characterization of pharmacokinetic attributes of a drug candidate, including its absorption profile and its distribution, metabolism, and elimination characteristics form an integral part of drug development. Many of the failures of drug candidates in development are due to their undesirable pharmacokinetic characteristics in humans. The pharmacokinetics of a lead compound would, therefore, have to be studied in detail and in several animal species, before it can be chosen as a development candidate. The pre-clinical pharmacokinetic data may then be used to predict the drug's absorption and disposition in humans (Lin, 1999). In today's drug discovery programs, accurate pharmacokinetic and metabolic data need to be available as early as when the results of the *in vitro* biological screening are obtained. The early evaluation of a drug candidate's pharmacokinetics and metabolism provides important feedback for rational drug design by medicinal chemists (Lin, 1999).

The primary mechanism of action for anticancer/antiviral nucleoside analogues is to disrupt target DNA synthesis within proliferating cancer cells or within replicating viruses. In order to be active, the nucleoside analogues must therefore reach their target cells, undergo cellular uptake, and then be efficiently phosphorylated to the 5'-triphosphate form by cellular or viral enzymes prior to incorporation into target DNA. The fate of nucleoside drugs, therefore, depends on the dose, route of administration, absorption, hepatic metabolism, and rate of elimination from blood, as well as, on rate of transport across plasma membranes and rate of intracellular phosphorylation and dephosphorylation. The final effect of nucleoside drugs ultimately depends on the ability of their active 5'-triphosphate derivatives to serve as substrates for incorporating enzymes such as reverse transcriptase and DNA polymerases. Since the activity and expression of the phosphorylating enzymes are in turn influenced by various factors including disease and/or immune status, large variability is expected for the pharmacokinetic evaluation and optimization of this class of compounds (Stretcher, 1995).

The common convention in cancer chemotherapy, as well as in the therapy of HIV infection, has been to use the highest tolerable dose to eradicate as many tumor cells as possible, and to achieve maximal inhibition of viral proliferation. Although this approach has proven valid in some cases, higher plasma concentrations of nucleosides do not necessarily correlate with higher intracellular concentrations of their active anabolites and a greater therapeutic effect (Back et al., 2001; Stretcher, 1995). Accordingly, it has been determined that in the treatment of some hematological cancers with nucleoside analogues, improved outcome and reduced toxicity can be achieved by monitoring nucleoside metabolites inside the target cells (Liliemark and Peterson, 1991). For instance, concentrations of cytarabine 5'-triphosphate in leukemic cells are predictive of remission in patients. However, concentrations of cytarabine 5'-triphosphate in leukemic cells are not any greater following high-dose cytarabine treatment (3 g/m^2) relative to an intermediate dose (1 g/m^2). This observation has been attributed to the saturable formation of the triphosphate anabolite in these cells (Plunkett and Gandhi, 1992).

Despite the limits of technologies developed to measure clinically relevant species and concentrations of nucleoside drugs, some progress has been made in understanding the relationships between pharmacokinetics and pharmacodynamics of these drugs. In cancer chemotherapy, it has been possible to individualize the chemotherapy dose *a priori* and *a posteriori*, based on the established relationships between systemic exposure to chemotherapy and response. Moreover, pharmacokinetic studies have played a major role in the development of various strategies to improve the therapeutic index of cancer chemotherapeutics (Masson and Zamboni, 1997).

Similar to anticancer nucleosides, dideoxynucleosides used in the treatment of HIV infection exhibit a narrow therapeutic window and a wide interpatient variability with respect to their pharmacokinetics. Thus, antiretroviral nucleosides appear to be good candidates for therapeutic drug monitoring. In practice, however, attempts to implement therapeutic drug monitoring for antiretroviral agents has been hindered by unspecific or surrogate measurements of antiviral efficacy and toxicity: While the primary endpoint of antiretroviral therapy is a reduction in mortality, the short-term effects are only measurable by monitoring various surrogate markers of the disease, such as CD4 counts, p24-antigenaemia and HIV viremia. Although assessment of the patient's health in terms of weight gain/ loss, energy levels, and the incidence of opportunistic infections, helps to monitor the clinical response to antiretroviral therapy, these measures are rather nonspecific endpoints that could be modulated by other factors such as chemoprophylaxis (Burger et al., 1995).

Moreover, it has been difficult to establish a relationship between plasma concentration and antiviral effect of antiretroviral nucleosides because it is the intracellular triphosphate form that constitutes the active moiety (Barry et al., 1996; Moore et al., 1999; Back et al[illegible]001). Although analytical methods for the measurement of intracellular triphosphates have recently been developed for some nucleosides, these methods require large volumes of blood from patients to be subjected to labour-intensive cell separation techniques, followed by analysis of the nucleoside triphosphate using a procedure that is only available in a few laboratories (Back et al, 2001). Thus, in the context of the large population studies that need to be conducted in order to investigate the pharmacokinetic-pharmacodynamic relationships of antiretroviral nucleosides, measurements of intracellular triphosphates of these agents is not a feasible option at this time (Back et al, 2001; Burger et al., 1995).

In view of the growing awareness among the clinical community of the potential benefits of pharmacokinetic optimization of nucleoside therapy, an increasingly greater role is being placed on pharmacokinetic and pharmacodynamic evaluations of nucleoside drugs. Improved dosage regimens would not only reduce the toxic side effects and improve the therapeutic outcomes, but would also reduce cost arising from non-optimized and excessive use of these drugs (Stretcher, 1995).

1.5.1. Dose-Dependent Pharmacokinetics and Nucleoside Therapy

Although the pharmacokinetics of most clinical drugs can be adequately described by first-order or linear processes, there are a number of important drugs that exhibit nonlinear pharmacokinetics either in their clinical dose range, or more frequently at higher doses (Lin, 1994). Both dose-related and time-dependent factors can cause non-linearity in the pharmacokinetic behavior of drugs, but only dose-dependent pharmacokinetics will be elaborated here. For drugs that follow linear disposition kinetics, the pharmacokinetic parameters describing drug absorption and elimination in the body do not change systematically with dose. In dose-dependent pharmacokinetics, however, pharmacokinetic parameters change with the size of dose administered or with dosing rate (Rowland and Tozer, 1995; Lin, 1994).

The presence of pharmacokinetic non-linearity often complicates the design of dosage regimens and prediction of efficicacy and toxicity. It is therefore important to study the influence of dose on the pharmacokinetics of new drugs and to investigate the causes of pharmacokinetic non-linearity when present (Lin, 1994).

A greater or less than proportional increase in the drug's area under the blood/plasma concentration-time curve (AUC) with increase in dose is the most commonly encountered manifestation of dose-dependent pharmacokinetics (Lin, 1994). Dose-dependent pharmacokinetics of a drug may come about as a result of non-linearity in any of the drug's pharmacokinetic processes including its absorption, distribution, metabolism and elimination. Nonlinear absorption or bioavailability may arise as a result of saturation of carrier-mediated transport mechanisms that are responsible for the passage of some drugs across gastrointestinal membranes. Other important mechanisms that can lead to nonlinear absorption include low aqueous solubility, saturation of presystemic metabolism, and dose-related changes in gastric emptying, gastrointestinal blood flow or motility (Ludden, 1991). Concentration-dependent plasma protein binding, saturable blood cell binding, and saturable tissue binding could result in dose-dependent pharmacokinetics due to nonlinear drug distribution. Finally, nonlinear elimination due to saturable hepatic metabolism and/or saturation of renal excretion is another important source of non-linearity in the pharmacokinetic behavior of certain drugs. Some of the mechanisms that are known to contribute to dose-dependencies in hepatic metabolism include depletion of various cofactors that are required for biotransformation reactions, inhibition of parent drug metabolism by its metabolites or "product inhibition", and drug-induced hepatotoxicity (Ludden, 1991; Lin, 1994).

The renal excretion of drugs and other substances is governed by four different processes: glomerular filtration, passive back diffusion, tubular secretion and tubular reabsorption. Of these processes, tubular secretion and tubular reabsorption are saturable as they involve carrier-mediated transport (van Ginneken and Russel, 1989). Many organic compounds are actively secreted via tubular secretion processes at a rate that increases in direct proportion to the plasma concentration until the transport approaches a limiting value, often referred to as T_M or maximum transport rate. Consequently, clearance by tubular secretion decreases as plasma concentration increases past the T_M Value (Rowland and Tozer, 1995). Saturable renal tubular secretion, however, rarely results in clinically significant non-linearities in plasma pharmacokinetics, as this process is usually accompanied by passive glomerular filtration and never occurs alone. With two competing pathways of elimination, only one of which is saturable, the non-linearity would only be apparent if the saturable pathway accounted for more than 30% of the overall elimination (van Rossum et al., 1974). The influence of saturable tubular secretion on plasma pharmacokinetics is further mitigated by the fact that many drugs are eliminated by non-renal pathways, in addition to the renal route (van Ginneken and Russel, 1989).

In cancer chemotherapy and antiretroviral therapy where high doses of drugs including nucleoside analogues are often administered, there is a greater theoretical possibility for occurrence of dose-dependent pharmacokinetics. Accordingly, dose-dependent pharmacokinetics have been observed more frequently for anticancer drugs than for other drugs. This is probably due to the fact that these drugs are studied over a wide range of doses during early evaluation and because high-dose cancer chemotherapy has been a common clinical approach (Powis et al., 1981).

Among nucleosides, dose-dependent pharmacokinetics have been reported for thymidine (Zaharko et al., 1979; Ensminger and Frei, 1978), 5-fluorouracil (Collins et al., 1980), arabinosyl cytosine (Dedrick et al., 1972), and 3-deazauridine (Benvenuto et al., 1979; Cysyk et al., 1978), as well as, for the antiviral nucleosides didanosine (Burger et al., 1995), carbovir (Brouwer et al., 1990), and acyclovir (Brigden and Whiteman 1985).

Saturation of elimination and/or uptake processes plays an important role in determining the occurrence of both toxic and therapeutic effects for drugs that exhibit dose-dependent pharmacokinetics. This is particularly relevant in the case of cytotoxic drugs including nucleoside analogues that have narrow therapeutic windows, and are capable of causing significant toxicity. It is therefore crucial to evaluate dose-range pharmacokinetics of new anticancer/antiviral drug candidates, in an attempt to design optimal dosage regimens and to evaluate their efficacy and toxicity.

1.6. References

Back DJ, Khoo SH, Gibbons SE, Merry C. The role of therapeutic drug monitoring in treatment of HIV infection. Br J Clin Pharmacol 2001;52:89S-96S.

Baldwin SA, Mackey JR, Cass CE, Young JD. Nucleoside transporters: Molecular biology and implications for therapeutic development. Mol Med Today 1999;5:216-224.

Balimane PV, Sinko PJ. Involvement of multiple transporters in the oral absorption of nucleoside analogues. Adv Drug Deliv Rev 1999;39:183-209.

Ban J, Weber G. Synergisitic action of tiazofurin and difluorodeoxycytidine on differentiation and cytotoxicity. Biochem Biophys Res Commun 1992;184:551-559.

Barry MG, Khoo SH, Veal GJ, Hoggard PG, Gibbons SE, Wilkins EGL, Williams O, Breckenridge AM, Back DJ. The effect of zidovudine dose on the formation of intracellular phosphorylated metabolites. AIDS 1996;10:1361-1367.

Benvenuto JA, Hall SW, Farquhar P, Stewart DJ, Benjamin RS, Loo TL. Pharmacokinetics and disposition of 3-deazauridine in humans. Cancer Res 1979;39:349-352.

Birnie GD, Kroeger H, Heidelberger C. Studies of fluorinated pyrimidines. XVIII. The degradation of 5-fluoro-2'-deoxyuridine and related compounds by nucleoside phosphorylase. Biochemistry 1963;2:566-572.

Blum MR, Liao SHT, Good SS, deMiranda P. Pharmacokinetics and bioavailability of zidovudine in humans. Am J Med 1988; 85(Suppl.2A):189-194.

Bouffard DY, Laliberte J, Momparler RL. Kinetic-studies on 2',2'-difluorodeoxycytidine (gemcitabine) with purified human deoxycytidine kinase and cytidine deaminase. Biochem Pharmacol 1993;45:1857-1861.

Bozzette SA, Kanouse DE, Berry S, Duan N. Health and function with zidovudine or zalcytabine as initial therapy for AIDS. A randomized controlled trial. Roche 3300/ACTG 114 Study Group. JAMA 1995;273:295-301.

Brigden D, Whiteman P. The clinical pharmacology of acyclovir and its prodrugs. Scand J Infect Dis 1985;47(Suppl.):33-39.

Broder S. Pharmacodynamics of 2',3'-dideoxycytidine: an inhibitor of human immunodeficiency virus. Am J Med 1990;88:2S-7S.

Brouwer KR, St. Clair RL, Lagarde J, Patanella JE, Walsh JS, Miwa GT. The pharmacokinetics of (–)-carbovir in rats. Drug Metab Dispos 1990;18:1078-1083.

Burger DM, Meenhorst PL, Beijnen JH. Concise overview of clinical pharmacokinetics of dideoxynucleoside antiretroviral agents. Pharmacy World & Science 1995;17:25-30.

Burris HA, Moore MJ, Andersen J, Green MR, Rothenberg ML, Madiano MR, Cripps MC, Portenoy RK, Storniolo AM, Tarassoff P, Nelson R, Dorr FA, Stephens CD, VanHoff DD. Improvements in survival and clinical benefit with gemcitabine as first-line therapy for patients with advanced pancreas cancer: A randomized trial. J Clin Oncol 1997;15:2403-2413.

Calabresi P, Cardoso SS, Finch SC, Kligerman MM, von Essen CF, Chu MY, Welch AD. Initial clinical studies with 5-iodo-2'-deoxyuridine. Cancer Res 1961;21:550-559.

Calabresi P, Chabner BA. Chemotherapy of neoplastic diseases. In: Goodman & Gilman "The pharmacological basis of therapeutics". Hardman JG, Limbird LE, Gilman A (editors). 10th edition, McGraw Hill (Health Professions Division); New York, 2001. pp. 1386-1459.

Calabresi P. Regional protection in cancer chemotherapy. I. Infusions of thymidine into external carotid artery of patients receiving systemic 5-iodo-2'-deoxyuridine. J Clin Invest 1962;41:1484-1491.

Camiener GW, Smith CG. Studies of the enzymatic deamination of cytosine arabinoside. I. Enzyme distribution and specific specificity. Biochem Pharmacol 1965;14:1405-1416.

Cardo DM, Culver DH, Ciesielski CA, Srivastava PU, Marcus R, Abiteboul D, Heptonstall J, Ippolito G, Lot F, McKibben PS, Bell DM. A case-control study of HIV seroconversion in health care workers after percutaneous exposure. Centers for Disease Control and Prevention Needlestick Surveillance Group. N Engl J Med 1997;337:1485-1490.

Carlow DA, Kerbel RS, Feltis JT, Elliott BE. Enhanced expression of class-I major histocompatibility complex gene (DK) products on immunogenic variants of a spontaneous murine carcinoma. J Natl Cancer Inst 1985;75:291-301.

Carmine AA, Brogden RN, Heel RC, Speight TM, Avery GS. Trifluridine: a review of its antiviral activity and therapeutic use in the topical treatment of viral eye infections. Drugs 1982;23:329-353.

Cass CE, Young JD, Baldwin SA, Cabrita MA, Graham KA, Griffiths M, Jennings LL, Mackey JR, Ng AM, Ritzel MW, Vickers MF, Yao SY. Nucleoside transporters of mammalian cells. In: Membrane transporters as drug targets. Vol 12. Amidon

GL and Sadee W (editors). Kluwer Academic/Plenum Publishers; New York, 1999. pp. 313-352.

Castellano D, Lianes P, Paz-Ares L, Hidalgo M, Guerra JA, Gomez-Martin C, Gomez H, Calzas J, Cortes-Funes H. A phase II study of a novel gemcitabine plus cisplatin regimen administered every three weeks for advanced non-small-cell lung cancer. Ann Oncol 1998;9:457-459.

Chabner BA, Drake JC, Johns DG. Deamination of 5-azacytidine by a human leukemia cell cytidine deaminase. Biochem Pharmacol 1973;22:2763-2765.

Chabner BA, Johns DG, Coleman CN, Drake JC, Evans WH. Purification and properties of cytidine deaminase from normal and leukemic granulocytes. J Clin Invest 1974;53:922-931.

Chaudhuri NK, Mukherjee KL, Heidelberger C. Studies of fluorinated pyrimidines. VII- the degradative pathway. Biochem Pharmacol 1959;1:328-341.

Chen CH, Vazquez-Padua M, Cheng YC. Effect of anti-human immunodeficiency virus nucleoside analogs on mitochondrial DNA and its implication for delayed toxicity. Mol Pharmacol 1991;39:625-628.

Chu CK, Schinazi RF, Ahn MK, Ullas GV, Gu ZP. Structure-activity relationships of pyrimidine nucleosides as antiviral agents for human immunodeficiency virus type 1 in peripheral blood mononuclear cells. J Med Chem 1989;32:612-617.

Cihak A, Lamar C, Pitot HC. Studies on the mechanism of the stimulation of tyrosine aminotransferase activity in vivo by pyrimidine analogs: the role of enzyme synthesis and degradation. Arch Biochem Biophys 1973;156:176-187.

Clarke RG, Lund EK, Johnson IT, Pinder AC. Apoptosis can be detected in attached colonic adenocarcinoma HT29 cells using annexin V binding, but not by TUNEL assay or sub-G_0 DNA content. Cytometry 2000;39:141-150.

Coates JA, Cammack N, Jenkinson HJ, Jowett AJ, Jowett MI, Pearson BA. (–)-2'-Deoxy-3'-thiacytidine is a potent, highly selective inhibitor of human immunodeficiency virus type 1 and type 2 replication in vitro. Antimicrob Agents Chemother 1992;36:733-739.

Collins JM, Dedrick RL, King FG, Speyer JL, Myers CE. Nonlinear pharmacokinetic models for 5-fluorouracil in man: intravenous and intraperitoneal routes. Clin Pharmacol Ther 1980;28:235-246.

Connor EM, Sperling RS, Gelber R, Kiselev P, Scott G, O'Sullivan MJ, VanDyke R, Bey M, Shearer W, Jacobson RL, Jimenez E, O'Neill E, Bazin B, Delfraissy J-F, Culnane M, Coombs R, Elkins M, Moye J, Stratton P, Balsley J. Reduction of maternal-infant transmission of human immunodeficiency virus type 1 with zidovudine treatment. Pediatric AIDS Clinical Trials Group protocol 076 Study Group. N Engl J Med 1994;331:1173-1180.

Cooney DA, Dalal M, Mitsuya H, McMahon JB, Nadkarni M, Balzarini J, Broder S, Johns DG. Initial studies on the cellular pharmacology of 2', 3'-dideoxycytidine, an inhibitor of HTLV-III infectivity. Biochem Pharmacol 1986;35:2065-2068.

Cretton EM, Zhou Z, Kidd LB, McClure HM, Kaul S, Hitchcock MJ. In vitro and in vivo disposition and metabolism of 3'-deoxy-2',3'-didehydrothymidine. Antimicorb Agents Chemother 1993;37:1816-1825.

Cysyk RL, Gormley PE, D'Anna ME, Adamson RH. The disposition of 3-deazauridine in mice. Drug Metab Dispos 1978;6:125-132.

Daher GC, Harris BE, Diasio RB. Metabolism of pyrimidine analogues and their nucleosides. Pharmacol Ther 1990;48:189-222.

Dahlberg JE, Mitsuya H, Blam SB, Broder S, Aaronson SA. Broad spectrum antiretroviral activity of 2',3'-dideoxynucleosides. Proc Natl Acad Sci USA 1987;84:2469-2473.

Darzynkiewicz Z, Juan G, Li X, Gorczyca W, Murakami T, Traganos F. Cytometry in cell necrobiology: Analysis of apoptosis and accidental cell death (necrosis). Cytometry 1997; 27:1-20.

Darzynkiewicz Z, Li X, Gong J, Hara S, Traganos F. Analysis of cell death by flow cytometry. In: Cell Growth and Apoptosis. Studzinski GP (editor). Oxford University press; New York, 1995. pp. 143-149.

Darzynkiewicz Z. Apoptosis in antitumor strategies: Modulation of cell cycle and differentiation. J Cell Biochem 1995;58:151-159.

Dedrick RL, Forrester DD, Ho DHW. In vitro-in vivo correlation of drug metabolism-deamination of 1-β-D-arabinofuranosylcytosine. Biochem Pharmacol 1972;21:1-16.

Diasio RB, Harris E. Clinical pharmacology of 5-fluorouracil. Clin Pharmacokinet 1989;16:215-237.

Dienstag JL, Perrillo RP, Schiff ER, Bartholomew M, Vicary C, Rubin M. Double-blind, randomized, 3-month, dose-ranging trial of lamivudine for chronic hepatitis B. Hepatology 1994;20:A199-A199 (Part 2).

Dive C, Hickmann JA. Drug-target interactions: Only the first step in the commitment to a programmed cell death? Br J Cancer 1991;64:192-196.

Dolin R. Antiviral chemotherapy and chemoprophylaxis. Science 1985;227:1296-1303.

Domin BA, Mahony WB, Zimmerman TP. Transport of 5-fluorouracil and uracil into human erythrocytes. Biochem Pharmacol 1993;46:503-510.

Dudley MN, Graham KK, Kaul S, Geletko S, Dunkle L, Browne M, Mayer K. Pharmacokinetics of stavudine in patients with AIDS or AIDS-related complex. J Infect Dis 1992;166:480-485.

Dudley MN. Clinical pharmacokinetics of nucleoside antiretroviral agents. J Infect Dis 1995;171:S99-S112.

Duschinsky R, Pleven E, Heidelberger C. The synthesis of 5-fluoropyrimidines. J Am Chem Soc 1957;79:4559-4560.

Ellison RR, Holland JF, Weil M, Jacquillat C, Boiron M, Bernard J, Sawitsky A, Rosner F, Gussoff B, Silver RT, Karanas A, Cuttner J, Spurr CL, Hayes DM, Blom J, Leone LA, Haurani F, Kyle R, Hutchison JL, Forcier RJ, Moon JH. Arabinosyl cytosine: A useful agent in the treatment of acute leukemia in adults. Blood 1968;32:507-523.

Endersen PC, Prytz PS, Aarbakke J. A new flow cytometric method for discrimination of apoptotic cells and detection of their cell cycle specificity through staining of F-actin and DNA. Cytometry 1995;20:162-171.

Ensminger WD, Frei E III. High-dose intravenous and hepatic artery infusions of thymdine. Clin Pharmacol Ther 1978;24:610-615.

Fadok VA, Voelker DR, Campbell PA, Cohen JJ, Bratton DL, Henson PM. Exposure of phosphatidylserine on the surface of apoptotic lymphocytes triggers recognition and removal by macrophages. J Immunol 1992;148:2207-2216.

Fernandes-Alnembri T, Takahashi A, Armstrong R, Krebs J, Fritz L, Tomaselli KJ, Wang L, Yu Z, Croce CM, Salveson G, Earnshaw WC, Litwack G, Alnemri ES. Mch3, a novel human apoptotic cysteine protease highly related to CPP32. Cancer Res 1995;55:6045-6052.

Fisher DE. Apoptosis in cancer therapy: Crossing the threshold. Cell 1994;78:539-542.

Friedman S. The inhibition of DNA (cytosine-5)methylases by 5-azacytidine: the effect of azacytosine containing DNA. Mol Pharmcol 1981;19:314-320.

Furman PA, Fyfe JA, St. Clair MH, Weinhold K, Rideout JL, Freeman GA, Lehrman SN, Bolognesi DP, Broder S, Mitsuya H, Barry DW. Phosphorylation of 3'-azido-3'-deoxythymidine and selective interaction of the 5'-triphosphate with human immunodeficiency virus reverse transcriptase. Proc Natl Acad Sci USA 1986;83:8333-8337.

Gao WY, Agbaria R, Driscoll JS, Mitsuya H. Divergent antihuman immunodeficiency virus activity and anabolic phosphorylation of 2', 3'-dideoxynucleoside analogs in resting and activated human cells. J Biol Chem 1994;269:12633-12638.

Gao WY, Shirasaka T, Johns DG, Broder S, Mitsuya H. Differential phosphorylation of azidothymidine, dideoxycytidine, and dideoxyinosine in resting and activated peripheral blood mononuclear cells. J Clin Investig 1993;91:2326-2333.

Glazer RI, Peale AL, Beisler JA, Abbasi MM. The effect of 5-azacytidine and dihydro-5-azacytidine on nuclear ribosomal RNA and poly(A) RNA synthesis in L1210 cells in vitro. Mol Pharmacol 1980;17:111-117.

Good SS, Durack DT, de Miranda P. Biotransformation in various species and in humans of 3'-azido-3'-deoxythymidine, a potential agent for the treatment of AIDS. Fed Proc 1986;45:444.

Gourdeau H, Clarke ML, Ouellet F, Mowles D, Selner M, Richard A, Lee N, Mackey JR, Young JD, Jolivet J, Lafreniere RG, Cass CE. Mechanisms of uptake and resistance to troxacitabine, a novel deoxycytidine nucleoside analogue, in human leukemic and solid tumor cell lines. Cancer Res 2001;61:7217-7224.

Grem JL. 5-Fluoropyrimidines. In cancer chemotherapy and biotherapy: Principles and practice. Chabner BA, Longo DL (editors). 3rd edition, Lippincott Williams & Wilkins Publishers; Philadelphia, 2001. pp.186-88.

Griffith DA, Jarvis SM. Nucleoside and nucleobase transport systems of mammalian cells. Biochim Biophys Acta 1996;1286:153-181.

Gustavson LE, Fukuda EK, Rubio FA, Dunton AW. A pilot study of the bioavailability and pharmacokinetics of 2', 3'-dideoxycytidine in patients with AIDS or AIDS-related complex. J Acquir Immune Defic Syndr 1990;3:28-31.

Hammer SM, Katzenstein DA, Hughes MD, Gundacker H, Schooley RT, Haubrich RH. A trial comparing nucleoside monotherapy with combination therapy in HIV-infected adults with CD4 cell counts from 200 to 500 per cubic millimeter. AIDS Clinical Trials Group Study 175 Study Team. N Engl J Med 1996;335:1081-1090.

Hammer SM, Squires KE, Hughes MD, Grimes JM, Demeter LM, Currier JS, Eron JJ Jr, Feinberg JE, Balfour HH Jr, Deyton LR, Chodakewitz JA, Fischl MA. A controlled trial of two nucleoside analogues plus indinavir in persons with human immunodeficiency virus infection and CD4 cell counts of 200 per cubic millimeter or less. AIDS Clinical Trials Group 320 Studt Team. N Engl J Med 1997;337:725-733.

Hart JS, Ho DH, George SL, Salem P, Gottlieb JA, Frei EI. Cytokinetic and molecular pharmacology studies of arabinosylcytosine in metastatic melanoma. Cancer Res 1972;22:2763-2765.

Hartmann KV, Heidelberger C. Studies on fluorinated pyrimidines XIII. Inhibition of thymidylate synthetase. J Biol Chem 1961;236:3006-3013.

Hayden FG. Antimicrobial agents. In: Goodman & Gilman "The pharmacological basis of therapeutics". Hardman JG, Limbird LE, Gilman A (editors). 10th edition, McGraw Hill (Health Professions Division); New York, 2001. pp. 1313-1336.

Heald AE, Hsyu PH, Yuen GJ, Robinson P, Mydlow P, Barlett JA. Pharmacokinetics of lamivudine in human immunodeficiency virus-infected patients with renal dysfunction. Antimicrob Agents Chemother 1996;40:1514-1519.

Heggie GD, Sommadossi JP, Cross DS, Huster WJ, Diasio RB. Clinical pharmacokinetics of 5-fluorouracil and its metabolites in plasma, urine, and bile. Cancer Res 1987;47:2203-2206.

Heinemann V, Xu YZ, Chubb S, Sen A, Hertel LW, Grindey GB, Plunkett W. Inhibition of ribonucleotide reduction in CCRF-CEM cells by 2',2'-difluorodeoxycytidine. Mol Pharmacol 1990;38:567-572.

Hercbergs A, Leith JT. Spontaneous remission of metastatic lung cancer following myxedema coma- an apoptosis related phenomenon? J Natl Cancer Inst 1993;85:1342-1344.

Hertel LW, Boder GB, Kroin JS, Rinzel SM, Poore GA, Todd GC, Grindey GB. Evaluation of the antitumor-activity of gemcitabine (2',2'-difluoro-2'-deoxycytidine)
Cancer Res 1990;50:4417-4422.

Hertel LW, Kroin JS, Misner JW, Tustin JM. Synthesis of 2-deoxy-2,2-difluoro-D-ribose and 2-deoxy-2,2-difluoro-D-ribofuranosyl nucleosides. J Org Chem 1988;53:2406-2409.

Hickman JA. Apoptosis induced by anticancer drugs. Cancer Metastasis Rev 1992;11: 121-139.

Hitchcock MJ, Jaffe HS, Martin JC, Stagg RJ. Cidofovir, a new agent with potent anti-herpesvirus activity. Antivir Chem Chemother 1996;7:115-127.

Ho HT, Woods KL, Bronson JJ, DeBoeck H, Martin JC, Hitchcock MJ. Intracellular metabolism of the antiherpes agent (s)-1-[3-hydroxy-2-(phosphonylmethoxy)propyl]cytosine. Mol Pharmacol 1992;41:197-202.

Horber DH, Ballmoos P, Schott H, Schwendener RA. Cell cycle-dependent cytotoxicity and induction of apoptosis by liposomal N^4 –hexadecyl-1-β-D-arabinofuranosylcytosine. Br J Cancer 1995;72:1067-1073.

Huang P, Plunkett W. Induction of apoptosis by gemcitabine. Semin Oncol 1995;22:19-25.

Huang P, Chubb S, Hertel LW, Grindey GB, Plunkett W. Action of 2',2'-difluorodeoxycytidine on DNA-synthesis. Cancer Res 1991; 51:6110-6117.

Huang P, Robertson LE, Wright S, and Plunkett W. High molecular weight DNA fragmentation: a critical event in nucleoside analogue induced apoptosis in leukemia cells. Clin Cancer Res 1995;1:1005-1013.

Inouye RT, Panther LA, Hay CM, Hammer SM. Antiviral agents. In: Clinical Virology. Richman DD, Whitley RJ, and Hayden FG (editors). 2nd edition, ASM Press; Washington, D.C., 2002. pp. 171-227.

Jeggo PA, Holliday R. Azacytidine-induced reactivation of a DNA-repair gene in Chinese-hamster ovary cells. Mol Cell Biol 1986;6:2944-2949.

Johnson MA, Moore KH, Yuen GJ, Bye A, Pakes GE. Clinical pharmacokinetics of lamivudine. Clin Pharmacokinet 1999;36:41-66.

Johnson SA. Nucloeside analogues in the treatment of haematological malignancies. Expert Opin Pharmacother 2001;2:929-943.

Jones PA, Taylor SM, Mohandas T, Shapiro LJ. Cell cycle-specific reactivation of an inactive X-chromosome locus by 5-azadeoxycytidine. Proc Natl Acad Sci USA 1982;79:1215-1219.

Karon M, Shirakawa S. The locus of action of 1-β-D-arabinofuranosylcytosine in the cell cycle. Cancer Res 1969;29:687-696.

Kaufman D, Chabner BA. Clinical strategies for cancer treatment: The role of drugs. In: Cancer chemotherapy and biotherapy. Chabner BA, Longo DL (editors). 2nd edition, Lippincott-Raven Publishers; Philadelphia, 1996. pp. 1-4.

Kaufman HE. The treatment of herpetic eye infections with trifluridine and other antivirals. In: Clinical Use of Antiviral Drugs. De Clercq E (editor). Nijhoff; Boston, 1988. pp. 25-38.

Kerr JFR, Winterford CM, Harmon BV. Apoptosis-its significance in cancer and cancer therapy. Cancer 1994;73:2013-2026.

Kinloch-De Loes S, Hirschel BJ, Hoen B, Cooper DA, Tindall B, Carr A. A controlled trial of zidovudine in primary human immunodeficiency virus infection. N Engl J Med 1995;333:408-413.

Klecker RW, Collins JM, Yarchoan R, Thomas R, Jenkins JF, Broder S, Myers CE. Plasma and cerebrospinal fluid pharmacokinetics of 3'-azido-3'-deoxythymidine: a novel pyrimidine analog with potential application for the treatment of patients with AIDS and related diseases. Clin Pharmacol Ther 1987;41:407-412.

Laidlaw IJ, Potten CS. Reduction in apoptosis relative to mitosis in histologically normal epithelium accompanies fibrocystic change and carcinoma of the premenopausal human breast. J Pathol 1992;167:25-32.

Lalezari J, Schacker T, Feinberg J, Gathe J, Lee S, Cheung T. A randomized, double-blind, placebo-controlled trial of cidofovir gel for the treatment of acyclovir-unresponsive mucocutaneous herpes simplex virus infection in patients with AIDS. J Infect Dis 1997;176:892-898.

Lalezari JP, Stagg RJ, Jaffe HS, Hitchcock MJ, Drew WL. A preclinical and clinical overview of the nucleotide-based antiviral agent cidofovir (HPMPC). Adv Exp Med Biol 1996;394:105-115.

Lazebnik YA, Kaufman SH, Desnoyers S, Poirier GG, Earnshaw WC. Cleavage of poly(ADP-ribose) polymerase by a proteinase with properties like ICE. Nature 1994;371:346-347.

Li LH, Olin EJ, Buskirk HH, Reineke LM. Cytotoxicity and mode of action of 5-azacytidine on L1210 leukemia. Cancer Res 1970;30:2760-2769.

Liliemark J, Peterson C. Pharmacokinetic optimization of anticancer therapy. Clin Pharmacokinet 1991;21:213-231.

Lin JH. Dose-dependent pharmacokinetics: Experimental observations and theoretical considerations. Biopharm Drug Dispos 1994;15:1-31.

Lin JH. Role of pharmacokinetics in the discovery and development of indinavir. Adv drug deliv rev 1999;39:33-49.

Lippe P, Tummarello D, Monterubbianesi MC, Silva RR, Giuliodori L, Mari D, Santo A, Pasini E, Cetto GL, Rossi D, Porfiri E, Cascinu S, Cellerino R. Weekly gemcitabine and cisplatin in advanced non-small-cell lung cancer: A phase II study. Ann Oncol 1999;10: 217-221.

Liteplo RG, Alvarez E, Frost P, Kerbel RS. Induction of thymidine kinase-activity in a spontaneously enzyme-deficient murine tumor-cell line by exposure in vivo to the DNA-hypomethylating agent 5-aza-2'-deoxycytidine - implications for mechanisms of tumor progression. Cancer Res 1985;45: 5294-5298.

Ludden TM. Nonlinear pharmacokinetics. Clinical implications. Clin Pharmacokinet 1991;20:429-446.

Lyer L, Ratain MJ. 5-Fluorouracil pharmacokinetics: Causes for variability and strategies for modulation in cancer chemotherapy. Cancer Investig 1999;17:494-506.

Mackey JR, Mani RS, Selner M, Mowles D, Young JD, Belt JA, Crawford CR, Cass CE. Functional nucleoside transporters are required for gemcitabine influx and manifestation of toxicity in cancer cell lines. Cancer Res 1998;58:4349-4357.

Majno G, Joris I. Apoptosis, oncosis and necrosis. An overview of cell death. Am J Pathol 1995;146:3-16.

Major PP, Egan EM, Herrick DJ, Kufe DW. Effect of Ara-C incorporation on deoxyribonucleic-acid synthesis in cells. Biochem Pharmacol 1982;31:2937-2940.

Masson E, Zamboni WC. Pharmacokinetic optimization of cancer chemotherapy. Effect on outcomes. Clin Pharmacokinet 1997;32:324-343.

Mauro DJ, De Riel JK, Tallarida R J, Sirover MA. Mechanisms of excision of 5-fluorouracil by uracil DNA glycosylase in normal human cells. Mol Pharmacol 1993;43:854-857.

Mikita T, Beardsley GP. Functional consequences of the arabinosylcytosine structural lesion in DNA. Biochemistry 1988;27:4698-4705.

Mitsuya H, Border S. Inhibition of the in vitro infectivity and cytopathic effect of human T-lymphotrophic virus type III/lymphadenopathy-associated virus (HTLV-III/LAV) by 2',3'-dideoxynucleosides. Proc Natl Acad Sci USA 1986;83:1911-1915.

Moore KHP, Barrett JE, Shaw S, Pakes GE, Churchus R, Kapoor A, Lloyd J, Barry MG, Back D. The pharmacokinetics of lamivudine phosphorylation in peripheral blood mononuclear cells from patients infected with HIV-1. AIDS 1999;13:2239-2250.

Moore MJ, Erlichman C. Pharmacology of anticancer drugs. In: The basic science of oncology. Tannock IF, Hill RP (editors). 3rd edition, McGraw-Hill Inc.; New York, 1998. pp.379-381.

Murakami T, Xun L, Gong J, Bhatia U, Traganos F, Darzynkiewicz Z. Drug concentration-dependent differences in cell cycle specificity. Cancer Res 1995;55:3093-3098.

Plagemann PG, Woffendin C. Dideoxycytidine permeation and salvage by mouse leukemia cells and human erythrocytes. Biochem Pharmacol 1989;38:3469-3475.

Plunkett W, Gandhi V. Pharmacokinetics of arabinosylcytosine. J Infusion Chemother 1992;2:169-176.

Plunkett W, Huang P, Searcy CE, Gandhi V. Gemcitabine: Preclinical pharmacology and mechanisms of action. Semin Oncol 1996;23:3-15 (Suppl 10).

Potten CS, Merrit A, Hickman J, Hall P, Faranda A. Characterization of radiation-induced apoptosis in the small intestine and its biological significance. Int J Radiat Biol 1994;65:71-78.

Powis G, Ames MM, Kovach JS. Dose-dependent pharmacokinetics and cancer chemotherapy. Cancer chemother pharmacol 1981;6:1-9.

Prusoff WH. Synthesis and biological activities of iododeoxyuridine, an analog of thymidine. Biochim Biophys Acta 1959;32:295-296.

Prusoff WH. Idoxuridine or how it all began. In: Clinical use of antiviral drugs. De Clercq E (editor). Nijhoff; Boston, 1988. pp. 15-24.

Raffanti S, Haas DW. Antimicrobial agents. In: Goodman & Gilman "The pharmacological basis of therapeutics". Hardman JG, Limbird LE, Gilman A (editors). 10th edition, McGraw Hill (Health Professions Division); New York, 2001. pp. 1349-1373.

Reed JC. Bcl-2 and the regulation of programmed cell death. J Cell Biol 1994;124:1-6.

Richardson B, Kahn L, Lovett EJ, Hudson J. Effect of an inhibitor of DNA methylation on T-cells .1. 5-Azacytidine induces T4 expression on T8+ T-cells. J Immunol 1986;137:35-39.

Ritzel MW, Ng AM, Yao SY, Graham K, Loewen SK, Smith KM, Hyde RJ, Karpinski E, Cass CE, Baldwin SA, Young JD. Recent molecular advances in studies of the concentrative Na^+-dependent nucleoside transporter (CNT) family: identification and characterization of novel human and mouse proteins (hCNT3 and mCNT3) broadly selective for purine and pyrimidine nucleosides (system *cib*). Mol Membr Biol 2001;18:65-72.

Roca B, Gomez CJ, Arnedo A. A randomized, comparative study of lamivudine plus stavudine, with indinavir or nelfinavir, in treatment-expereinced HIV-infected patients. AIDS 2000;14:157-161.

Rockwell S, Grindey GB. Effect of 2',2'-difluorodeoxycytidine on the viability and radiosensitivity of EMT 6 cells in vitro. Oncol Res 1992;4:151-155.

Rossi S, Whitfeld M, Berger TG. The treatment of acyclovir-resistant herpes zoster with trifluorothymidine and interferon alfa. Arch Dermatol 1995;131:24-26.

Rowland M, Tozer TN. In: Clinical Pharmacokinetics: Concepts and Applications, 3rd edition. Williams & Wilkins; Baltimore, 1995. pp. 394-419.

Shelton MJ, O'Donnell AM, Morse GD. Zalcitabine. Ann Pharmacother 1993;27:480-489.

Silvestri DL, Corey L, Holmes KK. Ineffectiveness of topical idoxuridine in dimethylsulfoxide for therapy for genital herpes. JAMA 1982;248:953-959.

Snoeck R, Van Ranst M, Andrei G, De Clercq E, De Wit S, Poncin M. Treatment of anogenital papillomavirus infections with an acyclic nucleoside phosphonate analogue. N Engl J Med 1995;333:943-944.

Sommadossi JP. Comparison of metabolism and in vitro antiviral activity of stavudine versus other 2',3'-dideoxynucleoside analogues. J Infect Dis 1995;171(Suppl 2):S88-S92.

Sorm F, Piskala A, Cihak A, Vesely J. 5-Azacytidine, a new, highly effective cancerostatic. Experientia 1964;20:202-203.

Spector RA, Kati WM, Anderson KS, Johnson KA. Inhibition of human cytomegalovirus by trifluorothymidine. Antimicrob Agents Chemother 1983;23:113-118.

Spruance SL, Pavia AT, Mellors JW, Murphy R, Gathe J, Stool E, Jemsek JG, Dellamonica P, Cross A, Dunkle L. Clinical efficacy of monotherapy with stavudine compared with zidovudine in HIV-infected zidovudine experienced patients. A randomized, double-blind, controlled trial. Bristol-Myers Squibb Stavudine/019 Study Group. Ann Intern Med 1997;126:355-363.

Spruance SL, Stewart JC, Freeman DJ, Brightman VJ, Cox JL, Wenerstrom G. Early application oftopical 15% idoxuridine in dimethylsulfoxide shortens the course of herpes simplex labialis: a multicenter placebo-controlled trial. J Infect Dis 1990;161:191-197.

Stadler WM, Murphy B, Kaufman D. Phase II trial of gemcitabine (GEM) plus cisplatin (CDDP) in metastatic urothelial cancer (UC). Proc Annu Meet Am Soc Clin Oncol 1997;16:A1152(abst).

Stallings RL, Crawford BD, Tobey RA, Tesmer J, Hildebrand CE. 5-Azacytidine-induced conversion to cadmium resistance correlates with early S-phase replication of inactive metallothionein genes in synchronized CHO cells. Somat Cell Mol Genet 1986;12:423-432.

Staszewski S, Morales-Ramirez J, Tashima KT, Rachlis A, Skiest D, Stanford J, Stryker R, Johnson P, Labriola DF, Farina D, Manion DJ, Ruiz NM. Efavirenz plus zidovudine and lamivudine, efavirenz plus indinavir, and indinavir plus zidovudine and lamivudine in the treatment of HIV-1 infection in adults. Study 006 Team. N Engl J Med 1999;341:1865-1873.

Stretcher B. Pharmacokinetic optimisation of antiretroviral therapy in patients with HIV infection. Clin Pharmacokinet 1995;29:46-65.

Tattersall MH, Ganeshaguru K, Hoffbrand AV. Mechanisms of resistance of human acute leukemia cells to cytosine arabinoside. Br J Haematol 1974;27:39-46.

Uchida M, Brown N, Ho DHW. Enzymatic conversion of 5-fluoro-2'-deoxyuridine to 5-fluorouracil or 5-fluoro-2'-deoxyuridine-5'-monophosphate in human tissues. Anticancer Res 1990;10:779-783.

Van Ginneken CAM, Russel FGM. Saturable pharmacokinetics in the renal excretion of drugs. Clin Pharmacokinet 1989;16:38-54.

Van Leeuwen R, Lange JM, Hussey EK, Donn KH, Hall ST, Harker AJ, Jonker P, Danner SA. The safety and pharmacokinetics of a reverse transcriptase inhibitor, 3TC, in patients with HIV infection: a phase I study. AIDS 1992;6:1471-1475.

Van Rossum JM, Van Ginneken CAM, Henderson PTH, Ketelaars HCJ, Vree TB. Pharmacokinetics of biotransformation. In: Kinetics of drug action, handbook of experimental pharmacology. Van Rossum JM (editor). Vol 47, Springer; Berlin, 1974. pp. 125-167.

Vaux DL. Toward an understanding of the molecular mechanisms of physiological cell death. Proc Natl Acad Sci USA 1993;90:786-789.

Vesely J, Cihak A. 5-Azacytidine - mechanism of action and biological effects in mammalian cells. Pharmacol Ther (Part A) 1978;2:813-840.

Vogler WR, Miller DS, Keller JW. 5-Azacytidine (NSC 102816): a new drug for the treatment of myeloblastic leukemia. Blood 1976;48:331-337.

Von Hoff DD, Slavik M, Muggia FM. 5-Azacytidine. A new anticancer drug with effectiveness in acute myelogenous leukemia. Ann Intern Med 1976;85:237-245.

Weaver VM, Lach B, Walker PR, Sikorska M. Role of proteoplysis in apoptosis: Involvement of serine proteases in internucleosomal DNA fragmentation in immature lymphocytes. Biochem Cell Biol 1993;71:488-500.

Wingard LB, Brody TM, Larner J, Schwartz A. Neoplastic cells: Drugs affecting cell growth and viability. In: Human pharmacology: molecular-to-clinical. Kist K (editor). 1st edition, Mosby-Year Book Inc.; Missouri, 1991(a). pp. 589-591.

Wingard LB, Brody TM, Larner J, Schwartz A. Neoplastic cells: Drugs affecting cell growth and viability. In: Human pharmacology: molecular-to-clinical. Kist K (editor). 1st edition, Mosby-Year Book Inc.; Missouri, 1991(b). pp. 720.

Wohlhueter RM, McIvor RS, Plagemann PGW. Facilitated transport of uracil and 5-fluorouracil, and permeation of orotic acid into cultured mammalian cells. J Cell Physiol 1980;104:309-319.

Wyllie AH, Kerr JF, Currie AR. Cell death, the significance of apoptosis. Int Rev Cytol 1980;68:251-306.

Yao SY, Ng AM, Loewen SK, Cass CE, Baldwin SA, Young JD. An ancient prevertebrate Na^+-nucleoside cotransporter (hfCNT) from the pacific hagfish (*Eptatretus stouti*). Am J Physiol 2002; 283:C155-C168.

Yuasa H, Matsuhisa E, Watanabe J. Intestinal brush border transport mechanisms of 5-fluorouracil in rats. Biol Pharm Bull 1996;19:94-99.

Yuen GJ, Morris DM, Mydlow PK, Haidar S, Hall ST and Hussey EK. Pharmacokinetics, absolute bioavailability, and absorption characteristics of lamivudine. J Clin Pharmacol 1995;35:1174-1180.

Zaharko DS, Botter BJ, Chiuten D, Wiernik PH. Pharmacokinetic studies during phase I trials of high-dose thymidine infusions. Cancer Res 1979;398:4777-4781.

Zimmerman TP, Mahony WB, Prus KL. 3'-Azido-3'-deoxythymidine. An unusual nucleoside analogue that permeates the membrane of human erythrocytes and lymphocytes by nonfacilitated diffusion. J Biol Chem 1987;262:5748-5754.

2. Objectives

The main objective of this thesis research was to evaluate physiochemical and pharmacokinetic properties of representative members of two new classes of pyrimidine nucleoside analogues recently synthesized for evaluation as anticancer/antiviral agents. The investigated analogues consist of selected 5-substituted derivatives of 1-(2-deoxy-β-D-ribofuranosyl)-2,4-difluorobenzene and 1-(2,3-dideoxy-3-nitrooxy-β-D-ribofuranosyl) uracil. The latter has a nitric oxide (NO) donor moiety at the 3' position of the sugar ring and the former is an isosteric analogue of deoxythymidine.

2.1. Evaluation of the novel synthetic *C*-nucleoside, 1-(2-Deoxy-β-D-ribofuranosyl)-2,4-difluoro-5-iodobenzene (5-IDFPdR)

1-(2-Deoxy-β-D-ribofuranosyl)-2,4-difluoro-5-iodobenzene (5-IDFPdR, MW: 356) is one of several unnatural 1-(2-deoxy-β-D-ribofuranosyl)-2,4-difluoro-5-substituted-benzenes recently synthesized for evaluation as anticancer, antiviral, and/or diagnostic imaging agents (see Figure 3.1). This class of *C*-nucleosides was designed to exploit several potential advantages relative to classical 5-substituted-2'-deoxyuridines, including stability towards phosphorolysis by pyrimidine phosphorylase, increased lipophilicity that may improve their ability to cross the blood-brain-barrier, and a greater resistance towards catabolism and deiodination.

The objectives of this study were to determine lipophilicity, in vitro enzyme stability, protein binding, and in vivo pharmacokinetic properties of 1-(2-deoxy-β-D-ribofuranosyl)-2,4-difluoro-5-iodobenzene (5-IDFPdR), which was designed to serve as a novel *C*-nucleoside mimic of IUdR. In addition to the in vitro physiochemical and in vivo pharmacokinetic studies, the cytotoxicity of 5-IDFPdR was assessed in a variety of cancer cell lines and its induced cell-cycle effects were studied in a murine tumor cell line (KBALB) using flow cytometry. Moreover, the results of antiviral evaluations of 5-IDFPdR in a variety of antiviral assay systems [HSV-1, HSV-2, varicella-zoster virus (VZV), vaccinia virus, vesicular stomatitis, cytomegalovirus (CMV) and human immunodeficiency viruses (HIV-1 & HIV-2)] are summarized.

2.2. Evaluation of 5-iodo-3'-*O*-nitro-2'-deoxyuridine (INUdR), a novel nitric oxide (NO)-releasing 5-iodo-2'-deoxyuridine (IUdR) prodrug

NO-donor pyrimidine nucleoside hybrids have a number of desirable features. While released NO could exert antitumor or antiviral activity by itself, the nucleoside component of these hybrid drugs is expected to synergistically enhance the cytotoxic or antiviral effects of these compounds. The 5'-monophosphate of the nucleoside component could irreversibly inhibit thymidylate synthase (TS), while the nucleoside 5'-triphosphate could inhibit DNA chain elongation by serving as an unnatural substrate for, or an inhibitor of, DNA polymerase. Accordingly, a number of 5-substituted-2'-deoxyuridines, having a NO-donor moiety on the sugar ring were recently synthesized for evaluation as anticancer and/or antiviral agents. These included a group of 3'-*O*-nitro-2'-deoxyuridines (see Figure 4.1), 3'-*O*-nitro-2'-deoxycytidines, and 5'-*O*-nitro-2'-deoxyuridines. The objectives of this study were to evaluate lipophilicity, in vitro enzyme stability, protein binding, in vitro nitric oxide release, and in vivo pharmacokinetic properties of INUdR, as a 3'-*O*-nitro-substituted mimic of IUdR. Furthermore, the results of INUdR cytotoxicity and antiviral evaluations are summarized.

Evaluation of 1-(2-Deoxy-β-D-ribofuranosyl)-2,4-difluoro-5-iodobenzene (5-IDFPdR), an Unnatural *C*-Nucleoside Mimic of Thymidine, as a Potential Anticancer/Antiviral Agent

---

Versions of this chapter have been published: "Biopharmaceutics & Drug Disposition", 2002, or in press: "Biopharmaceutics & Drug Disposition", 2003.

3. *C*-Nucleosides and their versatile applications

3.1. Introduction

The biological importance of many naturally occurring *C*- nucleosides has prompted considerable interest in the exploration of synthetic routes to produce not only these nucleosides but also structurally related analogues. *C*- nucleosides are nucleosides in which the anomeric carbon of the sugar moiety is attached directly to a carbon atom (rather than nitrogen) in the aglycone portion of the nucleoside. There have been numerous strategies developed for the successful synthesis of naturally occurring *C*-nucleosides, such as pseudouridine, showdomycin, formycin, pyrazomycin, and several structural congeners, many of which exhibit antitumor, antibacterial, antifungal or antiviral activity (Lerch et al., 1971; Brown et al., 1968; Kalvoda et al., 1970; Barton et al., 1990; Buchanan et al., 1991; Farkas et al., 1972).

In view of the remarkable biological activities exhibited by natural *C*-nucleosides, a large number of unnatural *C*-nucleosides containing substituted and unsubstituted heteroaromatics, such as pyrroles, pyridines, quinolines, imidazoles, pyrazoles, and thiazoles have been synthesized (Casiraghi et al., 1992; Belmans et al., 1985; Togo et al., 1994; Solomon et al., 1993; Togo et al., 1993; Bergstrom et al., 1991; Zhang et al., 1995; Du et al., 1995). Many of these compounds have also been found to exhibit a diverse range of biological activity (Chaudhuri et al., 1997).

Since the successful development of synthetic approaches for preparation of *C*-nucleosides, there has been growing interest in utilizing them as biophysical probes of noncovalent interactions in biological systems involving nucleic acids (Schweitzer and Kool, 1995), and as spectroscopic probes for the elucidation of DNA dynamics (Miller et al., 1995). Unnatural synthetic *C*-nucleosides have helped researchers to better understand natural nucleic acids and create novel nucleic acid structures (Ren et al., 1996), and have found application in studies of RNA-protein interactions (Puglisi et al., 1995).

In the process of DNA replication, highly specific incorporation of nucleotides into DNA by polymerase enzymes is known to be critical to the maintenance of high fidelity information transfer. Mismatched pairing at this step occurs only about once in every 1000 to 100000 insertions (Kornberg and Baker, 1992; Loeb and Kunkel, 1982). While specific base-base hydrogen binding, base stacking, base pair geometry, and interactions between the polymerase enzyme, DNA, and nucleotides have all been proposed to contribute to the high fidelity of DNA synthesis, the relative importance of these factors in the observed selectivity of nucleotide insertion remains unclear (Moran et al., 1997b).

In view of the limited number of naturally occurring nucleic acid base structures, and therefore the limited availability of probes based on these natural nucleosides, Kool and his coworkers initiated an exciting program to develop new synthetic analogues of the natural nucleosides to investigate the contribution of various mechanisms to the highly selective base pairing in DNA (Schweitzer and Kool, 1994). Accordingly, they designed nonpolar hydrophobic isosteres of pyrimidine nucleosides with the closest possible structural, steric and isoelectronic relationship to the natural structures that would, however, have a limited potential for hydrogen bonding. Compounds of this type could serve as valuable model compounds to probe the relative contributions of hydrogen bonding and base stacking in the formation of stable DNA duplex structures (Schweitzer and Kool, 1994).

In this respect, the 2,4-difluoro-5-methylphenyl isostere (5-MeDFPdR; Figure 3.1) was designed as a thymidine analogue, in which fluorine (F) is the isosteric replacement for oxygen (O), CH replaces NH, and the thymine N1 has been replaced by an sp^2 hybridized C-atom.

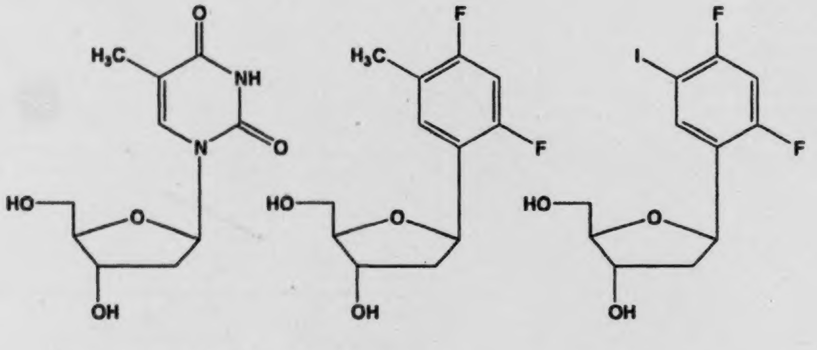

Thymidine **5-MeDFPdR** **5-IDFPdR**

Figure 3.1. Structures of thymidine, 1-(2-deoxy-β-D-ribofuranosyl)-2,4-difluoro-5-methylbenzene (5-MeDFPdR), and 1-(2-deoxy-β-D-ribofuranosyl)-2,4-difluoro-5-iodobenzene (5-IDFPdR)

Fluorine is one of the best substitutions for carbonyl-type oxygen both from a structural and an electronic standpoint. Data on atomic charges indicate that the 2,4-difluoro-5-methylphenyl isostere has the same absolute signs for the charges on every atom when compared to thymine, although smaller in magnitude. The reduced polarity of the 2,4-difluoro-5-methylphenyl isostere and related analogues is expected to make them more hydrophobic than the natural nucleosides, and to diminish their capability to form hydrogen bonds. Accordingly, 2,4-difluorotoluene (the aromatic group of 5-MeDFPdR) does not appear to form hydrogen bonds with potentially complementary partners based on the findings of NMR titration experiments. Furthermore, the calculated bond lengths obtained from AM1 semiempirical calculations for the natural thymine and the unnatural 2,4-difluorotoluene indicate that the difluoro-substituted thymidine analogue is a nearly perfect steric mimic of the natural thymidine. With such perfect steric and structural mimicry of natural thymidine, incorporation of the synthetic analogue into DNA is expected to be least disruptive to the geometry of the DNA helix (Schweitzer and Kool, 1994). Schweitzer and Kool subsequently incorporated the 2,4-difluoro-5-methylphenyl isostere and other designed hydrophobic purine and pyrimidine isosteres into synthetic oligodeoxynucleotides where they were base paired against each other and against the natural bases (Schweitzer and Kool, 1995). It was found that the hydrophobic base analogues were nonselective in pairing with the four natural bases (A, T, C, G) but selective for pairing with each other rather than with the natural bases. For example, the 2,4-difluoro-5-methylphenyl isostere, abbreviated as F', formed a high affinity F'-F' self-pair. The best stabilization occurred when the F'-F' pair is located at the end of the duplex, where the F'-F' pair is more stabilizing than a T-A pair. When situated internally, however, the affinity of the F'-F' pair is about equal to a T-T mismatch pair, which has two hydrogen bonds; the internal pairs may be destablized by imperfect steric mimicry, which could result in non-ideal duplex structure. This study suggested that formation of a stable duplex DNA-like structure is possible in the absence of conventional base-base hydrogen bonding. Solvation and desolvation effects appeared to best describe the observed selectivity of the designed hydrophobic isosteres, including the 2,4-difluoro-5-methylphenyl isostere (F'), for each other rather than for the natural bases. The results of this study illustrated the importance of solvation and desolvation in natural base pairing, and provided new evidence that hydrogen bonds may be more important for specificity of base pairing in DNA than for affinity. This study also indicated the possibility of using enzymatically replicable unnatural base pairs such as F'-F' to expand the biological and chemical genetic alphabet potential of DNA beyond the natural A-T and G-C pairs (Schweitzer and Kool, 1995). Subsequent studies showed that when F' is tested as a template for replication by the Klenow fragment [KF] of the *Escherichia coli* DNA polymerase I (pol I), dATP is inserted efficiently opposite F', while dCTP, dTTP and dGTP are not. Conversely, it was found that the 5'-triphosphate derivative of the 2,4-difluoro-5-methylphenyl isostere (dF'TP) is a very good substrate for *Escherichia coli* DNA polymerase I (pol I) and that dF'TP is inserted opposite A in a template strand by the Klenow fragment, with an efficiency (V_{max} / K_m) only 40-fold lower than the triphosphate of thymidine (dTTP). Moreover, it was inserted opposite A (relative to C, G, or T) with a selectivity almost as high as that observed for dTTP (Moran et al., 1997a). Thus, in spite of the poor hydrogen bonding abilities of F', the polymerase treats it almost as if it were thymine. The observation that Klenow fragment can efficiently replicate the inherently unstable A-F' or F'-A base pair with very high fidelity despite a lack of inherent base-pairing selectivity, lends support to the concept that hydrogen bonds may be less important in the fidelity of replication than previously believed. These observations have led researchers to conclude that nucleotide/template shape complementarity may be a primary factor governing nucleotide insertion by DNA polymerase (Moran et al., 1997a; Gukian and Kool, 1997).

In addition to their potential use as probes of the biological noncovalent interactions of oligonucleotides and nucleic acids in general, it is anticipated that nucleoside derivatives of 1-(2-deoxy-β-D-ribofurnaosyl)-2,4-difluoro-5-substituted-benzene may also have an inhibitory effect on DNA and RNA syntheses, owing to their potential for incorporation into nucleic acids (Mentel et al., 2000; Aketani et al., 2002). In this respect, these substituted benzenes may be considered a novel class of 5-substituted-2'-deoxyuridine (thymidine) mimics which may be cytotoxic to rapidly growing neoplastic cells and/or act as antiviral agents following the established mechanisms of action for other nucleosides (De Clercq, 1984). They may also find application as radiopharmaceutical imaging agents, or chemotherpaeutic agents to treat herpes simplex virus type-1 thymidine kinase positive (HSV-1 TK^+) gene transfected tumors (Oldfield et al., 1993; Wiebe et al., 1997). Replacement of the natural thymine base in thymidine by an unnatural aryl isostere in the nucleoside derivatives 1-(2-deoxy-β-D-ribofurnaosyl)-2,4-difluoro-5-substituted-benzene could bestow new and useful properties that natural nucleosides lack; these may include more favorable physiochemical and pharmacokinetic properties and/or reduced host cell cytotoxicity (Perigaud et al., 1992; Wang et al., 2001a).

Accordingly, a number of unnatural *C*-nucleosides, including a variety of 5-substituted [H, I, Br, Cl, F, Me, CF_3, NO_2, Et, $-CH{=}CH_2$, (*E*)-CH=CH-X, $-CH(N_3)CH_2X$, $-C(N_3){=}CH_2$, $-C{\equiv}CH$, $-C{\equiv}C-X$; where X=I, Br, Cl] derivatives of 1-(2-deoxy-β-D-ribofuranosyl)-2,4-difluorobenzene were recently designed as thymidine mimics and synthesized for evaluation as anticancer/ antiviral agents (Wang et al., 2001a,b;

Naimi et al., 2001). *C*-aryl nucleosides offer a number of potential advantages relative to classical 5-substituted-2'-deoxyuridines: The absence of an *N*-glycosidic bond is expected to increase their stability towards catabolic cleavage by pyrimidine phosphorylases, without the need for substitution on the sugar ring. In the case of *N*-nucleosides, substitutions on the sugar ring (e.g., 2'-ribofluoro, 2'-arabinofluoro, or 2'-arabino-hydroxy substitutions) are required to increase stability towards phosphorolysis or glycosidic bond cleavage (Mercer et al., 1989; Robins et al., 1991; Chou et al., 1987). Due to their inability to inhibit thymidylate synthetase (TS), these *C*-nucleoside mimics are expected to elicit reduced host cell toxicity. Moreover, their greater lipophilicity may alter tissue biodistribution, possibly enhancing their diffusion across the blood-brain-barrier to improve treatment of viral encephalitis and brain tumors, and as such offer an attractive alternative to making lipophilic prodrugs of nucleosides (Wang et al., 2001b; Wiebe and Knaus 1999).

3.2. Experimental

3.2.1. Materials

The novel unnatural 5-substituted [CH_3, I, CH_2CH_3] derivatives of 1-(2-deoxy-β-D-ribofuranosyl)-2,4-difluorobenzene, abbreviated as 5-MeDFPdR (244.1 Da), 5-IDFPdR (356 Da), and 5-EtDFPdR (258.1 Da) respectively, were synthesized by Drs. Naimi and Wang according to previously reported procedures (Wang et al., 2001a,b). 5-[^{125}I]IDFPdR was synthesized by Dr. Wei Yan Sun using an exchange reaction (Khalili et al., unpublished data). Thymidine, thymidine phosphorylase, thymine, polyethylene glycol 200 and 400, β-NADP, D-glucose-6-phosphate, and glucose-6-phosphate dehydrogenase were purchased from Sigma Chemical Co (Oakville, Ontario). β-Glucuronidase (*Escherichia coli*), and aryl sulfatase (*Helix pomatia*) were purchased from Boehringer Mannheim (Laval, Quebec). Na [^{125} I]I was purchased from Amersham (Mississauga, Ontario). Sprague Dawley rat liver microsomes were purchased from In Vitro Technologies (Baltimore, Maryland). Bovine serum albumin was obtained from Fischer Scientific (Nepean, ON). Centrifree™YM-30 devices (Amicon, Millipore Corporation; Bedford, MA) were used to separate free drug from the protein-bound drug in protein binding studies. *n*-Octanol used for the measurement of log P values was obtained from the Aldrich Chemical Company and was distilled prior to use. Dimethyl sulfoxide used for solubilization, was analytical reagent grade and obtained from BDH. All solvents used for HPLC analyses were of HPLC grade quality that were filtered and degassed before use.

A mechanical shaker (Dubnoff metabolic shaking incubator, Precision Scientific Co) was used for stability studies and partition coefficient determinations. A Vortex Genie™ (Scientific Industries, Inc. Bohemia, N. Y. 11716, USA) was used for mixing samples. Centrifugations of small samples were performed in an Eppendorf 5412 microcentrifuge; large samples were centrifuged in a Dynac centrifuge (Becton, Dickinson and Company, Parsippany, N. J. 07054). A Baxter centrifuge (Biofuge 17R) with fixed angle rotor was used in the protein binding study. A VWR scientific pH meter (model 8005) was used for pH measurements. A Branson 2200 sonicator was used for sonications. An Olympus CK40 microscope (Carsen Group Inc., Precision Instrument

Division, Markham, Ontario) was used for cell culture studies. A Neubauer improved bright-line hemocytometer was used for counting the cells.

3.2.2. Cell lines, cell culture media and materials

Two sets of adherent cell lines were used in MTT cytotoxicity assays, the KBALB/KBALB-STK cell lines and the 143B/143B LTK cell lines. When flow cytometry studies were performed, only KBALB/KBALB-STK cell lines were examined. The KBALB cell line is a transformed sarcoma cell line that was obtained from the American Type Culture Collection (ATCC). The KBALB-STK cell line was kindly provided by Dr. Scott Freeman (Tulane University). The KBALB-STK cell line was derived by exposing KBALB cells to supernatants from an ecotropic ψ-2 producer cell line. The latter producer cell line had been transfected with a construct that contains the HSV-1 TK gene under the direction of the SV-40 early promoter/enhancer and *neo*^{R} gene driven by the 5'-LTR.

The 143B cell line is an osteosarcoma cell line, obtained from ATCC. This cell line is a thymidine kinase negative (TK$^-$) mutant of R-970-5 that is tumorigenic in nude mice. The R-970-5 cell line is a human TK$^+$ osteosarcoma cell line that can be obtained from ATCC. The 143B-LTK cell line is derived from parental 143B cells, through transduction with a replication incompetent amphotropic Moloney murine leukemia virus vector (LSNtk) with the HSV-1 TK gene being directed by the 5'- LTR and *neo*^{R} gene under the control of a SV-40 early promoter/enhancer (Morin et al., 2000). The cell lines were maintained in Dulbecco's Modified Eagle Medium (DMEM) supplemented with 10% fetal bovine serum (FBS), and 1% antibiotic/antimycotic (containing penicillin G, streptomycin sulfate, and amphotericin B, 100X). Trypsin-EDTA was used for the purpose of trypsinization of the cells prior to the subculturing. KBALB-STK and 143B-LTK cells were maintained in media that in addition to the above components, contained geneticin (G418, 1 mg/mL), while 143B cells were maintained in a medium fortified with 5-bromo-2'-deoxyuridine (15 µg/mL). Cells were cultured in an incubator at 37 °C, in a 5% CO_2 atmosphere. DMEM, antibiotic/antimycotic and trypsin-EDTA were purchased from GIBCO BRL. Fetal bovine serum (FBS) was purchased from Cansera Company and was heat inactivated at 56 °C for 40 minutes. Geneticin antibiotic (G-418), trypan blue, propidium iodide and MTT [3-(4,5-dimethylthiazol-2-yl)-2,5-diphenyltetrazolium bromide] were obtained from Sigma Co. PBS was prepared in-house (contains 140 mM NaCl, 260 mM KCl, 8.1 mM Na_2HPO_4, 1.47 mM KH_2PO_4).

3.2.3. High performance liquid chromatography

Quantitative analyses of samples for all experiments were performed using a High Performance Liquid Chromatography (HPLC) system comprised of two Waters 501 pumps, a U6K manual injector or Waters Wisp 712 B autoinjector, Waters 486 UV detector and a Diamir data station. All samples were chromatographed on a reverse phase Radial-Pak™ cartridge column (8NVC184µ, Nova-Pak, C18; Waters), or using a YMC™ reverse phase HPLC column (YMC ODS-AQ™, 25 cm x 4.6 mm; Waters), preceded by precolumn inserts of the same packing. Both columns were maintained at the room temperature. Separations were performed using various mixtures of water and acetonitrile or various mixtures of 20 mM ammonium acetate buffer at pH 3.5 and acetonitrile.

3.2.4. Stability of 5-IDFPdR in solution (water and PBS) and upon incubation with rat plasma

To determine 5-IDFPdR stability in solution, stock solutions (100 μM) of 5-IDFPdR in water and PBS buffer (pH 7.4) were prepared and stored at 25 °C. Aliquots (50 μL) of these stock solutions were removed at specified time intervals (0.5, 1, 1.5, 2, 4, 6, 8, 16, 24, 48, 72, 96, 120 h), and analyzed by quantitative HPLC using acetonitrile-water (4:6, v/v) as eluent at a flow rate of 1 mL/min and UV detection at 273 nm. To determine stability in plasma, aliquots (10 μL) of a 1 mM solution of 5-IDFPdR in water were added to rat plasma (90 μL) to produce a 100 μM solution that was incubated at 37 °C in a water bath. At specified intervals (as above), aliquots (50 μL) were removed, mixed with methanol (100 μL), and centrifuged for 15 min at 12,800 rpm. Aliquots (50 μL) of the supernatants were analyzed by quantitative HPLC according to the procedure detailed for the water and buffer stability studies.

3.2.5. Enzymatic stability of 5-IDFPdR toward phosphorolysis by *E. coli* thymidine phosphorylase

The stability of 5-IDFPdR and 5-iodo-2'-deoxyuridine (IUdR) toward *E. coli* thymidine phosphorylase was assessed following published literature methods (Balzarini et al., 2000; Schwartz, 1978). Briefly, a mixture (500 μL) containing 10 mM Tris-HCl (pH 7.6), 1 mM EDTA, 2 mM potassium phosphate, 150 mM NaCl and 100 μM 5-IDFPdR, IUdR, or dThd (as positive control) was incubated at 22 °C, with and without *E. coli* thymidine phosphorylase (0.025 U) and 100 μM 2-deoxyribose-α-1-phosphate.

At different time points (0, 20, 40, and 60 min), aliquots (50 μL) were withdrawn and heated (nominally 95 °C) on a boiling hot water bath for 5 min to inactivate the enzyme. The samples were then rapidly cooled on ice and analyzed by HPLC using either acetonitrile:water (5:95, v/v) as eluent with UV detection at 270 nm and 290 nm for thymidine and IUdR, respectively, or acetonitrile:water (30:70 v/v) with UV detection at 273 nm for 5-IDFPdR.

3.2.6. In vitro incubation of 5-IDFPdR with rat liver microsomes

For in vitro metabolism studies with rat liver microsomes, incubation mixtures were prepared in glass test tubes containing rat liver microsomes (2 mg; 100 μL) to which potassium phosphate buffer (640 μL; 100 mM) and a stock solution of 5-IDFPdR (10 mM, 10 μL) were added. The NADPH regenerating system (NRS) was prepared in a separate set of glass test tubes, to contain β-NADP (0.5 mg/mL), glucose-6-phosphate (2.0 mg/mL) and glucose-6-phosphate dehydrogenase (1.5 units/mL) in 2 % $NaHCO_3$ solution. The incubation tubes, as well as the NRS tubes, were placed in a water bath (37 °C) and shaken occasionally. To start the reaction, NRS solution (250 μL) was added to each incubation test tube. At the end of each incubation time (0, 5, 15, 30, 45, 60 min), the test tube was quickly removed from the water bath, 5-MeDFPdR (50 μL of a 0.4 mg/mL, 1.64 mM solution) was added as internal standard, followed by methanol (1 mL) to terminate the enzymatic reaction, based on a modification of the microsome manufacturer's incubation procedure. The incubation mixtures were extracted into ethyl acetate (6 mL), which was then transferred into separate test tubes. The solvent was evaporated, and the residue was reconstituted in acetonitrile for HPLC analysis, using an acetonitrile-water gradient: after an initial hold time of 5 min, the gradient was developed from 80 % water to 70 % water over 1 min, and held at this concentration for 7 min. The initial solvent composition was then reestablished over 2 min, after which the column was re-equilibrated for 10 min before the next sample injection.

3.2.7. Determination of partition coefficients (log P)

Partition coefficients for 5-IDFPdR and 5-MeDFPdR (the internal standard selected for pharmacokinetic studies) were determined using the shake flask method (Hansch and Elkins, 1971), which involves partitioning a test compound between water saturated *n*-octanol and *n*-octanol saturated water, followed by quantitation of the analyte in either phase using UV spectrophotometry or HPLC.

n-Octanol was refluxed for 4 h and distilled *n*-octanol was collected at 196 °C. *n*-Octanol and water were mutually saturated by stirring equal volumes of octanol and water overnight. The two phases were then separated using a separatory funnel and each fraction was stored in a brown bottle at room temperature for subsequent use. The test compound (2 mg) was partitioned between water-saturated *n*-octanol (2 mL) and *n*-octanol-saturated water (4 mL). The tubes were shaken for 24 h at 22 °C in a mechanical shaker. The two phases were then separated and the concentration of test compounds in *n*-octanol phase was quantified by UV spectrophotometry at 273 nm using pre-established standard curves. Partition coefficients (log P values) were calculated from the log of the ratio of test compounds' concentration in the *n*-octanol phase to their concentration in the water phase, according to the following equation (Shargel and Yu, 1999; Hansch and Elkins, 1971):

$$\log P = \log [C_{n\text{-octanol}} / C_{\text{water}}] \qquad \text{Eq. 1}$$

The Interactive Analysis Log P computational program [Interactive Analysis (IA), Bedford, MA] developed by Marc Parham (mparham@interactiveanalysis.com) was used to calculate theoretical log P values.

3.2.8. Protein binding of 5-IDFPdR

Albumin represents the major component of plasma proteins responsible for reversible drug binding. The binding of 5-IDFPdR to bovine serum albumin (BSA) was assessed by incubating 5-IDFPdR at several concentrations (0.2 mL, $1\text{x}10^{-3}$ M to $6\text{x}10^{-6}$ M) with bovine serum albumin (BSA; 3.8 mL; 4.5 g/L, $1.22\text{x}10^{-4}$ M) in PBS (pH 7.4) for 1 h, at 37 °C. At the end of the incubation period, triplicate aliquots (1 mL) of drug-protein solutions were transferred to Centrifree™YM-30 devices and centrifuged at 2000x *g* for 25 min to separate free drug from protein-bound drug. These ultrafiltrates were kept at 4 °C for HPLC analysis using the same isocratic method described under 3.2.4. The free 5-IDFPdR concentrations in the ultrafiltrates were determined from standard curves that had been established by measuring peak areas for the samples containing known concentrations of 5-IDFPdR dissolved in the plain ultrafiltrate. Binding to albumin was calculated by the formula:

$$\text{Percent bound} = [(D_t - D_f) / D_t] \times 100 \qquad \text{(Eq. 2)}$$

D_f is the concentration of the free (unbound) drug present in ultrafiltrates and D_t is the total drug concentration (bound and free) present in the samples before ultrafiltration.

The precision of the analytical method, as assessed by intra- and interday relative standard deviations at low, medium, and high 5-IDFPdR concentrations (1×10^{-5} M, 1×10^{-4} M, 1×10^{-3} M) averaged about 8 %. The accuracy of the assays, as determined by comparing the results of the precision study with known 5-IDFPdR concentrations (in plain ultrafiltrate), was ~ 93 %.

3.2.9. In vitro cytotoxicity assay

To screen for the cytotoxicity of the drugs investigated, the widely used MTT cell viability assay was employed. The MTT assay is based on the cleavage of the tetrazolium salt MTT into a blue colored formazan product by the mitochondrial enzyme succinate dehydrogenase. This reduction only occurs in living cells so the amount of the formazan produced is proportional to the number of living cells present (Mossman, 1983).

Murine KBALB, KBALB-STK cells, and human 143B, 143B-LTK cells were cultured in complete DMEM medium supplemented with 10% fetal bovine serum (FBS). Exponentially growing cells were trypsinized, centrifuged, and suspended in growth medium and diluted to a concentration of approximately 8×10^3 cells per mL. The cells were then plated in 100 μL volumes (800 cells) into 96-well microplates and incubated for 24 hours at 37 °C in 5% CO_2. The compounds were dissolved in DMEM and added to the cells in 100 μL volumes to produce a range of final drug concentrations (10^{-3} to 10^{-7} M). The control wells were filled with 100 μL of plain drug-free medium. The blank rows contained 200 μL of medium alone (no cells). The plates were incubated for 3 days in an incubator at 37 °C and 5% CO_2. MTT working solution was prepared freshly on the day of the assay by 1:5 dilution of the MTT stock solution in prewarmed DMEM. MTT stock solution was prepared by dissolving MTT in PBS (5 mg/mL), and filtering the mixture through a 0.2 μ millipore filter. On the day of the assay, 50 μL of the freshly prepared MTT working solution was added to each well and the plates were incubated at 37 °C for 4 hours. At the end of the 4 hours, the medium was carefully aspirated from the wells, leaving approximately 20 μL in each well. DMSO (150 μL) was then added to each well and the plates were shaken slowly on a shaker for times up to 15 minutes to dissolve the formazan crystals. The plates were then read at 540 nm on a scanning multi-well spectrophotometer (ELISA reader).

3.2.10. Flow cytometry study

5-IDFPdR-induced changes in the cell cycle of a murine tumor cell-line were determined using a flow cytometer (1-laser, Becton Dickinson). Briefly, KBALB cells were incubated in DMEM containing various concentrations of 5-IDFPdR (0, $5\text{x}10^{-4}$M, $4\text{x}10^{-4}$M, $3\text{x}10^{-4}$M, $2\text{x}10^{-4}$M, $5\text{x}10^{-5}$M) for 6 days at 37 °C and 5% CO_2. On day 3 of incubations, the medium in each well was gently replaced with fresh medium containing 5-IDFPdR. Following the incubation period, trypsin-detached KBALB cells were washed in PBS and fixed with 70% ethanol. The cells were stored in fixative in a refrigerator overnight. About $1\text{x}10^6$ alcohol-fixed cells were then washed in PBS, centrifuged at 200x*g* for 5 min to pellet down the cells and to remove the supernatant. The resulting cell pellets were stained by suspending them in 1 mL of a propidium iodide/Triton X-100 lysis-staining solution that also contained DNase-free RNase A for 30 min at room temperature. The lysis-staining solution was prepared by adding 2 mg

DNase-free RNase A and 200 μL of 1 mg/mL propidium iodide (PI) to 10 mL of 0.1 % (v/v) Triton X-100 (Darzynkiewicz and Juan, 1997). The relative DNA content of the stained cells was then analyzed by flow cytometry.

3.2.11. Animal pharmacokinetic studies

Male Sprague-Dawley rats (250-350 g) purchased from Health Sciences Laboratory Animal Services (HSLAS) were used for the pharmacokinetic studies. The animals were handled in accordance with the guidelines of the Canadian Council on Animal Care and all experimental protocols and procedures were approved by the University of Alberta Health Sciences Animal Welfare Committee. All animals were housed in the Dentistry-Pharmacy Building Animal Services Facility and fed conventional rodent foods. During and after administration of the dose, the rats were placed in individual metabolic cages. Rats were fasted (water *ad libidum*) overnight prior to oral dosing (po) and for 4 h post dose. The animals were maintained under a 12-hour light/dark cycle with free access to water.

For pharmacokinetic studies, external right jugular vein cannulae were implanted under metofane anesthesia one day prior to dosing. Rats were fasted for 8 h, with free access to water, before the dosing. On the day of the experiment, 5-IDFPdR was dissolved in PEG 200:water (8:2 v/v), and rats were dosed at 5, 15 and 54 mg/kg intravenously (iv-bolus via the jugular vein cannula) and at 20, 40 and 54 mg/kg orally (by oral gavage). Just prior to the administration of the dose, blood (0.3 mL) was withdrawn. In iv–bolus studies, part of the pre-dose blood (0.15 mL) was pushed through the cannula immediately after the dose, followed by saline (2 x 0.2 mL), to wash out any residual dose out of the cannula. Blood (~ 270 μL) was collected into heparinized tubes at 2, 5, 10, 15, 20, 30, 45, 60, 90, 120, 150, 180, and 210 min following the iv-bolus dose. The same sampling schedule was used following the oral dose, but five additional blood samples were taken at 240, 270, 300, 330, and 360 min post dose. Each blood sample withdrawal was followed by injection of an equal volume of normal saline via the catheter. Shortly following blood sampling, exact volume (250 μL) of blood was transferred from each original blood collection tube to another test tube, followed immediately by the addition of 5-MeDFPdR (100 μL, 0.4 mg/mL, 1.64 mM) as internal standard to each blood test tube. Aliquots of a cold mixture of acetonitrile:DMSO (92:8 v/v, 650 μL) were then added to precipitate the proteins and extract the compounds of interest. These mixtures were vortexed for 1 min and centrifuged for 15 min at 1500x*g*. The supernatants were withdrawn, dried under a stream of dry nitrogen and reconstituted in HPLC mobile phase (150 μL) for quantitative analyses. Urine was collected (metabolic cage) for 24 h following the dose, and was stored at – 20 °C until analysis.

In biliary excretion studies rats were anesthetized by intraperitoneal injection of a mixture of 90 mg/kg Ketaset® (Wyeth-Ayerst Canada Inc., 100 mg/mL) and 10 mg/kg Rompun® (Bayer Inc., 20 mg/mL). Catheters were then implanted into the bile duct via a small abdominal incision, and into the right jugular vein. Blank bile was obtained just before the administration of the dose. 5-IDFPdR was then administered via the jugular vein catheter, at 5, 15 and 54 mg/kg to three sets of rats (n=3 in each set). Bile was collected at 1 h intervals up to 8 h following the dose.

3.2.11.1. Enzymatic hydrolysis assays.

The presence of glucuronides and/or sulfate conjugates of 5-IDFPdR in urine and bile aliquots were determined by incubation with β-glucuronidase and aryl sulfatase, using a modified literature method [Evelo et al., 1984]:

Urine Incubations. Aliquots of glucuronidase (8 units of *E. coli* β-glucuronidase in 1 mL 0.2 M KH_2PO_4/Na_2HPO_4, pH 6.2) were added to urine aliquots (1 mL), and the mixtures were incubated overnight at 37 °C. As control in each case, buffer with no enzyme was added to the urine aliquots (1 mL) of the same batch. At the end of the incubation time, 5-MeDFPdR (100 μL, 0.4 mg/mL) was added to the samples as internal standard, followed immediately by addition of methanol (1 mL). The mixtures were then vortexed and evaporated to dryness. The dried samples were reconstituted in HPLC mobile phase (200 μL) and centrifuged for 5 min at 1500x*g*. Aliquots (50 μL) of the supernatant were then analyzed by HPLC. The aryl sulfatase incubation study followed a similar protocol, except that a potassium acetate buffer (0.1 M, pH 5.2) was used to buffer the urine.

Bile Incubations. Glucuronides and sulfate conjugates in 0-8 h bile samples were determined by incubation of bile samples with β-glucuronidase and aryl sulfatase following the same protocol as described above for urine hydrolysis. In this case, however, due to a smaller volume of bile, smaller aliquots (200 μL) of bile were subjected to enzymatic hydrolysis. At the end of the incubation and following the addition of internal standard (5-EtDFPdR, 100 μL, 0.4 mg/mL), ethyl acetate (2 mL) was added to the bile sample and the compounds of interest were extracted by liquid-liquid extraction into the organic (ethyl acetate) phase. The ethyl acetate extracts were dried under a stream of nitrogen, and the dried samples were reconstituted in the HPLC mobile phase (200 μL) and analyzed by HPLC. The glucuronic acid conjugate and sulfate conjugate concentrations were calculated as the difference between the area under the curve of 5-IDFPdR in the treated and control samples.

3.2.11.2. Quantitative analyses of biological samples

All quantitative analyses were performed using the HPLC system described in section 3.2.3. The following methods were developed for quantitation of analytes in blood, bile and urine:

Method I: Analysis of the blood sample extracts was achieved by eluting column B isocratically with ammonium acetate buffer (20 mM, pH 3.5): acetonitrile (75:25), at a flow rate of 0.7 mL/min, with UV detection at 273 nm.

Method II: Reconstituted urine and bile extracts were analyzed similarly using ammonium acetate buffer (20 mM, pH 3.5): acetonitrile (78:22) as mobile phase, using a flow rate of 0.7 mL/min and with UV detection at 273 nm.

3.2.11.3. Quantitation limits and analytical recovery

The standard curves for 5-IDFPdR in rat blood, bile and urine covered a range of concentrations from 0.1 μg/mL to 100 μg/mL (blood and bile) and 0.2 to 125 μg/mL (urine), respectively. The standard curves of 5-IDFPdR in all three matrices were linear over the concentration range examined. The lowest detectable concentration of 5-IDFPdR was 0.01 μg/mL (100 μL sample volume). The precision of the analytical methods, as assessed by intra- and interday relative standard deviations at low, medium, and high 5-IDFPdR concentrations (0.5, 5.0 and 50 μg/mL) was less than 10%. The accuracy of the assays, as determined by comparing the results of the precision study with the known blood 5-IDFPdR concentrations, was always over 90%. To obtain an estimate of the analytical recovery for each matrix, peak areas of the extracted 5-IDFPdR samples containing low, medium and high concentrations (0.5, 5.0 and 50 μg/mL) of 5-IDFPdR were compared with those of direct injections of the same amount of 5-IDFPdR (n = 3 at each concentration). The mean recoveries ranged from 85 % for urine samples to 90 % and 94 % for blood and bile samples, respectively.

3.2.11.4. Pharmacokinetic analyses

The pharmacokinetic parameters of 5-IDFPdR at the studied doses were determined using open one- or two-compartment models (WinNonlin version 1.1™). The goodness of fit for the chosen compartment models was evaluated based on the sum of the weighted squared residuals, and Akaike's criterion.

The concentration C as a function of time in one- or two compartment models is given by the following formulae:

$C = C_o e^{-kt}$ (one compartment model) and $C = Ae^{-\alpha t} + Be^{-\beta t}$ (two compartment model)

C_o and k represent concentration at time zero and the elimination rate constant from the central compartment in one compartment model, respectively. A and B are zero time intercepts associated with the distribution and elimination phase, while α and β represent the distribution and elimination phases associated rate constants.

Significance of differences between the mean values of different pharmacokinetic parameters at various dose levels was calculated by a student's t test. Statistical significance was determined at the 95 % confidence level ($P<0.05$).

The urinary and biliary recoveries of unchanged and total (unchanged and conjugated) drug were calculated from the ratios of the amount of unchanged and/or total drug divided by the dose.

3.2.12. Blood-to-plasma ratio

The in vitro distribution of 5-[^{125}I] IDFPdR between blood cells and plasma was studied by incubating 5-[^{125}I] IDFPdR with fresh, heparinized rat blood (1.75, 3.5, and 35 µg/mL of blood) at 37 °C for 1 h. The blood samples were then centrifuged at 5000x*g* to separate the plasma. The radioactivity in blood and plasma was counted in a Beckman gamma well counter. The blood-to-plasma ratio was then determined from the ratio of radioactivity in equal volumes of blood and plasma.

3.3. Results

3.3.1. Stability of 5-IDFPdR in solution (water and PBS), and in incubates of rat plasma

5-IDFPdR was chemically stable in both water and PBS throughout the stability studies (120 h, 25 °C), and it was observed that 5-IDFPdR was stable in these solutions at 25 °C for at least two months. 5-MeDFPdR was equally stable in solution at 25 °C, with no HPLC-detectable degradation products during a two-month period. Upon incubation of 5-IDFPdR with rat plasma for up to 24 h at 37 °C, there was less than 10% reduction of the parent compound peak area.

3.3.2. Stability of 5-IDFPdR toward phosphorolysis by *E. coli* thymidine phosphorylase

Phosphorolysis, the catabolic cleavage of glycosidic bonds, inactivates many nucleosides. In this study, thymidine phosphorolysis was carried out as a positive control, which yielded thymine (28 %, 1 h incubation), as monitored by HPLC. As postulated, 5-IDFPdR did not undergo catabolic cleavage in the presence of *E. coli* thymidine phosphorylase, as there was no change in 5-IDFPdR peak area and no appearance of any new peaks on the HPLC chromatograms of incubation mixtures. IUdR was, however, cleaved by thymidine phosphorylase to a greater extent than thymidine itself (38 %, 1 h incubation), yielding 5-iodouracil.

3.3.3. In vitro incubation of 5-IDFPdR with rat liver microsomes

Replicate studies of the NADPH-dependent mirosomal metabolism of 5-IDFPdR were performed at three different concentrations of 5-IDFPdR (60 μM, 100 μM, and 1 mM). A decrease of the parent compound (5-IDFPdR) peak area was observed only over the 60 min incubation period (less than 8 % of the zero time point peak area). Attempts to identify a minor metabolite peak collected from HPLC and purified by numerous reinjections of the same fraction by mass spectrometry were inconclusive.

3.3.4. Partition coefficients

The experimental and calculated log P values for 5-IDFPdR, 5-MeDFPdR, and thymidine (dThd) are listed in Table 3.1.

Table 3.1. Experimental and calculated log P values of 5-IDFPdR, 5-MeDFPdR and dThd

Compound	Experimental log P	Calculated* log P
5-IDFPdR	2.87	2.80
5-MeDFPdR	1.90	1.96
dThd	-1.19**	-0.81

* Interactive Analysis Log P computational program
** Parang, 1997

The calculated log P values of 5-IDFPdR and 5-MeDFPdR are in good agreement with the experimental values obtained using the shake-flask method.

3.3.5. Protein binding of 5-IDFPdR

The extent of 5-IDFPdR binding to bovine serum albumin, in vitro at 37 °C, ranged from 70 % to 75 % over the range of 5-IDFPdR concentrations studied (Table 3.2). The examined concentration range includes the range of in vivo 5-IDFPdR concentrations (6×10^{-6} to 4×10^{-4} M) observed in pharmacokinetic studies.

Table 3.2. Percent bovine serum albumin binding of 5-IDFPdR at various 5-IDFPdR concentrations.

5-IDFPdR Concentration (M)	Mean Percent Bound (± S.D.)
6×10^{-6}	75 ± 0.4
1×10^{-5}	69 ± 2.2
4×10^{-5}	70 ± 0.2
8×10^{-5}	72 ± 0.7
1×10^{-4}	73 ± 0.2
4×10^{-4}	71 ± 0.2
8×10^{-4}	67 ± 0.5
1×10^{-3}	69 ± 0.7

3.3.6. In vitro cytotoxicity and flow cytometry studies

The results of cytotoxicity evaluations of 5-IDFPdR in KBALB, KBALB-STK, 143B, and 143B-LTK cell lines, as determined by the MTT assay, are illustrated in Figure 3.2.

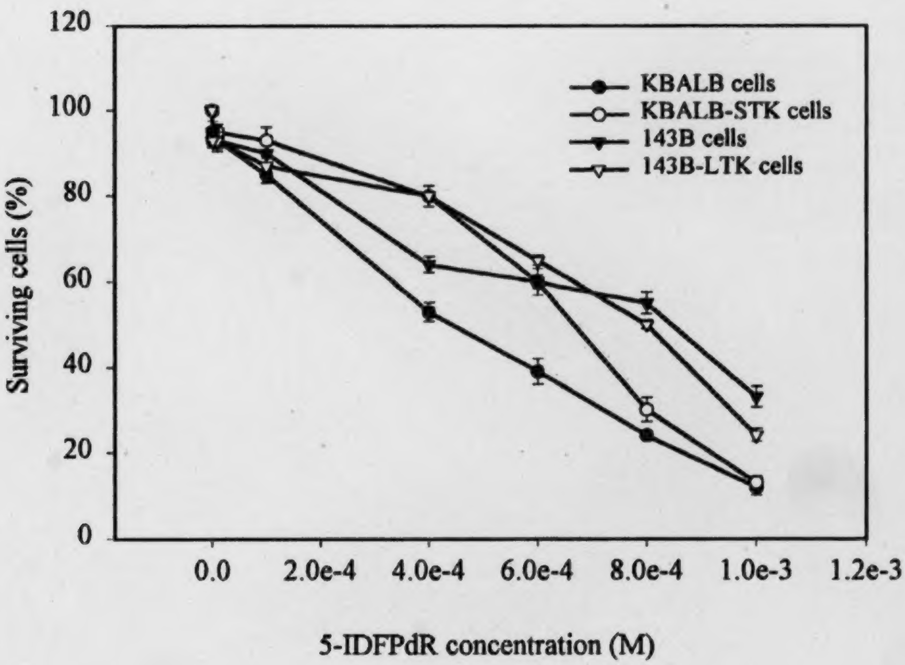

Figure 3.2. Percent of cells surviving following 72h exposure to various concentrations (M) of 5-IDFPdR. Error bars represent the standard deviations (S.D.) of the mean values for triplicate measurements.

Table 3.3 tabulates the IC_{50} (M), i.e. the concentration of the test compound that kills 50 % of the cells, for 5-IDFPdR and the reference compounds IUdR, FUdR, and thymidine. In comparison with these reference nucleosides, 5-IDFPR exhibited lower toxicity against the examined cancer cell lines, with the exception of 143B and 143B-LTK human osteosarcoma cell lines, where 5-IDFPdR was more toxic than IUdR. The results in Table 3.3 indicate that IUdR and FUdR are far more toxic to murine cancer cell lines than human cancer cell lines. This may be in part due to species-specific differences between the murine and human cancer cell lines. Moreover, 143B (human) cell line completely lacks thymidine kinase, and 143B-LTK (human) cell line has been transduced with a vector (LSNtk), in which 5'-LTR rather than SV-40 early promoter/enhancer element is promoting expression of viral thymidine kinase (HSV-1 TK). Although both 5'-LTR and SV-40 have varying degrees of promoter efficiency depending on the cell type, the Moloney murine leukemia virus 5'-LTR is thought to be less effective in promoting transcription than SV-40 early promoter/enhancer element in some cell lines (Guild et al., 1988; Wagner et al., 1985). The complete lack of thymidine kinase in the case of 143B cell line and a possibly lower expression of viral thymidine kinase by the promotory activity of 5'-LTR in 143B-LTK cell line may have contributed to the lesser sensitivity of these human cancer cell lines to the toxic effects of IUdR and FUdR. There are however no significant differences between the cytotoxicity of 5-IDFPdR against murine and human cancer cell lines, which may indicate that 5-IDFPdR has more unique metabolic activation pathways and requirements.

IUdR exhibited greater cytotoxicity against KBALB-STK cell line than the HSV-TK deficient parental KBALB cell line. This likely indicates that IUdR is more efficiently phosphorylated by the viral thymidine kinase expressing KBALB-STK cell line than by the viral thymidine kinase deficient parental KBALB cell line.

Table 3.3. Mean IC_{50} values of 5-IDFPdR and reference compounds FUdR, IUdR, and thymidine in various cell lines. Values in parantheses represent the standard deviations (S.D.) of the mean (n =3). The cited cytotoxicity data of FUdR and thymidine obtained from Wang et al. do not include S.D. values.

	KBALB	KBALB-STK	143B	143B-LTK
5-IDFPdR	4.1×10^{-4} (3.0×10^{-5})	6.5×10^{-4} (4.8×10^{-5})	8.2×10^{-4} (9.7×10^{-5})	7.9×10^{-4} (8.1×10^{-5})
IUdR	9.8×10^{-5} (1.0×10^{-5})	1.0×10^{-5} (1.1×10^{-6})	7.0×10^{-3} (4.0×10^{-4})	7.5×10^{-3} (7.7×10^{-4})
FUdR[a]	6.0×10^{-11}	8.8×10^{-11}	9.0×10^{-5}	1.0×10^{-4}
Thymidine[a]	9.5×10^{-5}	1.0×10^{-4}	ND[b]	ND[b]

[a] Data obtained from Wang et al, 2001
[b] ND: not determined

The DNA content of KBALB cells that were incubated for 6 days with various concentrations of 5-IDFPdR was measured using the DNA fluorochrome propidium iodide (PI). As described in section 3.2.10, the assay uses ethanol to fix and permeabilize KBALB cells, aiding access of PI dye to DNA in intact cells and allowing DNA content analysis of stained cell by flow cytometry. The intensity of the fluorescence signal from each cell following staining with propidium iodide or other DNA stains is directly proportional to the DNA content of the cell. Therefore, apoptotic cells, following staining of their cellular DNA, can be recognized as cells with low DNA stainability, forming a characteristic hypodiploid or sub-G_1 peak on the DNA histogram (Darzynkiewicz and Juan, 1997). Since measurement of DNA content also provides insight into the cell cycle position of the nonapoptotic cells, the cell cycle specificity of apoptosis can also be investigated using this approach (Darzynkiewicz et al., 1997). The main limitation of the DNA extraction approach is its low specificity in the detection of apoptosis. The sub-G_1 peak may include not only apoptotic cells, but also mechanically damaged cells, cells with altered chromatin structure, cells with lower DNA content (e.g., a sample containing cell populations with heterogeneous DNA indices), cell debris, nuclear fragments, and isolated chromosomes released from mitotic cells (Darzynkiewicz et al., 1997).

The fluorescence histograms of propidium iodide stained KBALB cells treated with near-IC_{50} (M)-concentrations of 5-IDFPdR are shown in Figure 3.3. On the basis of differences in DNA content, one can identify a population of G_0 / G_1 cells with low DNA content values (a peak around 200), G_2 / M cells with DNA content twice that of G_0 / G_1 cells (around 400), and S phase cells with intermediate DNA content (between 200 and 400). The M1-markers in panels A to D of Figure 3.3 show an estimate of the proportion of KBALB cells in the sub-G_1 zone, which in addition to apoptotic cells may also include cell debris and mechanically damaged cells (see above). These DNA content histograms further confirm the cytotoxicity findings of the MTT assay: Exposure of the KBALB cells to increasingly higher concentrations of 5-IDFPdR (within the $IC_{50} = 10^{-4}$ M range) led to an increase in the proportion of dying cells (apoptotic and necrotic), as demonstrated by a growing sub-G1 peak. Furthermore, there were no concentration related changes (e.g. accumulations) in the fraction of the cells within other phases of the cell cycle, which may indicate that 5-IDFPdR does not block the progression of KBALB cells through the cell cycle. This may be indicative of a lack of cell cycle specificity of 5-IDFPdR, although further studies would be needed to confirm this observation.

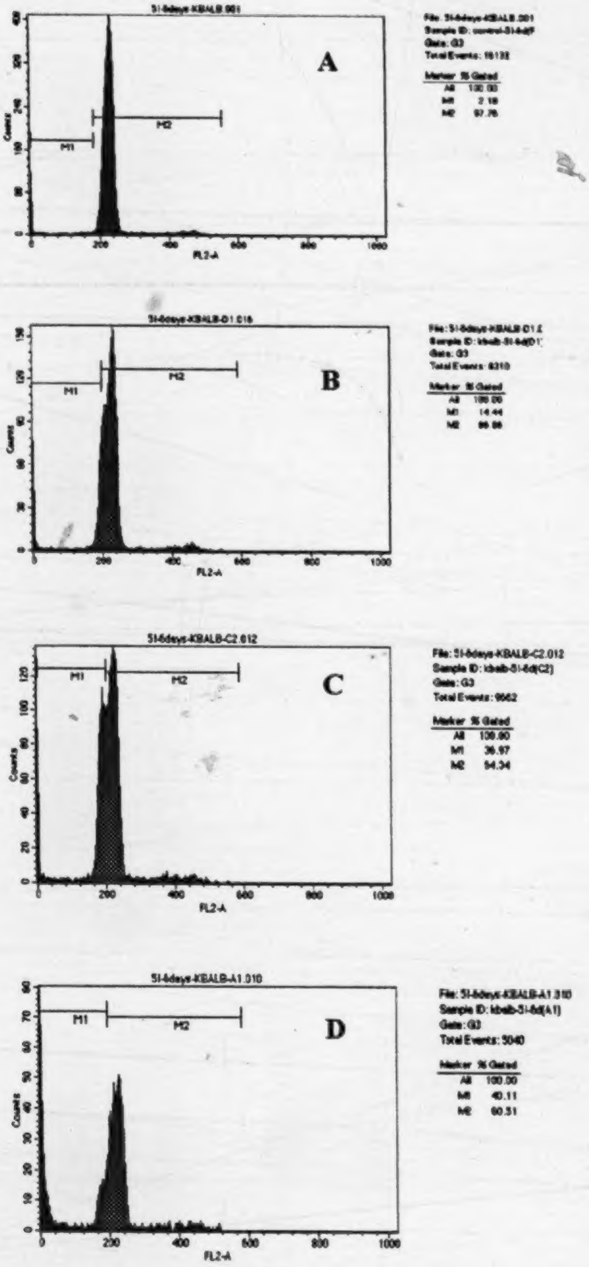

Figure 3.3.
Fluorescence histograms of KBALB cells stained with propidium iodide. The fluorescence on the x-axis represents the DNA content of cells; the counts on the y-axis represent the number of cells.

A: KBALB control cells.

B: KBALB exposed to 5-IDFPdR ($2x10^{-4}$ M)

C: KBALB exposed to 5-IDFPdR ($3x10^{-4}$ M)

D: KBALB exposed to 5-IDFPdR ($5x10^{-4}$ M)

3.3.7. Animal pharmacokinetic studies

Pharmacokinetic parameters and blood concentration-time profiles following iv and po dosing of 5-IDFPdR at 5,15 and 54, and at 20, 40 and 54 mg/kg, respectively are summarized in Tables 3.4 and 3.5 and illustrated in Figures 3.4 and 3.5.

Table 3.4. Pharmacokinetic parameters of 5-IDFPdR in iv dosed male SD rats. Values are means (S.D.), n = 3 or 4.

Dose (mg/kg)	$AUC_{(0-\infty)}$ (μg.min/mL)	$AUC_{(norm)}^*$ (kg.min/mL)	β half-life (min)	Cl_T (mL/min/kg)	V_{ss} (mL/kg)
5	175 (10)	0.13 (0.01)	8.4 (0.8)	28.7 (1.1)	294.9 (28.4)
15	472 (57)	0.13 (0.01)	8.0 (0.6)	32.1 (3.9)	331.9 (20.5)
54	2872 (149)	0.19 (0.02)	22.0 (16.6)	18.6 (0.9)	376.1 (63.5)

*AUC_{norm} is calculated from AUC/dose in each case.
Unpaired t- test was used to compare the means of various pharmacokinetic parameters at various dose levels. A *P*-value of less than 0.05 was considered to be significant.

Table 3.5. Pharmacokinetic parameters of 5-IDFPdR in po dosed male SD rats. Values are means (S.D.), n = 3 or 4.

Dose (mg/kg)	$AUC_{(0-\infty)}$ (μg.min/mL)	$AUC_{(norm)}^*$ (kg.min/mL)	β-half life (min)	T_{max} (min)	Cl_{po} (mL/min/kg)
20	538 (49)	0.09 (0.01)	24.5 (3.6)	8.8 (0.3)	37.4 (3.4)
40	1684 (125)	0.13 (0.01)	128.6 (137.8)	15.1 (0.7)	23.9 (1.8)
54	3154 (206)	0.21 (0.01)	176.1 (68.9)	15.5 (1.3)	17.1 (1.2)

*AUC_{norm} is calculated from AUC/dose in each case.
Unpaired t- test was used to compare the means of various pharmacokinetic parameters at various dose levels. A *P*-value of less than 0.05 was considered to be significant.

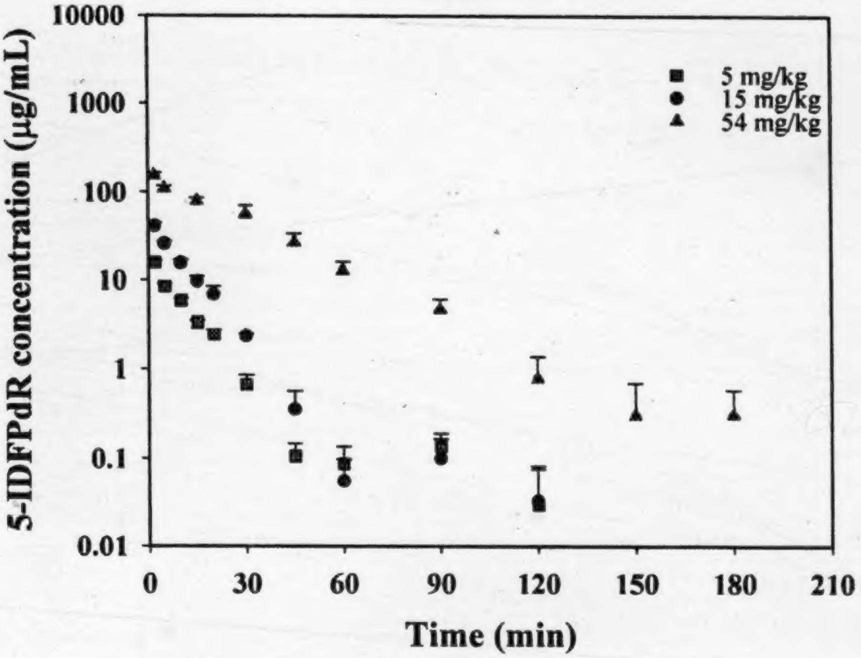

Figure 3.4. Mean (+S.D.) concentrations of 5-IDFPdR in rat blood following intravanous bolus administration at 5, 15 and 54 mg/kg (n=3 or 4).

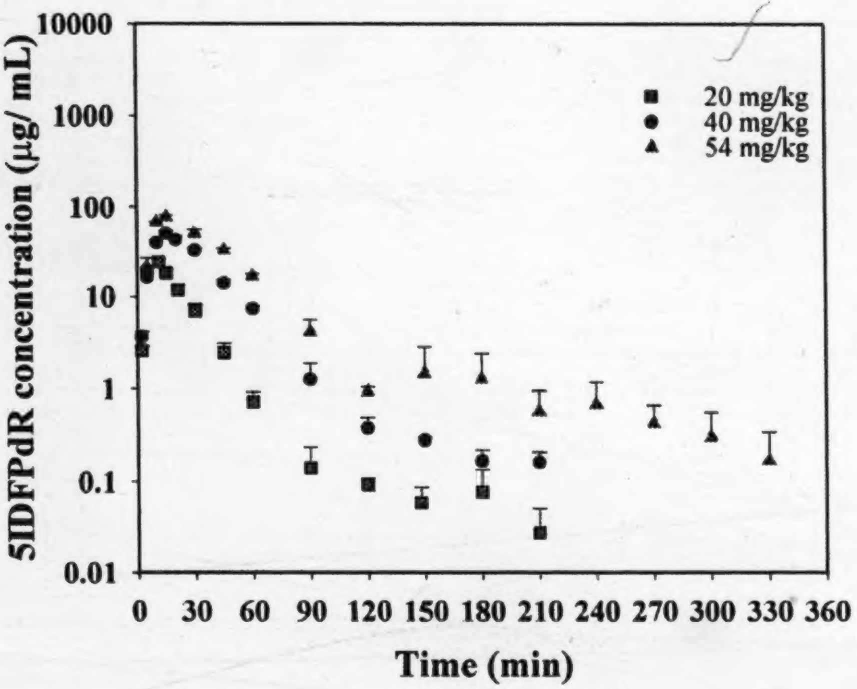

Figure 3.5. Mean (+S.D.) concentrations of 5-IDFPdR in rat blood following oral administration at 20, 40 and 54 mg/kg (n=3 or 4).

The results of urinary recovery of 5-IDFPdR following iv and po dosing, and the results of biliary recovery of 5-IDFPdR following iv administration to male SD rats at the three different dose levels (see above) are summarized in Tables 3.6, 3.7 and 3.8. The quantified metabolites consist only of glucuronides and sulfate conjugates.

Table 3.6. Percent of the 5-IDFPdR dose recovered as unchanged and unchanged plus metabolites in the urine, and mean renal clearance after iv and po administration of 5-IDFPdR to rats at three different dose levels. The data represent the mean (S.D.) values, n = 3.

5-IDFPdR	Intravenous doses (mg/kg)			Oral doses (mg/kg)		
	5	15	54	20	40	54
($^{1}X_{uu}$ /dose)*100	1(0.3)	1(0.5)	1.7(0.3)	0.7(0.2)	1.2 (0.3)	2.3(0.2)
($^{1}X_{u}$ /dose)*100	8(3)	8(2.2)	9(2.7)	4(1.1)	4.1(1.5)	11.7(0.5)
Cl_r (mL/min/kg)	0.29	0.32	0.32	0.26	0.28	0.39

[1] X_{uu} and X_u are the amounts of unchanged and total 5-IDFPdR (including only the glucuronide and sulfate conjugates) recovered in the urine, respectively.

Cl_r (mL/min/kg) has been calculated from the ratio of the mean amount of unchanged 5-IDFPdR excreted in the urine over the mean AUC at each dose level.

Unpaired t- test has been used to compare the means at various dose levels. A *P*-value of less than 0.05 is considered to be significant: There are no significant differences in X_{uu} and X_u values between the iv and po dosed rats at the highest dose (54 mg/kg). There is however, a statistically significant difference between the X_u value at the highest oral dose (54 mg/kg) relative to the X_u value at the intermediate oral dose (40 mg/kg).

Table 3.7. Mean percent of the 5-IDFPdR dose recovered as sulfates and glucuronides in the urine after iv and po administration of 5-IDFPdR to rats at three different dose levels.

5-IDFPdR -	Intravenous doses (mg/kg)			Oral doses (mg/kg)		
conjugates (%)	5	15	54	20	40	54
β-glucuronides	2.2	4.0	4.9	1.4	2.7	6.9
sulfates	4.8	3.0	2.3	1.9	1.0	2.5

Table 3.8. Mean percent of the 5-IDFPdR dose recovered as unchanged, and unchanged plus metabolites in the bile following iv administration of 5-IDFPdR to rats at three different dose levels. The data represent the mean (S.D.) values, n = 3.

5-IDFPdR	5 mg/kg	15 mg/kg	54 mg/kg
([1]A_{bu}/dose)*100	undetectable	0.10 (0.01)	0.11(0.02)
([2]A_b/dose)*100	10.3 (0.5)	3.8 (0.4)	1.3 (0.2)
[2]A_b (mg)	0.18 (0.01)	0.21 (0.01)	0.22 (0.03)

[1] A_{bu} is the amount of unchanged 5-IDFPdR excreted in the bile.

[2] A_b represents the amount of total 5-IDFPdR (i.e., unchanged plus glucuronides and sulfates) at each dose level.

Table 3.9. Mean absolute amounts (mg) of 5-IDFPdR glucuronides and sulfate conjugates recovered in the bile following iv administration of 5, 15 and 54 mg/kg doses (the mean of the actual administered doses are given in parantheses). Data are mean (S.D.) values from 3 rats at each dose level.

5-IDFPdR	5 mg/kg (1.7 mg)	15 mg/kg (5.3 mg)	54 mg/kg (16.1 mg)
β-glucuronides	0.17 (0.02)	0.18 (0.01)	0.18 (0.03)
sulfates	$5.3\text{x}10^{-3}$ ($2.0\text{x}10^{-3}$)	$1.3 \text{ x } 10^{-2}$ ($5.0\text{x}10^{-3}$)	$8.1 \text{ x } 10^{-3}$ ($7.0\text{x}10^{-3}$)

3.3.8. Blood-to-plasma ratio of 5-IDFPdR

The results of an in vitro distribution study of 5-[^{125}I] IDFPdR between blood cells and plasma, following incubation of 5-[^{125}I] IDFPdR with fresh rat blood at 37 °C for 1 h at 1.75, 3.5, and 35 μg/mL concentrations are summarized in the Table 3.8.

Table 3.8. In vitro blood-to-plasma ratio of 5-IDFPdR (rat blood)

5-IDFPdR concentration in blood (μg/mL)	Blood-to-Plasma Ratio
1.75	4.9 (0.2)
3.5	4.2 (0.1)
35	3.8 (0.1)

Data represent the mean (S.D.) of triplicate measurements at each concentration

3.4. Discussion

5-IDFPdR, a 3rd generation *C*-aryl nucleoside mimic, was found to be both very lipophilic (log P = 2.8), and very stable in vitro. The high lipophilicity of this compound, compared to IUdR (log P= -0.95) [Ghosh and Mitra, 1991], would be expected to alter tissue biodistribution, especially through facile diffusion across the blood-brain-barrier (BBB), and into other lipoidal tissues. In contrast to classical 5-substituted-2'-deoxyuridines such as IUdR, which readily undergo deglycosylation (phosphorolysis) in the presence of pyrimidine phosphoylases (Ghosh and Mitra, 1992, Klecker et al., 1995), 5-IDFPdR was found to be resistant to phosphorolysis by bacterial thymidine phosphorylase.

In contrast to the fairly low plasma protein binding reported for thymidine (~22%) [Borg et al., 1997] and 3'-azido-3'-deoxythymidine (AZT; ~20%) [Burger et al., 1995], bovine serum albumin binding for 5-IDFPdR was found to be moderate (70 to 75 %) and not concentration dependent over the examined range of 5-IDFPdR concentrations (see Table 3.2).

5-IDFPdR exhibited low cytotoxicity ($IC_{50} = 10^{-4}$ M range) against KBALB, KBALB-STK, 143B, and 143B-LTK cancer cell lines, as assessed by MTT cytotoxicity assay (see Figure 3.2 and Table 3.3). Moreover, it exhibited similar cytotoxicity against nontransfected (KBALB, 143B) and the corresponding HSV-1 TK transfected cancer cell lines (KBALB-STK, 143B-LTK).

Cellular DNA content analysis by flow cytometry showed an increase in fraction of KBALB cells in sub-G1 zone of DNA content histograms with increasing 5-IDFPdR concentrations. While this fraction likely contains some apoptotic cells, mechanically damaged cells, cell debris and necrotic cells would also appear in this region, due to the low sensitivity of DNA extraction assays in detection of apoptosis. More sensitive apoptosis detection assays would have to be performed before a true assessment of the extent of apoptosis induced by 5-IDFPdR can be made. Such assays may involve the simultaneous use of two different dyes, such as Annexin V and PI, to allow for differentiation between populations of live cells, from the early apoptotic cells, and from the late apoptotic or necrotic cells, on the basis of their differential staining with the two markers (Van England et al., 1998; Fadok et al., 1992; Koopman et al., 1994).

In antiviral assays, 5-IDFPdR appeared to be inactive (at concentrations up to 400 μg/mL) against a variety of viral strains (for details see Wang et al., 2001b), including HSV-1, HSV-2, varicella-zoster virus (VZV), vaccinia virus, vesicular stomatitis, cytomegalovirus (CMV) and human immunodeficiency viruses (HIV-1 & HIV-2).

There are a variety of plausible explanations for the observed lack of cytotoxicity of 5-IDFPdR and related 1-(2-deoxy-β-D-ribofuranosyl)-2,4-difluoro-5-substituted benzenes. In vitro studies indicate that 5-IDFPdR is a good substrate for mitochondrial thymidine kinase (TK2), but not cellular thymidine kinase (TK) [Wiebe LI, Sun W, Zhou A, Naimi E, Stahlshmidt A, Al-Madhoun A, Machulla H-J, Eriksson S, Knaus EE, unpublished data]. The low affinity of 5-IDFPdR for cellular thymidine kinase may result in an inefficient phosphorylation of 5-IDFPdR to the 5'-monophosphate form, which could partially account for the observed lack of cyotoxicity of 5-IDFPdR. The observed negligible differences in anticancer activities of 5-IDFPdR and related 1-(2-deoxy-β-D-ribofuranosyl)-2,4-difluoro-5-substituted benzenes between nontransfected (KBALB, 143B) and the viral TK transfected (KBALB-STK, 143B-LTK) cancer cell lines, and the reported negligible differences in their antiviral activities against TK^+ versus TK^- viral strains (Wang et al., 2001b) may support the "lack of efficient phosphorylation" hypothesis.

It has been reported that 5-MeDFPdR-triphosphate is inserted into replicating DNA strands by the Klenow fragment of *E. Coli* DNA polymerase 1, and that DNA chain elongation continues even after insertion of 5-MeDFPdR (Moran et al., 1997a,b). Thus, it is possible that these *C*-nucleosides become incorporated into DNA, but are inherently nontoxic, possibly due to a perfect mimicry to naturally occurring deoxyribonucleosides.

Alternatively, it is possible that these compounds are devoid of anticancer/antiviral activity, due to their inability to inhibit thymidylate synthase (TS), which is a well known molecular target for the cytotoxic/cytostatic effects exhibited by numerous active nucleoside analogues, such as 5-fluoro-2'-deoxyuridine, (*E*)-5-(2-iodovinyl)-2'-deoxyuridine and 5-(1-azidovinyl)-2'-deoxyuridine (Balzarini et al., 1995). Future biochemical studies would be needed to determine the molecular targets of this class of nucleoside mimics, and to definitively uncover the underlying reasons for their apparent lack of significant anticancer/antiviral activity.

The pharmacokinetics of 5-IDFPdR was studied in male Sprague-Dawley rats following iv-bolus administration of 5, 15, and 54 mg/kg doses, and oral administration of 20, 40 and 54 mg/kg doses (Tables 3.4 and 3.5, Figures 3.4 and 3.5). The hapatobiliary excretion of 5-IDFPdR was studied following iv-bolus administration of 5, 15, and 54 mg/kg doses (Tables 3.8 and 3.9). Following iv administration at 5 and 15 mg/kg, 5-IDFPdR was eliminated from blood in a biphasic fashion with an elimination half-life of 8-9 min. Accordingly, a good fit to a two compartment model was obtained at these two dose levels. Upon increasing the dose from 5 to 15 mg/kg, the total body clearance (Cl_T) was only very slightly increased from ~ 28 mL/min/kg to ~ 32 mL/min/kg, the AUC was increased almost proportionally to the dose and AUC_{norm} remained practically unchanged, providing an overall picture of linear kinetics. Increasing the dose 3.6 fold, from 15 to 54 mg/kg, however, led to an almost 6 fold increase in the AUC and a 44% increase in the dose normalized AUC (~0.19 kg.min. mL^{-1}). Accordingly, there was a decreased Cl_T (~19 mL/min/kg) accompanied by an increased elimination half-life (~22 min) at the highest dose relative to the lower doses.

The blood concentration-time profiles of 5-IDFPdR following oral administration of 20 and 40 mg/kg doses also fit the two compartment model. At the highest administered iv and oral doses (54 mg/kg), the blood concentration-time profiles differed somewhat from animal to animal and could be fitted with either one or two compartment models. AUC_{norm} increased by 49% as the oral dose increased from 20 to 40 mg/kg, and further by 55% as the dose was increased from 40 mg/kg to 54 mg/kg. Moreover, there was a decrease in Cl_T from 37 mL/min/kg at the 20 mg/kg dose to 17 mL/min/kg at the 54 mg/kg oral dose and a significant increase in elimination half-life with increasing oral doses (Table 3.5).

The results of the 5-IDFPdR urinary recovery study (Table 3.6) show a slight increase in the fraction of unchanged 5-IDFPdR and unchanged plus metabolites (only glucuronides and sulfate conjugates of 5-IDFPdR were quantified in these studies) as the iv dose was increased from 15 to 54 mg/kg. A more pronounced increase in the urinary recovery of these fractions was, however, observed with increase in the oral dose: the fractions of unchanged and unchanged plus metabolites were increased from 0.7 and 4% to 2.3 and 11.7 %, respectively, as the oral dose increased from 20 to 54 mg/kg. The overall recovery of unchanged 5-IDFPdR in the urine was very small (0.7-2.3 %) regardless of the dose. Of the phase II metabolites (glucuronides and sulfates) recovered in the urine, the glucuronide conjugates prevailed at the highest iv/oral dose, while sulfates accounted for the greater part of metabolic recovery at the lowest dose (Table 3.7).

The mean fractions of the dose recovered in bile following iv dosing at 5, 15 and 54 mg/kg as unchanged 5-IDFPdR and as unchanged plus glucuronide and sulfate conjugates are summarized in Table 3.8. Approximately 0.1 % of the dose was recovered as unchanged 5-IDFPdR in the bile. More than 97 % of the unchanged compound was recovered from bile samples collected in the first two hours following iv dosing. At all three doses, the glucuronide conjugates of 5-IDFPdR accounted for most of the metabolites recovered (Table 3.9). While fraction of the unchanged 5-IDFPdR in the bile appears to have remained the same with the increase in dose, the fraction of glucuronides recovered was reduced from ~ 10 % at 5 mg/kg to ~ 3.4 % at 15 mg/kg, and was further decreased to ~ 1 % as the dose was increased to 54 mg/kg.

Overall, the results of these studies suggest that 5-IDFPdR exhibits nonlinear, and more specifically, dose-dependent pharmacokinetics. Dose-dependent pharmacokinetics are commonly reflected in a greater than or less than proportional increase in the area under the drug concentration-time curve (AUC) with increase in dose (Lin, 1994). The mechanisms of dose-dependent pharmacokinetics of drugs vary widely, and nonlinearities in any or all pharmacokinetic processes, including absorption, distribution, metabolism and elimination, could contribute to the overall dose-dependent phenomenon. In this study, increasing the orally administered 5-IDFPdR dose led to a greater than proportional increase in AUC. A disproportionate increase in AUC with dose was also observed following administration of the highest intravenous dose (54 mg/kg). The dose-normalized AUC's were not superimposable, as would be expected in the case of linear kinetics, and they increased with increasing oral and iv doses (except upon increasing the iv dose from 5 mg/kg to 15 mg/kg). This phenomenon may be attributed to an increase in absorption and/or a decrease in elimination with increasing dose.

The fairly high blood clearance (37 mL/min/kg) of 5-IDFPdR relative to the hepatic blood flow of rats (40 to 60 mL/min/kg) following administration of the lower oral dose (20 mg/kg) suggests that 5-IDFPdR at lower doses might be a high hepatic extraction drug with low systemic bioavailability, and that dose-dependence in absorption may contribute to the overall observed pharmacokinetic nonlinearity. It would then be expected that with increasing oral doses, the first-pass metabolism would gradually become more saturated, the bioavailability would increase and would eventually become marginally dose-dependent. Because of nonlinear kinetics, however, an accurate determination of oral bioavailability was not possible based on the present study design. Mere estimates of bioavailability may be obtained by comparison of the mean AUC_{po} with mean AUC_{iv} at the same dose (54 mg/kg). Based on this comparison, an Fa value slightly greater than one is obtained, as mean AUC_{po} was marginally greater than mean AUC_{iv} ($P = 0.0493$). The accuracy of this bioavailability estimate, however, remains questionable due to the presence of nonlinear kinetics and may be overestimated (Kempf et al., 1995).

While non-linearity in the absorption of 5-IDFPdR remains a plausible mechanism that may have contributed to the observed nonlinear kinetics, more accurate dose-range assessments of bioavailability would be needed before such hypothesis could be validated. For drugs exhibiting nonlinear kinetics, concomitant administration of the intravenous reference dose and the oral dose would provide more accurate estimates of bioavailability. Using a tracer dose of the isotopically labeled drug as the reference iv treatment, the concurrent iv and oral treatments can be easily distinguished. Both labeled and unlabeled analytes may then be simultaneously tracked and quantitated using LC/MS/MS technology (Yeh et al., 1999).

As indicated earlier, elimination of 5-IDFPdR from the body was reduced with an increase in dose (Tables 3.4 and 3.5): Cl_T decreased from 32 mL/min/kg at 15 mg/kg (iv) to 19 mL/min/kg at 54 mg/kg (iv). An even more pronounced decrease in Cl_T was observed with increasing oral doses: increasing the oral dose two-fold (from 20 mg/kg to 40 mg/kg) led to ~ 36 % decrease in Cl_T (from 37 mL/min/kg to 24 mL/min/kg) and a further dose increase from 40 to 54 mg/kg (1.35-fold) led to ~ 30 % reduction in Cl_T values (from 24 mL/min/kg to 17 mL/min/kg).

In the case of linear kinetics, the fraction of the drug and metabolites recovered in the urine would be expected to remain the same regardless of the dose. In the case of 5-IDFPdR, however, it was observed that the urinary recovery of unchanged 5-IDFPdR as well as urinary recovery of unchanged plus metabolites (only glucuronides and sulfate conjugates of 5-IDFPdR were quantified in the present study) were somewhat increased at the highest dose (Table 3.6).

Both saturable renal excretion and saturable non-renal metabolism (including saturable hepatic metabolism) may contribute to the overall nonlinear elimination of the drugs. Saturation of renal clearance is unlikely to be contributing to the decreased total body clearance of 5-IDFPdR with increase in oral dose, as the renal clearance estimates obtained from the ratio of total drug excreted unchanged in the urine (X_U^∞) over AUC, suggest that renal clearance plays a minor role in the elimination of 5-IDFPdR. Moreover, renal clearance either remained almost unchanged when the iv/oral doses were increased or was increased as the oral dose increased from 40 mg/kg to 54 mg/kg (Table 3.6).

The increased recovery of the unchanged 5-IDFPdR in the urine with increase in oral dose could in theory be due to increased bioavailability, increased renal clearance, or capacity-limited metabolism of 5-IDFPdR as illustrated through following equations (Rowland and Tozer, 1995):

$X_U^\infty/\text{dose} = fe \cdot \text{Fa}$ and $fe = Cl_r / (Cl_r + Cl_{nr})$

(X_U^∞ is the total amount of compound excreted unchanged in the urine, *fe* is the fraction excreted unchanged, Fa is the bioavailability, Cl_r and Cl_{nr} represent the renal and nonrenal clearances.)

The increased urinary recovery of 5-IDFPdR metabolites at higher oral dose could have also been theoretically caused by an increased (dose-dependent) bioavailability with increase in dose, although estimated Fa at an intermediate dose of 5-IDFPdR (calculated from the dose-corrected ratio of $AUC_{po\ (20\ mg/kg)}$ divided by $AUC_{iv\ (15\ mg/kg)}$) suggests that Fa is quite high even at the intermediate dose. Thus, an increase in Fa upon increasing the administered dose may not be as important a contributor to the observed increase in recovery of both unchanged 5-IDFPdR and its metabolites. Increased renal clearance and/or saturable hepatic metabolism might have contributed to the increased urinary recovery of unchanged drug at the highest oral dose, but the extent of their possible contribution cannot be discerned here.

Since total body clearance, which represents the sums of renal and metabolic clearances, was reduced at higher doses and renal clearance was insignificant and either unaffected by an increase in the dose or else increased at higher doses, it may be postulated that 5-IDFPdR exhibits saturable hepatic and/or non-renal metabolism ($Cl_{nr} \downarrow$).

If hepatic metabolism of 5-IDFPdR were to be saturated at the higher doses, the observed greater urinary recovery of certain 5-IDFPdR metabolites (e.g., glucuronides) at the highest dose might indicate that phase II conjugation reactions other than glucuronidation are becoming saturated at very high doses of 5-IDFPdR. It is, for instance, known that among phase II conjugation reactions, glucuronidation reactions may demonstrate saturation kinetics at very high drug concentrations due to their high capacity. In contrast, conjugations with glycine, sulfate, and glutathione tend to be saturated even at therapeutic drug concentrations, due to their lesser capacity (Shargel and Yu, 1995). The observation that glucuronide conjugates of 5-IDFPdR accounted for the greater part of metabolic recovery at the highest iv/oral dose (Table 3.7), whereas sulfate conjugates prevailed at the lowest dose, seems to support the dose-dependent and capacity-limited saturation of phase II metabolic reactions for 5-IDFPdR.

The 5-IDFPdR biliary metabolite recovery data (Tables 3.8 and 3.9) suggest that formation and/or biliary transport of 5-IDFPdR glucuronides and sulfates would have been saturating at iv doses lower than our lowest administered iv dose (5 mg/kg). In general, reduced formation of such conjugated metabolites could occur as a result of reduced availability of cofactors such as UDPGA (uridine diphosphate glucuronic acid) and PAPS (3'-phosphoadenosine-5'-phosphosulfate) and/or the transferase enzymes that are required for the formation of the conjugates and would be depleted at times of high demand (Lin, 1994; Shargel and Yu, 1999). In the case of 5-IDFPdR, urinary recoveries of these conjugates, especially glucuronides, was not reduced at higher doses, suggesting that saturable formation of these metabolites by the liver is unlikely to be the cause of their reduced recovery in the bile at higher doses. Instead, saturable transport of these metabolites into the bile may offer a better explanation for the observed saturation in the biliary excretion of 5-IDFPdR metabolites. It is known that active biliary transport systems such as the canalicular multispecific organic anion transporter and P-glycoproteins play an important role in excretion of xenobiotics and their glucuronide conjugates in the rats (Shimamura et al., 1994). Saturation of the active transport by one or more of these transporters, which may be involved in the efficient biliary excretion of 5-IDFPdR metabolites, might offer an explanation for the observed saturation in the biliary excretion of 5-IDFPdR metabolites.

Nonlinear distribution due to saturable plasma protein binding, saturable blood cell binding and/or saturable tissue binding may also have played a role in the nonlinear handling of 5-IDFPdR. It is known that volume of distribution is directly related to plasma protein binding and inversely related to tissue binding, as shown by the following equation:

$$V_d = V_p + V_t * (f_u / f_t)$$

V_d is the volume of distribution, V_p is the plasma volume, V_t is the volume of tissues, and f_u and f_t are the fractions of unbound drug in the plasma and tissue, respectively. From this equation, it can be seen that saturation of plasma protein binding, which results in increased f_u levels, could lead to an increase in the volume of distribution of the drug with dose. Conversely, saturation of tissue binding and the resulting increased f_t levels would reduce the volume of distribution (Lin, 1994). In addition to their opposing effects on the volume of distribution, saturable plasma protein binding and saturable tight tissue binding may lead to lesser or greater than proportional increases in AUC with increase in dose, respectively. In the case of 5-IDFPdR, saturable tissue binding may have further contributed to the observed greater than proportional increase in AUC with dose. This possibility would, however, have to be explored in studies in which nonlinearity of tissue binding are assessed by examining the ratio of the drug concentration in a given tissue to that in plasma. Nonetheless, the possible presence of saturable tight tissue binding does not preclude the possibility for coexistence of saturable plasma protein binding. The observed increase in the volume of distribution (Vss) of 5-IDFPdR with increase in iv dose (Table 3.4), may well be an indication of saturable plasma protein binding. Further studies are needed to determine whether nonlinear distribution due to the saturable binding to plasma proteins and/or saturable tissue binding is playing a role in the nonlinear kinetics of 5-IDFPdR.

In addition to saturable plasma protein and tissue binding, saturable blood cell binding can introduce concentration-dependence in the blood-to-plasma concentration ratio of a given drug. Over the examined range of 5-IDFPdR concentrations (1.75 to 35 µg/mL), 5-IDFPdR appears to have a greater distribution into blood cells relative to plasma and there is a slight concentration dependence in the observed blood-to-plasma ratios. It is therefore quite likely that at very high blood concetrations of 5-IDFPdR, saturable blood cell binding contributes to the observed nonlinear increase in AUC. Further pharmacokinetic studies based on plasma concentrations of 5-IDFPdR at various doses would be needed to explore the extent of dose-dependence in blood-to-plasma concentration ratio of 5-IDFPdR.

In conclusion, 5-IDFPdR exhibits dose-dependent pharmacokinetics. Decreased elimination of 5-IDFPdR with increasing dose, as supported by longer elimination half-lives at higher doses, is one likely mechanism contributing to the dose-dependent behavior of this compound. Saturable non-renal metabolism might explain the reduced total body clearance of 5-IDFPdR at higher doses, despite the unchanged or increased urinary clearance.

For drugs exhibiting nonlinear kinetics, the dosage regimens may need to be carefully designed to avoid potential unpredictable toxicity and/or lack of pharmacological response associated with the disproportional changes in steady state drug concentrations on changing dose. Manifestation in the rat of nonlinear kinetics at doses of 5-IDFPdR, which may be of therapeutic relevance, warrants extended dose-range evaluations of this compound in future preclinical and clinical studies to establish safe and efficacious dosage regimens.

3.5. References

Aketani S, Tanaka K, Yamamoto K, Ishihama A, Cao H, Tengeiji A, Hiraoka S, Shiro M, Shionoya M. Syntheses and structure-activity relationships of nonantural β-*C*-nucleoside 5'-triphosphates bearing an aromatic nucleobase with phenolic hydroxy groups: Inhibitory activities against DNA polymerases. J Med Chem 2002;45:5594-5603.

Barton DHR, Ramesh M. Tandem nucleophilic and radical chemistry in the replacement of the hydroxyl group by a carbon carbon bond - a concise synthesis of showdomycin. J Am Chem Soc 1990;112:891-892.

Belmans M, Esmans E, Dommisse R, Lepoivre J, Alderweireldt F, Balzarini J, De Clercq E. Synthesis and biological evaluation of a series of substituted 2-pyridine *C*-nucleosides .1. Coupling reaction of organo-metallic pyridine compounds with 2,4-3,5-di-o-benzylidene-aldehydo-D-ribose. Nucl & Nucleotides 1985;4:523-538.

Bergstrom DE, Zhang PM. An efficient route to C-4 linked imidazole nucleosides - synthesis of 2-carbamoyl-4-(2'-deoxy-beta-D-ribofuranosyl)imidazole. Tetrahedron letters 1991;32:6485-6488.

Borg N, Zhou X-X, Johansson N-G, Oeberg B, Staehle L. Distribution to the brain and protein binding of 3'- and 5-substituted 2',3'-dideoxyuridine derivatives, studied by microdialysis. Antivir Chem Chemother 1997; 8:47-53.

Brown DM, Burdon MG, Slatcher RP. A synthesis of pseudouridine and of 5-beta-D-ribofuranosyluridine. J Chem Soc, section C 1968;1051-1053.

Buchanan JG, Jumaah AO, Kerr G, Talekar RR, Wightman RH. *C*-nucleoside studies .22. Cine-substitution in 1,4-dinitropyrazoles - further model studies, an improved synthesis of formycin and pyrazofurin and the synthesis of some 3(5)-alkylsulfonyl-4-amino-5(3)-beta-D-ribofuranosylpyrazoles. J Chem Soc, Perkins Trans 1(5) 1991,1077-1083.

Burger DM, Meenhorst PL, Beijnen JH. Concise overview of the clinical pharmacokinetics of dideoxynucleoside antiretroviral agents. Pharm World Sci 1995;17:25-30.

Casiraghi G, Cornia M, Rassu G, Delsante C, Spanu P. Synthesis and transformation of pyrrole C-glycoconjugates. Tetrahedron 1992;48:5619-5628.

Chaudhuri NC, Ren RX-F, Kool ET. *C*-Nucleosides derived from simple aromatic hydrocarbons. Synlett 1997:341-347.

Chou TC, Kong XB, Fanucchi MP, Cheng YC, Takahashi K, Watanabe KA, Fox JJ. Synthesis and biological effects of 2'-fluoro-5-ethyl-1-beta-D-arabinofuranosyluracil. Antimicrob Agents Chemother 1987;31:1355-1358.

Collins JM, Unadkat JD. Clinical pharmacokinetics of zidovudine- an overview of current data. Clin Pharmacokinet 1989;17:1-9.

Cretton EM, Waterhous DV, Bevan R, Sommadossi J-P. Glucuronidation of 3'- azido-3'-deoxythymidine by rat and human liver microsomes. Drug Metab Dispos 1990;18:369-372.

Darzynkiewicz Z, Juan G. DNA content measurement for DNA ploidy and cell cycle analysis. Current protocols in cytometry 1997; 7.5.1-7.5.24. John Wiley & Sons, Inc.

De Clercq E. Biochemical aspects of the selective antiherpes activity of nucleoside analogues. Biochem Pharmacol 1984;33:2159-2169.

Du JF, Qu FC, Lee DW, Newton MG, Chu CK. 1,3-Dioxolane *C*-nucleosides - asymmetric-synthesis of 4 stereoisomers of 2-[2-(hydroxymethyl)-1,3-dioxolan-5-yl)]-1,3-thiazole-4-carboxamide. Tetrahedron Lett 1995;36:8167-8170.

Evelo CTA, Versteegh JFM, Blaauboer BJ. Kinetics of the formation and secretion of the aniline metabolite 4-aminophenol and its conjugates by isolated rat hepatocytes. Xenobiotica 1984;14:409-416.

Fadok VA, Voelker DR, Cammpbell PA, Cohen JJ, Bratton DL, Henson PM. Exposure of phosphatidylserine on the surface of apoptotic lymphocytes triggers specific recognition and removal by macrophages. J Immunol 1992;148:2207-2216.

Farkas J, Flegelova Z, Sorm F. Synthesis of pyrazomycin. Tetrahedron Lett 1972;22:2279-2280.

Ghosh MK and Mitra AK. Brain parenchymal metabolism of 5-iodo-2'-deoxyuridine and 5'-ester prodrugs. Pharm Res 1992;9:1048-1052.

Ghosh MK and Mitra AK. Effects of 5'-ester modification on the physiochemical properties and plasma protein binding of 5-iodo-2'-deoxyuridine. Pharm Res 1991;8:771-775.

Gibaldi M, Perrier D. Pharmacokinetics. 2nd edition, Marcel Dekker, Inc.; New York and Basel, 1982.

Guckian KM, Kool ET. Highly precise shape mimicry by a difluorotoluene deoxynucleoside, a replication-competent substitute for thymidine. Angew Chem Int Ed Engl 1997;36:2825-2827.

Guild BC, Finer MF, Housman DE, Mulligan RC. Development of retroviral vectors useful for expressing genes in cultured embryonal and hematopoietic cells in vivo. J Virol 1988;62:3795-3801.

Hansch C, Elkins D. Partition coefficients and their uses. Chem Rev 1971;71:525-554.

Kalvoda L, Farkas J, Sorm F. Synthesis of showdomycin. Tetrahedron Lett 1970;26:2297-2300.

Kempf DJ, Marsh KC, Denissen JF, McDonald E, Vasavanonda S, Flentge CA, Green BE, Fino L, Park CH, Kong XP, Wideberg NE, Saldivar A, Ruiz L, Kati WM, Sham HL, Robins T, Stewart KD, Hsu A, Plattner JJ, Leonard JM, Norbeck DW. ABT-538 is a potent inhibitor of human immunodeficiency virus protease and has high oral bioavailability in human. Proc Natl Acad Sci 1995;92:2484-2488.

Khalili P, Naimi E, Knaus EE, Wiebe LI. Pharmacokinetics and metabolism of the novel synthetic *C*-nucleoside, 1-(2-deoxy-β-D-ribofuranosyl)-2,4-difluoro-5-iodobenzene: a potential mimic of 5-iodo-2'-deoxyuridine. Biopharm Drug Dispos 2002;23:105-113.

Klecker RW, Jenkins JF, Kinsella TJ, Fine RL, Strong JM, and Collins JM. Clinical pharmacology of 5-iodo-2'-deoxyuridine and 5-iodouracil and endogenous pyrimidine modulation. Clin Pharmacol Ther 1985;38:45-51.

Koopman G, Reutelingsperger CPM, Kuijten GA, Keehnen RM, Pals ST, Van Oers MH. Annexin V for flow cytometric detection of phosphatidylserine expression on B cells undergoing apoptosis. Blood 1994;84:1415-1420.

Kornberg A, Baker T. In: DNA Replication. 2nd edition, Freeman WH; New York, 1992. P.113.

Lerch U, Burdon MG, Moffat JG. C-glycosyl nucleosides. I. Studies on the synthesis of pseudouridine and related compounds. J Org Chem 1971;36:1507-1513.

Lin JH. Dose-dependent pharmacokinetics: Experimental observations and theoretical considerations. Biopharm Drug Dispos 1994;15:1-31.

Lin JH. Role of pharmacokinetics in the discovery and development of Indinavir. Adv Drug Deliv Rev 1999;39:33-49.

Loeb LA, Kunkel TA. Fidelity of DNA synthesis. Ann Rev Biochem 1982:51:429-457.

Mentel R, Kurek S, Wegner U, Janta-Lipinski M, Guertler L, Matthes E. Inhibition of adenovirus DNA polymerase by modified nucleoside triphosphate analogs correlate with their antiviral effects on cellular level. Med Microbiol Immunol 2000;189:91-95.

Mercer JR, Xu LH, Knaus EE, Wiebe LI. Synthesis and tumor uptake of 5-Br-82-labeled and 5-I-131-labeled 5-halo-1-(2-fluoro-2-deoxy-beta-D-ribofuranosyl)uracils. J Med Chem 1989;32:1289-1294.

Miller TR, Alley SC, Reese AW, Solomon MS, McCallister WV, Mailer C, Robinson BH, Hopkins PB. A probe for sequence-dependent nucleic-acid dynamics. J Am Chem Soc 1995,117:9377-9378.

Montgomery JA. Approaches to antiviral chemotherapy. Antiviral Res 1989;12:113-132.

Moran S, Ren RX-F, Kool ET. A thymidine triphosphate shape analog lacking Watson-Crick pairing ability is replicated with high sequence selectivity. Proc Natl Acad Sci USA 1997a;94:10506-10511.

Moran S, Ren RX-F, Rumney S, Kool ET. Difluorotoluene, a nonpolar isostere for thymidine, codes specifically and efficiently for adenine in DNA replication. J Am Chem Soc 1997b; 119:2056-2057.

Mossman T. Rapid colorimetric assay for cellular growth and survival-Application to proliferation and cyto-toxicity assays. J Immunol Methods 1983;65:55-63.

Naimi E, Wiebe LI, Balzarini J, De Clercq E, Knaus EE. Synthesis of 1-(2-deoxy-β-D-ribofuranosyl)-2,4-difluoro-5-(2-halo-1-hydroxyethyl)benzenes and related derivatives: "Thymine replacement" analogs of deoxythymidine for evaluation as antiviral and anticancer agents. Drug Development Research 2001:52:492-499.

Oldfield EH, Ram Z, Culver KW, Blaese RM, De Vroom HL, Anderson WF. Hum Gene Ther 1993;4:39-69.

Parang K, 1997. Evaluation of myristic acid analogs & 5'-O-ester prodrugs of dThd, AZT & FLT. Ph.D. Thesis, University of Alberta, p.133.

Perigaud C, Gosselin G, Imbach JL. Nucleoside analogues as chemotherapeutic agents: a review. Nucleosides Nucleotides 1992;11:903-945.

Puglisi JD, Chen L, Blanchard S, Frankel AD. Solution structure of a bovine immunodeficiency virus TAT-TAR peptide-RNA complex. Science 1995;270:1200-1203.

Ren XF, Schweitzer BA, Sheils CJ, Kool ET. Formation of stable DNA loops by incorporation of nonpolar, non-hydrogen-bonding nucleoside isosteres. Angew Chem Int Ed Engl 1996;35:743-746.

Robins MJ, Manfredini S, Wood SG, Wanklin RJ, Rennie BA, Sacks SL. Nucleic acid related compounds. 65. New syntheses of 1-(beta-D-arabinofuranosyl)-5(E)-(2-iodovinyl)uracil (IVAraU) from vinylsilane precursors. Radioiodine uptake as a marker for thymidine kinase positive herpes viral infections. J Med Chem 1991;34:2275-2280.

Rowland M, Tozer TN. Clinical Pharmacokinetics: Concepts and Applications. 3rd edition. Williams & Wilkins; Baltimore, USA, 1995.

Schwartz M. Thymidine phosphorylase from *Escherichia Coli*. Methods Enzymol 1978; LI;442-445.

Schweitzer BA, Kool ET. Aromatic nonpolar nucleosides as hydrophobic isosteres of pyrimidine and purine nucleosides. J Org Chem 1994, 59:7238-7242.

Schweitzer BA, Kool ET. Hydrophobic, non-hydrogen-bonding bases and base pairs in DNA. J Am Chem Soc 1995;117:1863-1872.

Shargel L, Yu A. Applied Biopharmaceutics & Pharmacokinetics. 4th edition. Appleton & Lange; Stamford, Connecticut, 1999.

Solomon MS, Hopkins PB. Chemical synthesis and characterization of duplex DNA containing a new base pair - a nondisruptive, benzofused pyrimidine analog J Org Chem 1993;58:2232-2243.

Stretcher BN. Pharmacokinetic optimization of antiretroviral therapy in patients with HIV infection. Clin Pharmacokinet 1995;29:46-65.

Tan XL, Chu CK, Boudinot FD. Development and optimization of anti-HIV nucleoside analogs and prodrugs: A Review of their cellular pharmacology, structure-activity relationships and pharmacokinetics. Adv Drug Deliv Rev 1999;39:117-151.

Togo H, Aoki M, Kuramochi T, Yokoyama M. Radical decarboxylative alkylation onto heteroaromatic bases with trivalent iodine compounds. J Chem Soc Perkin Trans 1(20) 1993:2417-2427.

Togo H, Ishigami S, Fujii M, Ikuma T, Yokoyama M. Synthesis of *C*-nucleosides via radical coupling reaction. J Chem Soc Perkin Trans 1(20)1994;2931-2942.

Tovell DR, Samuel J, Mercer JR, Misra HK, Xu L, Wiebe LI, Tyrrell DL, Knaus EE. The in vitro evaluation of nucleoside analogues as probes for use in the non-invasive diagnosis of herpes simplex encephalitis. Drug Des Deliv 1988;3:213-221.

Trang JM, Prejean JD, James RH, Irwin RD, Goehl TJ, Page JG. Zidovudine bioavailability and linear pharmacokinetics in female B6C3F1 mice. Drug Metab Dispos 1993;21:189-193.

Van Engeland M, Nieland LJW, Ramaekers FCS, Schutte B, Reutelingsperger CPM. Annexin V-affinity assay: A review on an apoptosis detection system based on phosphatidylserine exposure. Cytometry 1998;31:1-9.

Wagner EF, Vanek M, Vennstrom B. Transfer of genes into early embryonal carcinoma cells by retrovirus infections: efficient expression from an internal promoter. EMBO J 1985;4:663-666.

Wang ZX, Duan W, Wiebe LI, Balzarini J, De Clercq E, Knaus EE. Synthesis of 1-(2-deoxy-β-D-ribofuranosyl)-2,4-difluoro-5-substituted-benzenes: 'thymine replacement' analogs of thymidine for evaluation as anticancer and antiviral agents. Nucleosides Nucleotides Nucleic Acids 2001a;20:41-58.

Wang ZX, Duan W, Wiebe LI, Balzarini J, De Clercq E, Knaus EE. Synthesis of 1-(2-deoxy-β-D-ribofuranosyl)-2,4-difluoro-5-substituted-benzene thymidine mimics, some related α-anomers, and their evaluation as antiviral and anticancer agents. Nucleosides Nucleotides Nucleic Acids 2001b;20:11-40.

Yeh KC, Stone JA, Carides AD, Rolan P, Woolf E, Ju WD. Simultaneus investigation of indinavir nonlinear pharmacokinetics and bioavailability in healthy volunteers using stable isotope labeling technique: study design and model-independent data analysis. J Pharm Sci 1999; 88:568-573.

Zhang HC, Brakta M, Daves GD. Palladium-mediated coupling reactions of an amino-substituted heterocycle - direct synthesis of *C*-nucleosides related to adenosine. Nucleosides & Nucleotides 1995;14:105-116.

Evaluation of 5-Iodo-3'-*O*-nitro-2'-deoxyuridine (INUdR), a 5-Substituted-2'-deoxyuridine with an Unnatural 3'-ONO_2 Substituent on the Sugar Ring, as a Potential Nitric Oxide-Releasing Anticancer/Antiviral Agent

---

A version of this chapter is in press: "European Journal of Pharmaceutical Sciences", 2003.

4. Nitric oxide and nitric oxide donors

4.1. Introduction

Nitric oxide (NO) is an important endogenous free radical species, which is involved in a wide range of physiological and pathophysiological processes (Moncada et al., 1991). NO involvement has been found in almost every aspect of human biological processes from controlling blood pressure to neurotransmission. Within the immune system, NO fights infectious diseases, parasites, and tumor cells. NO has also been implicated in heart disease, asthma, hypertension, impotency, shock, and cognitive processes (Hou et al., 1999 and references therein). In the mammalian system, NO is synthesized directly from the amino acid L-arginine by the enzyme NO synthase (NOS) [Moncada et al., 1989]. It has now been established that there are three distinct isoforms of NOS: the endothelial (eNOS) and neuronal (nNOS) NO synthases, that were identified in the vasculature endothelium and neuronal tissues, respectively, and are constitutively expressed, and the inducible NO synthase (iNOS) that was identified first in macrophages and is not present in non-activated cells (Nathan and Xie, 1994; Forstermann, 1994). The latter isoform, iNOS, is unique among the NOS isoforms in that its expression is induced by various inflammatory stimuli and its activity is independent of intracellular Ca^{2+} levels (Stuehr and Griffith, 1992). Upon exposure to inflammatory cytokines or endotoxins, iNOS is expressed in macrophages, liver, vascular endothelial and smooth muscle cells, chondrocytes, myocardium, and many other tissues and cell types (Bredt and Synder, 1994).

4.1.1. An Overview of Some Nitric Oxide Functions within the Immune System

It is known that viral infections caused by RNA or DNA viruses can induce iNOS expression, and the NO synthesized by iNOS can inhibit viral replication (Mannick, 1995). Whether produced endogenously by iNOS or generated from exogenously added NO donors, NO has been shown to have antiviral properties in some animal models (Akarid et al., 1995; Mikami et al., 1996) and in a variety of cell lines: Replication of several viruses, including herpes simplex virus type 1 (Croen, 1993), vesicular stomatitis virus (Bi and Reiss, 1995), vaccinia virus (Harris et al., 1995), coxsackievirus (Lowenstein et al., 1996), poliovirus (Komatsu et al, 1996), and rhinovirus (Sanders et al., 1998), has been shown to be inhibited by induction of NO synthase, or by the addition of NO-donors. Mechanistically, NO appears to interfere with specific stages in the life cycle of viruses. For instance, NO inhibits vaccinia virus DNA synthesis, late protein translation, and virion assembly (Melkova and Esteban, 1995; Harris et al, 1995). Similarly, NO has been reported to inhibit coxsackievirus replication in part by inhibiting viral RNA synthesis (Zaragoza et al., 1997). In addition to interfering with viral targets, it is possible that NO also inhibits various host cell processes that are necessary for viral replication, although in most cases, the precise identity of the host and viral targets of NO are not known (Zaragoza et al., 1997). Although NO is frequently an important mediator in intracellular inhibition of viral replication, it is not the only inhibitor, as many of the interferon inducible proteins can also block viral pathways (Staeheli, 1990). Moreover, NO does not exert antiviral activity against some viruses and in some instances, it may even contribute to the pathogenesis of viral infection (Kreil and Eibl, 1996). Thus, it is not clear if NO has a role in viral clearance or pathogenesis (Reiss and Komatsu, 1998).

In addition to the antimicrobial role of NO, which has been observed for all groups of infectious pathogens in various mammalian species, other host-protective functions of NO within the immune system include its anti-tumor and autotoxic functions. A number of studies have demonstrated that NO causes cytostasis of various tumor cell lines (Hibbs et al., 1988; Stuehr and Nathan, 1989; Sveinbjornsson et al., 1996). Various mechanisms that may account for the observed tumor cell death caused by NO and its reactive nitrogen intermediates have subsequently been identified. Inhibition of mitochondrial iron-sulfur enzymes of the respiratory chain, inhibition of the citric-acid-cycle enzyme *cis*-aconitase (Drapier and Hibbs, 1988), inactivation of the ribonucleotide reductase enzyme (Lepoivre et al., 1990), consumption of cellular adenosine triphosphate by activating the nuclear DNA-repair enzyme poly (ADP-ribose) polymerase (Szabo' et al., 1994), activation of caspases (Brockhaus and Brun, 1998), and accumulation of the wild-type p53, a central regulator of cell growth and apoptosis (Forrester et al., 1996) have all been implicated as mechanisms by which NO exerts its anti-tumor effects. Here again, the function of NO in tumor immunology cannot be easily predicted, as this molecule has also been implicated in promotion of tumor growth, vascularization, and invasiveness (Jenkins et al., 1995; Thomsen et al., 1997). The frequent expression of nitric oxide synthase in human cancers is suggestive of a pathophysiological role for NO in carcinogenesis. Studies on the role of NO in tumor progression have indicated that tumor-associated NO production may promote cancer progression by providing a selective growth advantage to tumor cells with mutant p53 (rather than wild-type p53) and that inhibitors of iNOS may have a therapeutic effect in these tumors (Ambs et al., 1998). The stimulatory effect of NO on the expression of vascular endothelial growth factor (VEGF) by tumor cells and its strong selective pressure for iNOS-positive tumor cells expressing mutant p53 (as opposed to wild-type p53) may partially account for the pro-tumor function of NO in these cases (Chin et al., 1997; Ambs et al., 1998).

4.1.2. Current Approaches to the Development of Nitric Oxide Donors

As nitric oxide research continues to grow, there is an increasing interest in identification and therapeutic exploitation of suitable NO donors. Most of the current NO donors are labile and have a short duration of action. Lack of tissue specificity and development of physiological tolerance with the resulting loss of pharmacological activity further complicates the therapeutic use of NO donors. In the ongoing development of novel NO donors, therefore, attempts should be made to design and synthesize NO donors that are more stable, and are less likely to induce tolerance. Development of specific targeting NO donors or prodrugs and development of hybrid molecules that utilize the biological function of NO with other pharmaceutical moieties are among some of the current approaches in development of more desirable NO donor agents (Hou et al., 1999).

Activation of soluble guanylate cyclase by NO, which stimulates the production of cyclic GMP, and direct interaction of NO with target proteins in a chemical reaction known as *S*-nitrosylation which involves the transfer of NO to the sulfhydryl group of cysteine residues, constitute two major signaling pathways of nitric oxide (Moncada and

Higgs, 1993; Stamler et al, 1992; Jaffrey et al., 2001; Broillet, 1999). *S*-Nitrosylation modifies a number of different proteins posttranslationally and as such, offers the possibility to selectively target an individual protein for *S*-nitrosylation. This can be achieved by directing a NO donor capable of performing *S*-nitrosylation to the protein of interest (Badroff et al., 2002). This approach has recently been successfully utilized by Badroff and coworkers to inhibit the virus encoded enteroviral protease 2A, which is essential for replication of Coxsackie-B-viruses. This was achieved by the targeted delivery of NO to an individual cellular target, the Coxsackieviral protease 2A, by a peptide conjugated dinitrosyl-iron-di-L-cysteine complex (DNIC). The authors concluded that selective modulation of cellular processes by NO, i.e., an enhancement of NO's antiviral properties in this case, can be achieved through enhanced delivery of NO to the desired target by peptide-DNIC (Badroff et al., 2002).

Design and use of hybrid NO-donor drugs is yet another emerging strategy in the development of NO donors as therapeutic agents. Hybrid NO donor drugs have shown efficacy as calcium channel agonists and antagonists, potassium channel openers, β_1-adrenergic blockers, and anti-inflammatory agents (NSAIDs) [Shan and Knaus, 1999; Gasco et al., 1996]. In this regard, a nitro derivative of aspirin has recently been shown to reduce the infarct size caused by myocardial ischemia-reperfusion in the anesthetized rat more efficiently than aspirin (Rossoni et al., 2001). A NO-releasing derivative of ursodeoxycholic acid has been reported that selectively delivers NO to the liver and protects against development of portal hypertension (Fiorucci et al., 2001).

4.1.3. Novel Pyrimidine Nucleoside Nitric Oxide Donor Agents As Potential Anticancer/Antiviral Agents

Organic nitrates ($RONO_2$), which are esters of nitric acid and aliphatic alcohols, represent the oldest class of NO-donor compounds. This class of NO-donors includes the classical drug glyceryl trinitrate, beneficial effect of which in treatment of angina pectoris was first reported more than 100 years ago (Murrel, 1879). Today, organic nitrates, such as glyceryl trinitrate, isosorbide dinitrate and isosorbide mononitrate remain important drugs for the acute and preventive treatment of myocardial ischemia (Abrams, 1995; Parker and Parker, 1998). Organic nitrates consisting of 5' and/or 3' nitrate esters of pyrimidines, deoxyuridine and deoxycytidine have also been synthesized, although there were no biological data reported (Lichtenthaler and Muller, 1973; Duschinsky, 1978; Huang and Torrence 1978; Giziewicz et al., 1999). The 2'-*O*-nitro derivatives of arabinocytidine and arabinoadenine, on the other hand, have been shown to exhibit antileukemic activity [Chwang et al., 1983 (a & b)].

It is anticipated that the design of tumor selective NO-donor/nucleoside hybrid drugs, that release both NO and a nucleoside drug in a controlled manner, could provide an opportunity for the development of a novel class of double-barreled anticancer and/or antiviral drugs (Naimi et al., 2003). Accordingly, a number of 5-substituted-2'-deoxyuridines, having a NO-donor moiety on the sugar ring were recently synthesized for evaluation as anticancer and/or antiviral agents (Figure 4.1). The chemical synthesis, NO release, and anticancer and antiviral activities of some of these compounds have recently been reviewed (Naimi et al., 2003).

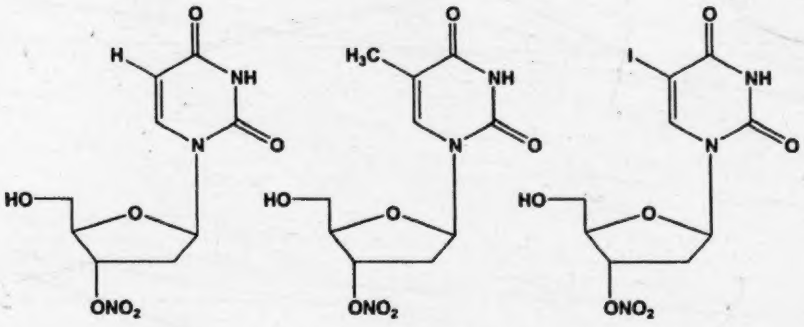

NUdR **NTdR** **INUdR**

Figure 4.1. Structures of selected 3'-O-nitro-2'-deoxyuridines

4.1.4. Detection and Quantification of Nitric Oxide (NO) in Stock Solutions of NO Donors and in Biological Matrices

Over the past decade, development of various analytical techniques helped to unravel numerous roles of NO in various biological systems. Some of the methods that have been employed for the analysis of NO include a chemiluminescence technique using the reaction of NO with ozone or luminol, electron spin resonance (EPR) spectrometry using an efficient NO trapping reagent, an electrochemical detection method using NO-specific electrodes, fluorometry using a fluorescent NO indicator, and spectrophotometric detection techniques based on the reaction of NO with oxyhemoglobin or oxymyoglobin, and based on the Griess reaction (Nagano and Yoshimura, 2002; Nims et al., 1996).

In the presence of oxygen, NO is readily autoxidized to nitrite (NO_2^-), which is the only stable final product of nitrogen oxide formed following decomposition in aqueous solutions in vitro. In extracellular fluids such as plasma or urine, however, nitrate (NO_3^-) appears to be the predominant stable end-product of NO metabolism. The measurement of the stable end-products of NO metabolism using the Griess reaction provides a rapid and simple way of NO quantitation, especially when NO production is to be assessed in a large number of samples (Titheradge, 1998). The Griess reaction (Figure 4.2) is based on a two-step diazotization reaction, and takes advantage of the nitrosative properties of nitrite for its detection and quantitation: Under acidic conditions, an NO_2^- derived nitrosating agent reacts with sulfanilic acid to produce the diazonium ion which then couples with an aromatic amine [N-(1-naphthyl)ethylenediamine] to form a chromophoric azo derivative with a characteristic maximum absorbance at 543 nm (Nims et al., 1996). Although not very sensitive, the Griess reaction is a relatively inexpensive and convenient method for estimating total NO production.

Quantitation of NO in biological samples (e.g., plasma, serum, urine) using the Griess reaction requires that NO_3^-, which is the predominant metabolite of NO in those matrices, be at first reduced to NO_2^- by an appropriate enzymatic conversion method (Grisham et al., 1996). Both NADPH-dependent nitrate reductase and formate-nitrate reductase can efficiently reduce nitrate to nitrite, which can then be quantitated using the Griess reaction (Titheradge, 1998).

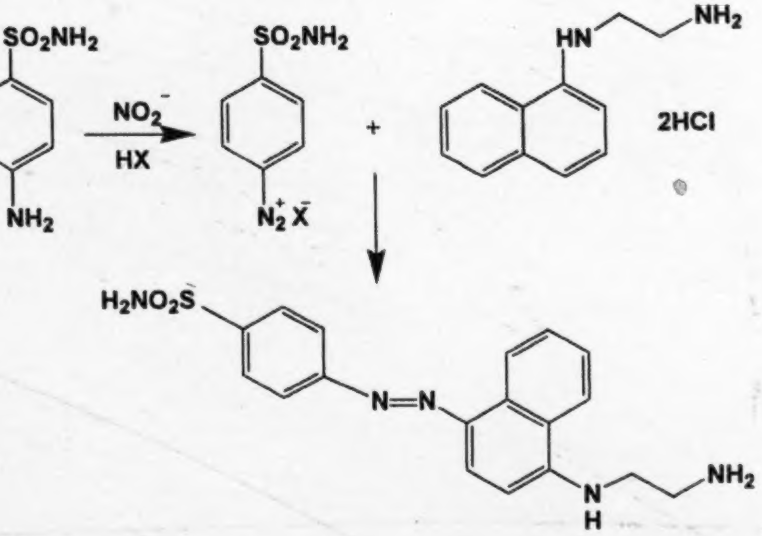
SO₂NH₂
NH₂
NO₂⁻
HX
SO₂NH₂
N₂⁺ X⁻
+
HN
NH₂
2HCl
H₂NO₂S
N=N
N
H
NH₂

Figure 4.2. Proposed reaction pathway for the Griess reaction (Miles et al., 1996)

4.2. Experimental

4.2.1. Materials

5-Iodo-3'-*O*-nitro-2'-deoxyuridine (INUdR, 399 Da), 3'-*O*-nitro-2'-deoxyuridine (NUdR, 273 Da), 3'-*O*-nitro-2'-deoxythymidine (NTdR, 287 Da), and 1-(2-deoxy-β-D-ribofuranosyl)-2,4-difluoro-5-methylbenzene (5-MeDFPdR, 244.1 Da) were synthesized according to previously reported procedures (Naimi et al., 2002; Wang et al., 2001). 5-Iodo-2'-deoxyuridine (IUdR) was purchased from ICN Biomedicals Inc. (Aurora, Ohio). Na[^{125} I]I used in the radiolabelling of INUdR was purchased from Amersham. [^{125} I] INUdR was radiolabeled by Dr. Wei Yan Sun through an iodine transmetalation reaction on the tributylstannyl precursor. Thymidine (dThd), HEPES buffer, pyruvic acid, thymine, L-cysteine (Cys), sulfanilamide, N-(1-naphthyl)ethylenediamine, isosorbide dinitrate (ISDN), sodium nitrite, glutathione (GSH), polyethylene glycol (PEG) 200, NADPH, FAD, lactate dehydrogenase, thymidine phosphorylase, and *Aspergillus* nitrate reductase were purchased from the Sigma Chemical Co. (Oakville, Ontario). *n*-Octanol was obtained from Aldrich Chemical Company (Milwaukee, WI). Bovine serum albumin (BSA) was obtained from Fischer Scientific (Nepean, ON). β-Glucuronidase (*Escherichia coli*), and aryl sulfatase (*Helix pomatia*) were purchased from Boehringer Mannheim (Laval, Quebec).

Centrifree™YM-30 and Ultra-15 centrifugal filter devices (Amicon, Millipore Corporation; Bedford, MA) were used to separate free from protein-bound drug in protein binding studies, and to purify rat sera prior to use in NO release assays, respectively. Waters Oasis® HLB (1 cc, 10 mg) extraction cartridges were used in the purification and extraction work-up of the rat plasma and urine samples prior to quantitative HPLC analyses. All solvents used for HPLC analyses were HPLC quality, and were filtered and degassed just prior to use.

4.2.2. High Performance Liquid Chromatography

The HPLC system was comprised of two Waters 501 pumps, a Waters Wisp 712 B autoinjector, a Waters 486 UV detector and a Diamir data station. All samples were analyzed on an YMC™ HPLC column (YMC ODS-AQ™, 25 cm x 4.6 mm) preceded by a guard column of the same packing. The column was maintained at room temperature and eluted at 0.7 mL/min using various mixtures of 20 mM ammonium acetate buffer at pH 3.5 and acetonitrile.

4.2.3. Stability of INUdR in solution (water, PBS, and in an acidic environment), and in incubates of rat plasma

The chemical stability of INUdR was studied in acidic medium (0.1 M HCl), in distilled water and in phosphate buffer solution (PBS, pH 7.4), at both ambient temperature (22 °C) and at 37 °C. Stock solutions (0.1 mM) of INUdR were prepared in 0.1 M HCl, in water, and in PBS (pH 7.4). An aliquot of each solution was kept at room temperature and another aliquot was incubated at 37 °C in tightly closed vials. At predetermined time intervals (0, 0.5, 1, 2, 4, 20, 24, 48, 72, 96, 120 h), aliquots (50 μL) of these stock solutions were removed and immediately analyzed by an isocratic HPLC method, using a mixture of ammonium acetate buffer (20 mM, pH 3.5): acetonitrile (80:20 v/v), a flow rate of 0.7 mL/min, and with UV detection at 290 nm.

To determine stability of INUdR in plasma, fresh rat plasma (90 μL) was spiked with INUdR (1mM, 10 μL) or with PBS (10 μL, pH 7.4) as blank, and incubated at 37 °C for selected times up to 24 h. As a comparison, stability of another IUdR mimic, 5-iodo-1-(2-deoxy-2-fluoro-β-D-arabinofuranosyl)uracil (FIAU), was also studied in the rat plasma following the same incubation protocol as INUdR. Similar to INUdR, the FIAU molecule bears a substitution on the sugar ring, designed to improve the nucleoside's stability in vitro and in vivo. At specified intervals (as above), aliquots (50 μL) of drug-plasma and plain plasma solutions were removed, mixed with acetonitrile (250 μL), and centrifuged at 12800 rpm to precipitate plasma proteins. Aliquots of the INUdR plasma extracts were analyzed by HPLC using the above method. To determine the identity of the major by-product of INUdR, formed upon incubation with rat plasma and detected on the HPLC chromatograms at λ=254 (invisible at λ=290, INUdR λ_{max}), the corresponding HPLC eluent fraction was collected and evaporated to dryness. This sample was then analyzed with an on-line HPLC-MS system. Mass spectra were obtained using electrospray in the positive ion mode. For HPLC analysis of FIAU plasma extracts, an isocratic mixture of ammonium acetate buffer (20 mM, pH 3.5): acetonitrile (90:10 v/v), at a flow rate of 0.7 mL/min was used, with UV detection at 283 nm.

4.2.4. Enzymatic stability of INUdR and NTdR toward phosphorolysis by *E. coli* thymidine phosphorylase

The stability of INUdR and NTdR toward phosphorolysis by *E. coli* thymidine phosphorylase was assessed following the same procedure described in section 3.2.5. For HPLC analysis, INUdR- and NTdR-containing samples were analyzed using an acetonitrile-ammonium acetate buffer (20 mM, pH 3.5) gradient with UV detection at 290 and 270 nm, respectively. After an initial hold time of 5 min, the gradient was developed from 5 % acetonitrile to 60 % acetonitrile over 8 min, and held at this concentration for 17 min. The initial solvent composition was then re-established over the next 30 min, and the column was allowed to re-equilibrate for 20 min before the next sample injection. Thymidine (dThd) samples were analyzed isocratically, using ammonium acetate buffer (20 mM, pH 3.5)-acetonitrile (95:5 v/v) with UV detection at 270 nm. The flow rates were maintained at 0.7 mL/min for all HPLC analyses.

4.2.5. Determination of partition coefficients (log P)

Partition coefficients were determined experimentally using the shake flask method (Hansch, Elkins, 1971), as well as by calculation using the Interactive Analysis Log P computational program program [Interactive Analysis (IA), Bedford, MA; developed by Marc Parham (mparham@interactiveanalysis.com], and are expressed as log P values. The method details have been described in section 3.2.7. Briefly, a known amount of each compound (2 mg) was partitioned between water-saturated *n*-octanol (2 mL) and *n*-octanol saturated water (2 mL), and samples were shaken for 24 h at 22 °C in a mechanical shaker. Following separation of the two phases, concentrations of the compounds in the *n*-octanol or water phase were determined using UV absorbance (Philips PU 8740 UV/VIS scanning spectrophotometer) at 290 nm for INUdR and at 270 nm for NTdR. Log P values were then calculated from the log ratio of the compound's concentration in *n*-octanol relative to its concentration in water.

4.2.6. Protein binding of INUdR and NTdR

The binding of INUdR and NTdR to bovine serum albumin (BSA; 3.8 mL, 4.5g/L, 1.22 x10^{-4}M) in PBS (pH 7.4) was examined at several concentrations of test compound (0.2 mL, 1x10^{-3} to 6x10^{-6} M) at 37 °C for 1 h. The procedural details have been described in section 3.2.8. Two isocratic methods were developed for HPLC quantitation of INUdR and NTdR in the ultrafiltrates: INUdR and NTdR were eluted using either 65:35 (v/v) or 80:20 (v/v) mixtures of ammonium acetate buffer (20 mM, pH 3.5): acetonitrile, with a flow rate of 0.7 mL/min and UV detection at 290 and 270 nm, respectively.

4.2.7. In vitro nitric oxide release assays

Nitric oxide release from INUdR in vitro was assessed in the presence of thiols [glutathione (GSH) and L-cysteine (Cys)] and in rat plasma. To estimate percent nitric oxide release from INUdR in the presence of thiols, the compound was dissolved in 0.1 M phosphate buffer solution (pH 7.4) at a final concentration of 1 mM, with or without various amounts of Cys or GSH (0 to 25 mM). ISDN was used as a reference NO-donor compound. The concentration range for Cys and GSH was chosen to cover the range of concentrations in human blood (10-20 mM) as reported by Ellman (1958). The samples were incubated at 37 °C for 0, 0.5, 1, and 16 h in tightly closed vials, under Argon. At the end of each incubation time, samples were removed from the incubator and freshly premixed Griess reagent (1 mL) was added to each drug solution (1 mL). Griess reagent was prepared by mixing equal volumes of 1 % sulfanilamide solution (prepared in 5 % v/v phosphoric acid/ distilled water) and 0.1 % N-(1-naphthyl)ethylenediamine hydrochloride solution. Shortly after addition of the Griess reagent (~ 10 min), the absorbance was measured at 540 nm using a Philips PU 8740 UV/VIS scanning spectrophotometer. For the standard curves, solutions of known nitrite concentrations (sodium nitrite solution, 0-60 μM) were prepared in 0.1 M PBS (pH 7.4) and their absorbance was measured following the addition of the Griess reagent.

Nitric oxide release in rat plasma was measured according to a slightly modified literature method (Grisham et al, 1996). Briefly, rat plasma was filtered through a Millipore Ultrafree-15 centrifugal device. Aliquots of INUdR solution in PBS (1×10^{-2} M, 10 μL) were then added to the filtered plasma (90 μL) and these spiked plasma samples were incubated in closed vials for 0, 1, and 16 h at 37 °C. At the end of each incubation time point, the samples were removed from the incubator and subjected to enzymatic treatment, followed by measurement of total nitrate plus nitrite concentrations using Griess reagent. The enzymatic treatment involved an initial 30 min incubation of each drug-plasma sample (100 μL) at 37 °C with 10 U/mL *Aspergillus* nitrate reductase (10 μL), 1 M HEPES buffer (pH 7.4, 25 μL), 0.1 mM FAD (25 μL), 1 mM NADPH (50 μL), and water (290 μL) in a total volume of 500 μL. As a blank, water (390 μL) was incubated with nitrate reductase, HEPES buffer, FAD and NADPH in a total volume of

500 µL at 37 °C for 30 min. Following this initial incubation, lactate dehydrogenase (5 µL, 1500 U/mL) and pyruvic acid (50 µL, 100 mM) were added to each sample tube and samples were incubated for an additional 10 min at 37 °C. The LDH/pyruvate system oxidizes any unreacted NADPH and, therefore, prevents inhibition of the following Griess reaction by this agent. Following the above enzymatic treatment steps, freshly prepared Griess reagent (1 mL) was added to each sample and samples were allowed to stand at room temperature for ~ 10 min. The absorbance of each sample was then determined at 540 nm, and total nitrate and nitrite concentrations were calculated from the slope of the standard curves established using known concentrations of nitrite and nitrate.

4.2.8. Animal pharmacokinetic studies

Animal care and handling procedures have been described in section 3.2.11. To study the pharmacokinetics of INUdR in the rat model, external right jugular vein cannulae were implanted into male SD rats (250-300 g), under metofane anesthesia, the day before the experiment. Rats were fasted for 8 h, with free access to water, before dosing. On the day of the experiment, INUdR was dissolved in PEG 200:water (4:6 v/v) and rats were dosed at 40 mg/kg intravenously (iv-bolus via the jugular vein cannula) or orally (by oral gavage). Blood was collected via the cannula, into heparinized tubes prior to dosing, and at 2 (in iv studies only), 5, 10, 15, 20, 30, 45, 60, 90, 120, 150, and 180 min following administration of the dose. In iv-bolus studies, the pre-dose blood (0.15 mL) was pushed through the cannula immediately after the dose, followed by saline (2x 0.15 mL) to wash out any residual dose on the walls of the cannulae. Following each blood withdrawal, an equal volume of normal saline was injected to replace the removed blood. Immediately following their collection, blood samples were centrifuged at 5000x*g* and plasma was separated and stored at –20 °C until analysis. Urine samples were collected (in metabolic cages) for 24 h following the dose, the urine volume was recorded, and the samples were pooled and stored at –20 °C until analysis. Waters Oasis® HLB (1 cc, 10 mg) extraction cartridges were used for the cleanup and extraction of INUdR from rat plasma and urine samples, prior to the quantitative HPLC analyses. Plasma sample solutions were prepared by addition of 5-MeDFPdR (0.2 mg/mL, 50 μL) as internal standard to each plasma sample (100 μL) and diluting the samples up to 500 μL with PBS (pH 7.0). Before loading the samples, every cartridge was first conditioned with methanol (1 mL) and then equilibrated with water (1 mL). Plasma sample solutions (500 μL) were then manually loaded onto the cartridges with 1 mL syringes and washed by pushing 1 mL of water: methanol solution (95:5 v/v) through the cartridge. Next, the analytes were eluted from the cartridge by pushing 1 mL of ethyl acetate through the cartridge. The ethyl acetate fractions were then dried under a stream of nitrogen, reconstituted in ammonium acetate buffer and subjected to HPLC analysis. For standards, aliquots of plain rat plasma (50 μL) were spiked with INUdR solutions (50 μL) of varying concentrations (0.2 to 6.4 x 10^{-5} mg/mL), followed by addition of internal standard (5-MeDFPdR; 0.2 mg/mL, 50 μL) and PBS (pH 7.0, 350 μL). These were then extracted using Waters Oasis® HLB extraction cartridges as described above. The extraction efficiency (91 ± 5 %) was estimated by comparing the peak areas of the extracted INUdR samples (with known concentrations) with those of direct injections of the same amount. HPLC was carried out isocratically, using ammonium acetate buffer: acetonitrile (72:28 v/v) as the mobile phase, at a flow rate of 0.7 mL/min with UV detection at 290 nm (INUdR λ_{max}) for the first 16 min of each run, and 270 nm thereafter to detect 5-MeDFPdR. Urine samples were prepared for HPLC analysis by filtration through sterile Acrodisc® 0.2 μm low protein binding disposable filters to remove any particulate matter, followed by addition of 5-MeDFPdR (0.2 mg/mL, 500 μL) as internal standard to aliquots (500 μL) of each urine sample. The urine aliquots (500 μL) were then loaded onto preconditioned Waters Oasis® HLB (1cc, 10 mg) extraction cartridges, washed with 1 mL of a water:methanol (90:10 v/v) solution and eluted by pushing ethyl acetate (1 mL) through the cartridge. The ethyl acetate extracts were evaporated to dryness, reconstituted in ammonium acetate buffer and filtered through Millex®-LH (0.45 μm, 4mm) syringe filters prior to HPLC analysis. The efficiency of extraction of urine samples by the above method was estimated at 80 ± 5%. For HPLC analysis of urine samples, a mixture of ammonium acetate buffer (20 mM, pH 3.5):acetonitrile (80:20 v/v) was used as the mobile phase, with UV detection carried out at 290 nm for the first 30 min, and at 270 nm thereafter, to detect the internal standard (5-MeDFPdR). The standard solutions were prepared from INUdR in blank urine (0.5 mg/mL to 0.8 μg/mL), to which 5-MeDFPdR (0.2 mg/mL, 500 μL) was added as internal standard. The samples were then extracted, dried, reconstituted, and analyzed as described above.

For studies aimed at quantitation of INUdR in the bile following iv-bolus administration of 40 mg/kg dose, male Sprague-Dawley rats (250-300 g) were anesthetized by intraperitoneal injection of a mixture of 90 mg/kg Ketaset® (Wyeth-

Ayerst Canada Inc., 100 mg/mL) and 10 mg/kg Rompun® (Bayer Inc., 20 mg/mL), and then catheters were surgically inserted into the bile duct and into the right jugular vein. Blank bile was collected from the biliary catheter just before administration of the dose. INUdR was then administered via the jugular vein catheter, and bile was collected at 1-hour intervals up to 8 h following the dose. Extraction of INUdR from bile samples was achieved by liquid-liquid extraction, using ethyl acetate. Briefly, 5-MeDFPdR (100 μL; 0.2 mg/mL) was added as internal standard to each 200 μL aliquot of bile, and the samples were diluted to 1 mL by addition of PBS (pH 7.0). Ethyl acetate (2 mL) was then added to each diluted bile sample, and the resulting mixture was vortexed for 5 min. Following separation of the two phases, the organic phase was removed and dried under a stream of nitrogen, and later reconstituted in ammonium acetate buffer for HPLC analysis. The standards were established by adding INUdR (50 μL) at various concentrations (0.004-1 mg/mL) to blank bile (150 μL), followed by addition of the internal standard and liquid-liquid extraction using ethyl acetate as described above. An extraction efficiency of 95 ± 2 % was estimated using this method for the bile samples. The HPLC analysis was performed using a mobile phase of ammonium acetate buffer (20 mM, pH 3.5): acetonitrile (78:22 v/v), and a flow rate of 0.7 mL/min with UV absorbance switched to 270 nm from 290 nm, after the first 30 min of each acquisition.

4.2.8.1. Enzymatic hydrolysis assays

To determine the presence of glucuronide and/or sulfate conjugates of INUdR, aliquots of rat urine and bile were incubated with β-glucuronidase and aryl sulfatase following the procedures described in section 3.2.11.1. Only the sample cleanup and

HPLC methods for detection of INUdR in enzyme treated samples will therefore be described here:

Urine Incubations. Aliquots of glucuronidase/sulfatase treated urine samples (total volume, 2100 μL) were extracted using Waters Oasis® HLB cartridges, following the same procedure used for untreated urine samples described above (4.2.8).

Bile Incubations. Cumulative amounts of glucuronide and sulfate conjugates in 8-hour bile samples were determined by incubation of bile samples with β-glucuronidase and aryl sulfatase following the same general method described for bile samples in section 3.2.11.1. At the end of the incubation and following the addition of internal standard (5-MeDFPdR, 100 μL, 0.2 mg/mL), each sample was diluted up to 1 mL by addition of 500 μL of PBS (pH 7.0). The resulting bile samples were extracted and analyzed by HPLC as described above (4.2.8) for enzymatically untreated bile samples. The glucuronic acid conjugate and sulfate conjugate concentrations were calculated from the difference between the area under the curve of INUdR in the treated and control samples.

4.2.9. Blood-to-plasma ratio

The in vitro distribution of [^{125}I] INUdR between blood cells and plasma was assessed by incubating three different concentrations of [^{125}I] INUdR with fresh, heparinized rat blood (1, 5, and 50 μg per mL of blood) following the same procedure described in section 3.2.12.

4.2.10. Pharmacokinetic Analysis

Various pharmacokinetic parameters of INUdR were estimated by applying area-moment analysis (WinNonlin version 1.1™) to the INUdR plasma time-concentration data. Total clearance (CL_T) was calculated by dividing the dose by the $AUC_{0\rightarrow\infty\,(iv)}$, and oral clearance (CL/Fa) was calculated by dividing the oral dose by the $AUC_{0\rightarrow\infty\,(po)}$. The elimination half-life ($T_{½}$) was calculated from $0.693/\lambda_z$ (λ_z = terminal slope), using a minimum of four data points. Mean residence time (MRT) was calculated from $AUMC_{0\rightarrow\infty}$ /$AUC_{0\rightarrow\infty}$, and steady-state volume of distribution (V_{ss}) was obtained by multiplying CL_T by MRT. Mean absorption time (MAT) was obtained by subtracting MRT_{iv} from MRT_{oral}, and the absorption half-life was estimated from 0.693 x MAT (Gibaldi M, 1991).

The urinary and biliary recoveries of unchanged drug were calculated from the ratios of the amount of unchanged INUdR over the dose. The bioavailability (Fa) for the 40 mg/kg oral dose was estimated from the mean ratio of the AUC_{oral} values relative to AUC_{iv} values obtained following the iv dosing of rats at 40 mg/kg.

4.3. Results

4.3.1. Stability of INUdR in solution (water, PBS, and in an acidic environment), and in incubates of rat plasma

INUdR was chemically unchanged in both water and PBS at experimental conditions of biological relevance (pH 1 and 7.4, 37 °C), as well as at 22 °C, 4 °C and –20 °C. Overall, INUdR was very stable under these conditions, with no observable degradation even at 37 °C in a very acidic medium (pH = 1). However, incubates of INUdR in rat plasma (37 °C) gradually degraded over time (Figure 4.3). A degradation product of INUdR in rat plasma was detected by HPLC at 254 nm that was invisible at 290 nm, the INUdR λ_{max}. Online LC-MS of the corresponding HPLC eluent fraction indicated loss of iodine from the parent molecule (*m/z* = 421.96, [M + Na^+]), giving rise to an intense daughter ion at *m/z* 295.1 Da [M + Na^+] for this metabolite. This deiodination was further confirmed by HPLC co-chromatography of the metabolite with an authentic sample of NUdR (i.e. deiodinated INUdR). As shown in Figure 4.3, about 20 % of INUdR was deiodinated within the first two hours of incubation in plasma, and ~ 70 % was converted to NUdR within 24 h.

Conversely, FIAU remained almost intact in incubates of rat plasma, with less than 2.8% degradation over a 24 h incubation period. Similar results have been reported for stability of FIAU in human whole blood (~ 2.5% degradation at the end of a 24 h incubation period) [Vaidyanathan et al., 1998].

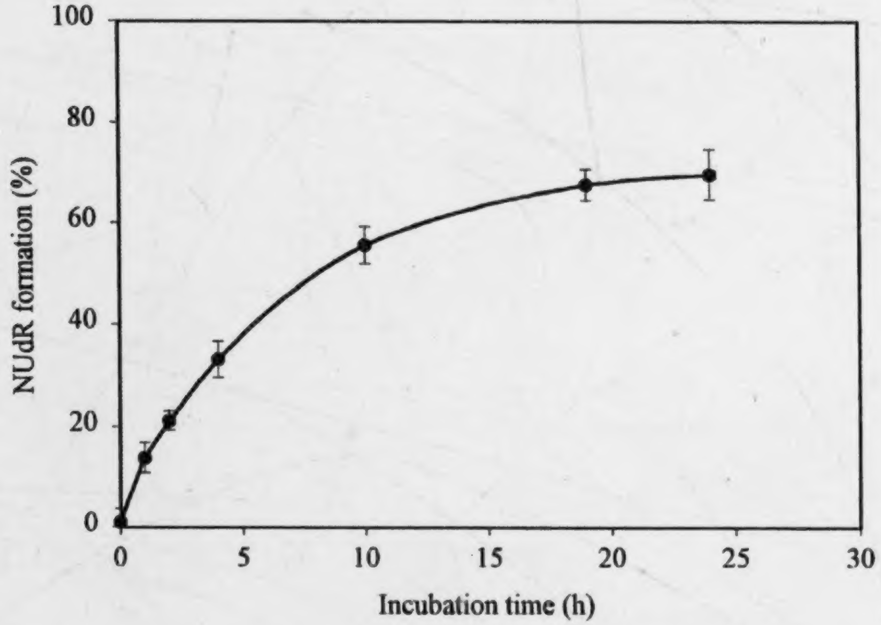

Figure 4.3. Formation of NUdR from INUdR as a function of incubation time (at 37 °C) in rat plasma. Error bars represent standard deviation (S.D.) of the mean (n = 3).

4.3.2. Enzymatic stability of INUdR and NTdR toward phosphorolysis by *E. coli* thymidine phosphorylase

Stability of pyrimidine nucleosides towards catabolic cleavage by pyrimidine phosphorylases is an important consideration in the design of novel anticancer/antiviral pyrimidine nucleosides. Glycosidic bond cleavage by these enzymes is a major inactivating mechanism for many of classical 5-substituted-2'-deoxyuridines (Desgranges et al., 1983). Current studies indicated that neither INUdR nor NTdR act as substrates for thymidine phosphorylase. There were no significant changes in the peak areas of either one of these compounds, and no apparent formation of new peaks on the HPLC chromatograms of incubation mixtures. Under identical experimental conditions, however, both TdR and IUdR underwent phosphorolysis and yielded thymine (28%) and 5-iodouracil (38%), respectively. HPLC co-chromatography of authentic thymine and 5-iodouracil with TdR and IUdR phosphorolysis mixtures confirmed the identity of catabolites, thymine and 5-iodouracil, respectively.

4.3.3. Partition coefficients (log P)

The experimental and calculated (Interactive Analysis Log P Predictor) log P values of INUdR, NTdR, thymidine and IUdR are summarized in Table 4.1.

Table 4.1. Experimental and calculated log P values for INUdR, IUdR, NTdR and dThd.

Compound	Experimental log P	Calculated* log P
INUdR	+1.12	+0.67
NTdR	+0.10	-0.37
IUdR	-0.96**	-0.5
dThd	-1.19***	-0.81

* Interactive Analysis Log P Program
** Narurkar and Mitra, 1988
***Parang, 1997

4.3.4. Protein binding of INUdR and NTdR

INUdR binding to bovine serum albumin (BSA) in vitro at 37 °C ranged from 65 to 77 % over a three-log range of INUdR concentrations (1×10^{-3} to 6×10^{-6} M) (Table 4.2). BSA binding of NTdR, on the other hand, ranged from 10 to 21 % at NTdR concentrations between 1×10^{-3} and 2×10^{-6} M (Table 4.3).

Table 4.2. Percent binding of INUdR to bovine plasma albumin at various INUdR concentrations.

INUdR Concentration (M)	Mean Percent Bound (± S.D.)
6×10^{-6}	77 ± 0.5
1×10^{-5}	76 ± 1.6
2×10^{-5}	77 ± 1.2
4×10^{-5}	75 ± 1.1
1×10^{-4}	73 ± 3.8
2×10^{-4}	71 ± 0.6
4×10^{-4}	68 ± 0.7
8×10^{-4}	65 ± 0.9
1×10^{-3}	65 ± 1.1

Table 4.3. Percent binding of NTdR to bovine plasma albumin at various NTdR concentrations.

NTdR Concentration (M)	Mean Percent Bound (± S.D.)
2×10^{-6}	21 ± 0.7
6×10^{-6}	17 ± 1.0
2×10^{-5}	16 ± 1.1
4×10^{-5}	13 ± 0.8
2×10^{-4}	12 ± 1.2
4×10^{-4}	11 ± 0.9
8×10^{-4}	11 ± 0.4
1×10^{-3}	10 ± 0.5

4.3.5. In vitro nitric oxide release of INUdR

INUdR and related 5-substituted-2'-deoxyuridines with NO donor substituents at the 3'- or 5'-position of the sugar ring were synthesized as double-barreled prodrugs, which would act as nitric oxide donor agents and simultaneously generate the corresponding anticancer and/or antiviral nucleoside. While bioactivation of organic nitrates to NO is thought to involve the NADPH-dependent cytochrome P450 pathway and specific isozymes of glutathione-*S*-transferase, the non-enzymatic release of NO presumably involves interactions of the organic nitrates with sulfhydryl groups of compounds such as Cys and GSH (Wang et al., 2002). The effects of Cys and GSH on NO release from INUdR and ISDN, an organic nitrate with two ONO_2 groups used as a positive control, are tabulated as well as illustrated in Tables 4.4 and 4.5 and Figures 4.4 and 4.5, respectively.

Table 4.4. Nitric oxide release from INUdR and ISDN in PBS, upon incubation with increasing cysteine concentrations, as % NO per molecule of INUdR or ISDN.

Time (h)	% NO Release in PBS							
	ISDN				INUdR			
	Cys-2.5	Cys-5	Cys-10	Cys-25	Cys-2.5	Cys-5	Cys-10	Cys-25
0	0.4 (0.1)	0.54 (0.01)	0.58 (0.12)	1.43 (0.18)	0.35 (0.07)	0.56 (0.02)	0.76 (0.06)	2.40 (0.13)
0.5	0.56 (0.03)	1.51 (0.04)	2.63 (0.09)	6.95 (0.30)	0.77 (0.04)	1.94 (0.07)	3.68 (0.12)	10.15 (0.15)
1	0.77 (0.03)	2.04 (0.12)	3.85 (0.08)	10.2 (0.2)	1.02 (0.11)	2.88 (0.10)	5.43 (0.16)	14.65 (0.40)
16	1.3 (0.3)	10.0 (0.5)	31.4 (1.2)	58.9 (1.7)	1.7 (0.1)	9.2 (0.2)	36.5 (0.5)	70.0 (3.4)

Table 4.5. Nitric oxide release from INUdR and ISDN in PBS, upon incubation with increasing glutathione concentrations, as % NO per molecule of INUdR or ISDN.

Time (h)	% NO Release in PBS							
	ISDN				INUdR			
	GSH-2.5	GSH-5	GSH-10	GSH-25	GSH-2.5	GSH-5	GSH-10	GSH-25
0	0.15 (0.02)	0.40 (0.13)	0.50 (0.09)	0.62 (0.10)	0.15 (0.02)	0.36 (0.03)	0.36 (0.01)	0.77 (0.06)
0.5	0.44 (0.01)	0.81 (0.05)	1.16 (0.02)	2.26 (0.33)	0.70 (0.06)	1.27 (0.06)	1.80 (0.03)	3.31 (0.07)
1	0.71 (0.06)	1.28 (0.05)	1.76 (0.10)	3.06 (0.06)	1.05 (0.02)	1.96 (0.09)	2.87 (0.11)	5.03 (0.15)
16	2.5 (0.1)	7.3 (0.2)	15.9 (2.5)	26.9 (1.0)	3.1 (0.6)	10.5 (0.2)	25.5 (1.6)	41.6 (1.8)

Data in Tables 4.4 and 4.5 represent the mean of three measurements (S.D.)

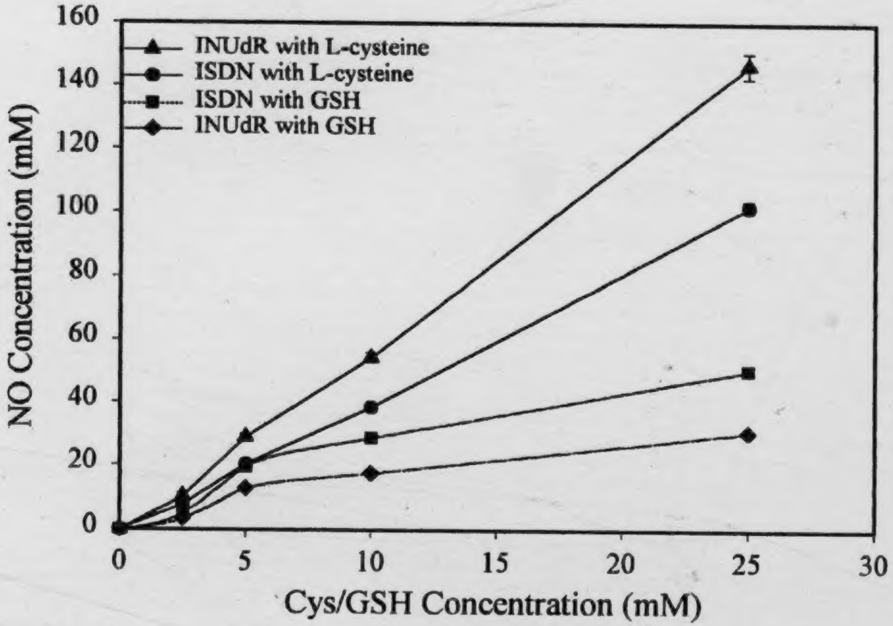

Figure 4.4. Mean nitrite generation from ISDN and INUdR in PBS as a function of increasing L-cysteine/glutathione concentrations following 1 h incubation at 37 °C. The error bars represent the standard deviation (S.D.) for triplicate measurements and in most cases are too small to be seen.

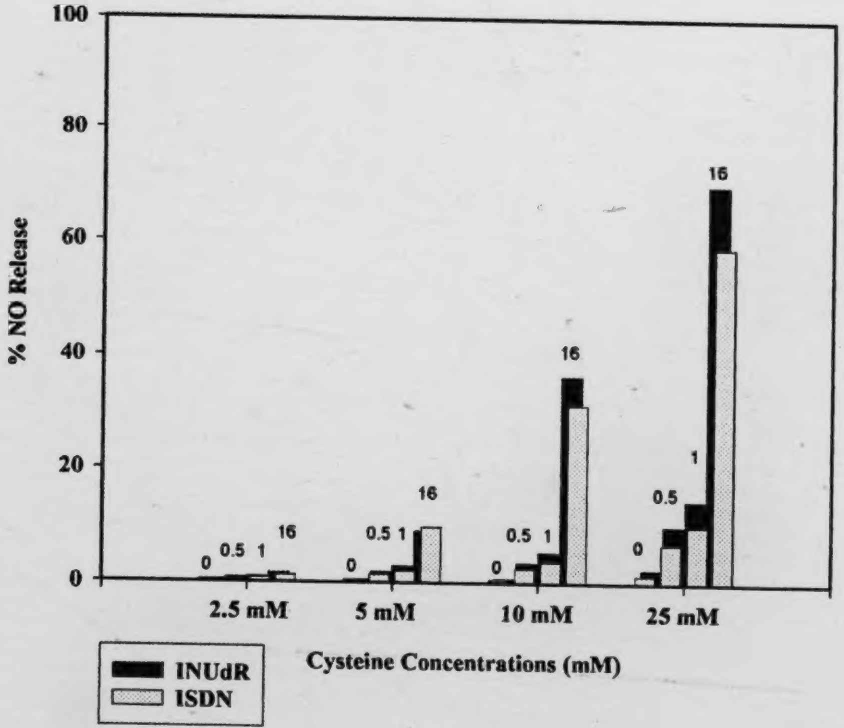

Figure 4.5. Mean percent NO release of INUdR/ISDN in PBS with increasing cysteine concentrations (0 to 25 mM) and for various incubation times. Standard deviations (S.D.) are listed in Table 4.4.
[The incubation times (0, 0.5, 1, 16 h) are shown on each bar.]

Table 4.6 summarizes the results of NO release by INUdR and ISDN following incubation with rat plasma for different durations of time.

Table 4.6. Nitric oxide release from INUdR and ISDN in incubates of rat plasma, as % NO per molecule of INUdR or ISDN. Values are mean (S.D.) of triplicate measurements.

Time (h)	**% NO Release in rat serum**	
	ISDN	**INUdR**
0	3.4 (0.8)	2.41 (1.0)
1	5.9 (1.1)	6.52 (1.6)
16	22.61 (2.7)	15.9 (2.2)

4.3.6. Pharmacokinetic Studies of INUdR

The mean plasma concentrations of INUdR (μg/mL), as a function of time after iv-bolus and oral administration of INUdR (40 mg/kg) to rats, are plotted in Figure 4.6. The pharmacokinetic parameters generated by area-moment analysis are summarized in Table 4.7.

Table 4.7. Pharmacokinetic parameters for INUdR in male SD rats following single intravenous and oral doses of INUdR (40 mg/kg). Data represent mean (S.E.), n = 3.

Parameter	**IV-bolus**	**Oral**
$T_{1/2}$ (h)	0.3 (0.07)	0.4 (0.04)
Cl_T (L/ h/ kg)	2.57 (0.24)	2.70* (0.30)
MRT (h)	0.34 (0.05)	0.73 (0.1)
V_{SS} (L/kg)	0.89 (0.16)	NA**
MAT (h)		0.39 (0.05)
$T_{1/2\ abs}$ (h)		0.27 (0.03)
Fa		0.95 (0.05)

*Oral clearance is obtained by dividing the oral dose by the $AUC_{0\to\infty\ (po)}$.

** NA: Not applicable

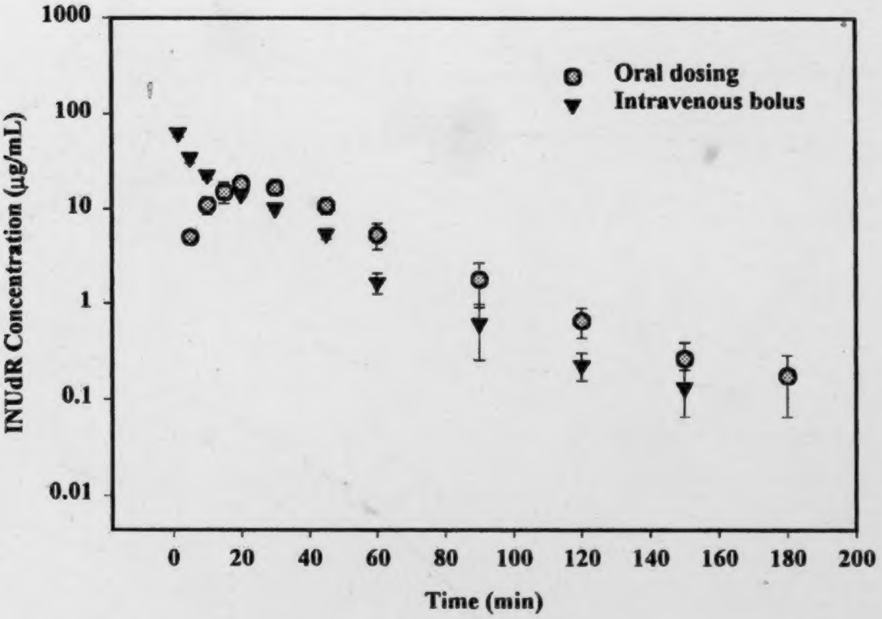

Figure 4.6. Concentration-time curves for INUdR in plasma following iv bolus and oral administration of INUdR (40 mg/kg) to rats. Data are for n = 3 (± S.E.)

The results of urinary recovery of INUdR, as unchanged and as glucuronides and sulfate conjugates, following intravenous and oral administration of INUdR (40 mg/kg) to male SD rats are summarized in Table 4.8. Biliary recoveries of unchanged INUdR, as well as, INUdR glucuronides and sulfates following intravenous administration of INUdR (40 mg/kg) to male SD rats are shown in Table 4.9.

Table 4.8. Percent of the INUdR dose recovered as unchanged, and as glucuronides and sulfates in the 24h urine specimens of each rat (n = 3) following intravenous administration of INUdR (40 mg/kg). The last columns in each dosing route category (iv or po) represent the mean (S.D.) recoveries (as percent of the dose) for the three rats.

INUdR recovery	**Intravenous dosing**				**Oral dosing**			
	Rat 1	Rat 2	Rat 3	Mean (S.D.)	Rat 1	Rat 2	Rat 3	Mean (S.D.)
[1]X_U%	15.0	38.0	28.0	27.0 (11.5)	22.0	34.0	37.0	31.0 (7.9)
[1]X_G%	7.0	11.0	10.0	9.3 (2.1)	5.0	12.0	6.0	7.7 (3.8)
[1]X_S%	NR*				NR*			

[1] X_U %, X_G %, and X_S % represent the percents of INUdR dose recovered in the urine as unchanged, glucuronides, and sulfates, respectively.

*NR: no INUdR sulfates were recovered

Table 4.9. Percent of the INUdR dose recovered as unchanged, and as glucuronides and sulfates in the bile specimens of each rat (n = 3) following intravenous administration of INUdR (40 mg/kg). The last column represents the mean (S.D.) recoveries (as percent of the dose) for the three rats.

INUdR recovery	**Intravenous dosing**			
	Rat 1	Rat 2	Rat 3	Mean (S.D.)
[2]X_{Ub}%	0.42	1.0	0.68	0.70 (0.29)
[2]X_{Gb}%	0.38	0.71	0.55	0.55 (0.17)
[2]X_{Sb}%	NR*			

[1] $X_{U\,b}$%, X_{Gb} %, and X_{Sb} % represent the percents of INUdR dose recovered in the bile as unchanged, glucuronides, and sulfates, respectively.

*NR: no INUdR sulfates were recovered

4.3.7. Blood-to-plasma ratio of INUdR

The results of an in vitro distribution study of [^{125}I] INUdR between blood cells and plasma, following incubation of [^{125}I] INUdR with fresh rat blood at 37 °C for 1 h at 1, 5, and 50 µg/mL concentrations are summarized in the Table 4.10.

Table 4.10. In vitro blood-to-plasma ratio of INUdR (rat blood)

INUdR concentration in blood (µg/mL)	Blood-to-Plasma Ratio
1.0	0.7 (0.05)
5.0	0.5 (0.03)
50.0	0.1 (0.02)

Data represent the mean (S.D.) of triplicate measurements at each concentration

4.4. Discussion

5-Iodo-3'-*O*-nitro-2'-deoxyuridine (INUdR) is a member of a group of 3'-*O*-nitro-2'-deoxyuridines recently synthesized for evaluation as anticancer/antiviral agents (Naimi et al., 2003; see appendix). The design of a nitric oxide (NO) donor/ nucleoside prodrug was based on the assumption that a dual mechanism of action of this type would release cytotoxic NO in a controlled manner and subsequently exert the biochemical toxicity of 5-iodo-2'-deoxyuridine (IUdR). Accordingly, these potentially synergistic actions could provide a greater cytotoxic or antiviral effect.

INUdR was stable under experimental conditions in phosphate buffer (PBS, pH 7.4), in water, and in acidic medium (pH=1) at both ambient temperature (22 °C) and 37 °C. Furthermore, INUdR has been found to be stable at 4 °C and –20 °C for months. In incubates of rat plasma, however, INUdR was unstable and degraded rapidly. The rapid and direct deiodination of INUdR to NUdR, as the only metabolite formed in incubates of rat plasma appears to be rather unusual, as in most reported cases of halopyrimidine dehalogenations, catabolic breakdown of the nucleoside has been thought to precede the reductive dehalogenation of the nucleobase (Smith et al., 1992). While introduction of a nitrooxy group at the 3'-position of the sugar ring appears to stabilize the *N*-glycosidic bond of INUdR against enzymatic cleavage (as described below), it does not appear to have any stabilizing effect against its deiodination in plasma. In the case of FIAU, however, substitution on the sugar ring at the 2'-position (fluorine in arabino position) appears to not only stabilize the C-N bond against catabolic cleavage, but also to either directly or indirectly reduce the rate of deiodinaion of FIAU (Vaidyanathan et al., 1998). Accordingly, FIAU remained almost intact in incubates of rat plasma, with less than 2.8% degradation over a 24 h incubation period. Similar results have been reported for the stability of FIAU in human whole blood (~ 2.5% degradation at the end of a 24 h incubation period) [Vaidyanathan et al., 1998]. The parent nucleoside, IUdR, with an unsubstituted sugar ring, is reportedly unstable both in vitro and in vivo. As demonstrated by Vaidyanathan et al., only 1% of the intact IUdR remains, at the end of a 24 h incubation with human whole blood. Unlike INUdR, dehalogenation of IUdR has been thought to occur as a result of reductive deiodination of the 5-iodouracil ring, which is formed subsequent to the catabolic break down of the nucleoside [Prusoff et al., 1960]. In fact, 5-iodouracil is the major metabolite, formed during incubation of IUdR with human whole blood (Vaidyanathan et al., 1998).

INUdR and NTdR, unlike IUdR and other classic *N*-glycosidic 5-substituted-2'-deoxyuridines, were resistant to phosphorolysis by thymidine phosphorylase. Formation of the 3'-nitrate ester appears to have resulted in an increased resistance towards catabolic breakdown by thymidine phosphorylase. Moreover, INUdR and NTdR were more lipophilic than parent nucleosides IUdR and dThd, respectively. Their greater lipophilicity may allow these compounds to diffuse more readily across cell membranes compared to IUdR, dThd, and other more hydrophilic nucleosides.

The results of in vitro binding of INUdR to bovine serum albumin (BSA) over a three-log range of INUdR concentrations (1×10^{-3} to 6×10^{-6} M) (Table 4.2) indicate that this compound is moderately protein bound (65-77%). Furthermore, the binding of

INUdR to BSA shows some degree of concentration dependence: At lower concentrations of INUdR (< $4x10^{-5}$M), the mean percent binding to BSA was about 76 %; at INUdR concentrations beyond $4x10^{-5}$ M, there was a gradual decline in mean percent binding to 65 %. This may be attributed to partial saturation of serum albumin binding sites for the drug. NTdR, on the other hand, exhibited low protein binding (10 to 21 %) at NTdR concentrations between $1x10^{-3}$ and $2x10^{-6}$ M (Table 4.3). NTdR protein binding is very similar to the reported ~ 22 % protein binding for dThd (Borg et al., 1997). Similar to INUdR, the binding of NTdR to BSA also gradually declined with increasing substrate (NTdR) concentrations. These results suggest that nonlinearity of serum/plasma protein binding may need to be considered and assessed in studies that require higher circulating concentrations of INUdR or NTdR, such as in vivo acute and subacute toxicity studies.

There was no spontaneous release of NO by either INUdR or ISDN in the absence of thiols. On the other hand, both Cys and GSH accelerated release of NO by ISDN and INUdR in PBS, in a concentration and time dependent manner, although Cys had a greater NO release enhancement effect. Overall, INUdR exhibited greater or equal NO release in PBS and plasma (except for the 16h plasma incubates) compared with the reference drug ISDN. Similar high NO release has also been reported for other 3'-*O*-nitro and 5'-*O*-nitro derivatives of 2'-deoxyuridine (Naimi et al., 2003; see appendix).

Although INUdR and related 3'- and 5'-*O*-nitro derivatives of 2'-deoxyuridine generally release a greater percent of NO compared to the reference drug isosorbide dinitrate upon incubation with thiols (Cys or GSH) or in serum, their reported cytotoxicities ($CC_{50} \approx 10^{-3}$ to 10^{-6} M range) are low. For instance, INUdR has been reported to be equitoxic to IUdR in vitro ($CC_{50} \approx 10^{-4}$ to 10^{-5} M) against a variety of cancer cell lines. Moreover, expression of the viral thymidine kinase does not provide a gene therapeutic effect for INUdR and related compounds, as demonstrated by their similar cytotoxicity against nontransfected (KBALB, 143B) and the corresponding HSV-1 TK transfected cancer cell lines (KBALB-STK, 143B-LTK) [Naimi et al., 2003; for details see appendix].

In a battery of antiviral activity assays, INUdR had some selectivity against herpes simplex virus type 1 (KOS), herpes simplex virus type 2 (G), and vaccinia virus ($IC_{50} = 48$ μg/mL). These results are consistent with the reported antiviral effects of NO in cell lines infected with herpes simplex virus type 1 (Croen, 1993) and vaccinia virus (Harris et al., 1995). INUdR did not reduce cell culture pathogenicity induced by parainfluenza-3 virus, Reovirus-1, and a variety of other viruses (Naimi et al., 2003; see appendix).

The lack of significant anticancer/antiviral activities of this novel class of NO-donor nucleosides may be due to a number of reasons:

For instance, it is possible that the sugar moiety is not phosphorylated by thymidine kinase to the 5'-monophosphate form. The observed negligible differences in anticancer/antiviral activities of these compounds between nontransfected (KBALB, 143B) and the viral TK transfected (KBALB-STK, 143B-LTK) cell lines provide some support for the lack of phosphorylation hypothesis. Alternatively, it is possible that these nucleoside nitrate esters are devoid of anticancer/antiviral activity, due to their inability to inhibit thymidylate synthase (TS), which is a key target for the cytotoxic/cytostatic effects exhibited by certain nucleoside analogues, such as 5-fluoro-2'-deoxyuridine (Santi et al., 1974), (*E*)-5-(2-iodovinyl)-2'-deoxyuridine and 5-(1-azidovinyl)-2'-deoxyuridine (Balzarini et al., 1995).

In in vivo pharmacokinetic studies, INUdR exhibited a short elimination half-life, following both iv-bolus ($T_{1/2} \approx 16$ min) and oral administration ($T_{1/2} \approx 23$ min) routes. The elimination half-life of INUdR in rats is, therefore, only slightly longer than that reported for IUdR (< 10 min in all studied species) [Mariani et al., 1993, Baranowska-Kortylewicz et al., 1996]. The $T_{1/2}$ and MRT following oral administration of INUdR were greater than those following intravenous administration (Table 4). While MRT values for any non-instantaneous mode of administration would always be greater than MRT following intravenous bolus administration, the half-life should normally be the same for different routes of administration. In those cases, however, where elimination is rate-limited by absorption (i.e. $K_a < K_e$ or $T_{1/2\ abs} > T_{1/2\ el}$), as is the case for flip-flop kinetics, the terminal slope of the oral administration profile would likely reflect the absorption rather than the elimination process and as such may not parallel the iv-bolus terminal slope. In the case of INUdR, the absorption half-life (0.27 h) following oral administration (0.693 x MAT) is the same as the elimination half-life following iv-bolus dosing (or $K_a = K_e$). The slightly higher oral half-life of INUdR may, therefore, suggest that its oral absorption is slightly prolonged but not to the extent of limiting its elimination (as would be expected for flip-flop kinetics). INUdR is a high clearance drug based on the comparison of its Cl_T (~ 2.57 L/h/kg or ~ 43 mL/min/kg) with the rat's average hepatic blood flow (40 to 60 mL/min/kg). The V_{ss} of INUdR following iv-bolus administration averaged 0.89 ± 0.16 L/kg, which is greater than the average total body water in rats (0.7 L/kg) [Gerlowski et al., 1983]. This observation suggests that INUdR is likely distributed intracellularly. Once distributed intracellularly, the nucleoside analogue may be partially trapped, in the form of its phosphorylated anabolites. The recovery of unchanged INUdR in urine was variable and averaged about 30 % (range: 15 to 38 %). INUdR glucuronides in the urine accounted for an estimated 5 to 12 % of the dose, but no sulfate conjugates of INUdR were detected in the urine specimens based on the enzymatic hydrolyses with aryl sulfatase enzyme. The absolute bioavailability of INUdR, based on the oral and intravenous plasma data, averaged about 95 % (Fa = 0.95). Following intravenous bolus administration of INUdR at 40 mg/kg, 0.4 to 1% of INUdR was recovered in bile samples as unchanged drug. The amount of INUdR in the bile samples collected after the third hour following the dose, fell below the limits of detection. A small amount of INUdR glucuronide (~ 0.5% of the dose) was recovered in the bile samples following incubation with glucuronidase enzyme. Aryl sulfatase hydrolysis of bile samples, however, did not reveal an increase in the parent INUdR concentrations and it was, therefore, concluded that there were no sulfate conjugates present.

There was no preferential uptake of INUdR into blood cells, as revealed from the study of in vitro distribution of [^{125} I]INUdR between blood cells and plasma. The blood-to-plasma ratio, as determined from the ratio of radioactivity in equal volumes of blood and plasma, ranged from 0.7 to 0.1 over the examined INUdR concentrations (1 to 50 µg/mL). Either whole blood or plasma samples may, therefore, be suitable for future pharmacokinetic studies of this compound.

4.4. References

Abrams J. The role of nitrates in coronary heart disease. Arch Intern Med 1995;155:357-364.

Akarid K, Sinet M, Desforges B, Gougerot-Pocidalo MA. Inhibitory effect of nitric oxide on the replication of a murine retrovirus in vitro and in vivo. J Virol 1995;69:7001-7005.

Ambs S, Merriam WG, Ogunfusika MO, Bennet WP, Ishibe N, Hussain P, Tzeng EE, Geller DA, Billiar TR, Harris CC. P53 and vascular endothelial growth factor regulate tumor growth of NOS2-expressing human carcinoma cells. Nat Medicine 1998;4:1371-1376.

Badorff C, Fichtscherer B, Muelsch A, Zeiher AM, Dimmeler S. Selective delivery of nitric oxide to a cellular target: A pseudosubstrate-coupled dinitrosyl-iron complex inhibits the enteroviral protease 2A. Nitric Oxide: Biology and Chemistry 2002;6:305-312.

Balzarini J, Degreve B, Esteban-Gamboa A, Esnouf R, De Clercq E, Engelborghs Y, Camarasa MJ, Perez-Perez MJ. Kinetic analysis of novel multisubstrate analogue inhibitors of thymidine phosphorylase. FEBS Lett 2000;483:181-185.

Balzarini J, Andrei G, Kumar R, Knaus EE, Wiebe LI, De Clercq E. The cytostatic activity of 5-(1-azidovinyl)-2'-deoxyuridine (AzVDU) against herpes simplex virus thymidine kinase gene transfected FM3A cells is due to inhibition of thymidylate synthase and enhanced by UV light (lambda =254 nm) exposure. FEBS Lett 1995;373:41-44; and references therein.

Baranowska-Kortylewicz J, Kortylewicz ZP, Hoffman D, Winoto A, Lai J, Dalrymple GV. Colon-specific prodrugs of 5-radioiodo-2'-deoxyuridine. Acta Oncol 1996;35,959-964.

Bi Z, Reiss CS. Inhibition of vesicular stomatitis virus infection by nitric oxide. J Virol 1995;69:2208-2213.

Borg N, Zhou XX, Johansson NG, Oeberg B, Staehle L. Distribution to the brain and protein binding of 3'- and 5-substituted 2', 3'-dideoxyuridine derivatives, studied by microdialysis. Antivir Chem Chemother 1997;8,47-53.

Bredt DS, Synder SH. Nitric Oxide: A physiological messenger molecule. Annu Rev Biochem 1994;63:175-179.

Brockhaus F, Brune B. U937 apoptotic cell death by nitric oxide: bcl-2 down-regulation and caspase activation. Exp Cell Res 1998;238:33-41.

Broillet MC. S-nitrosylation of proteins. Cell Mol Life Sci 1999;55:1036-1042.

Chin K, Kurashima Y, Ogura T, Tajiri H, Yoshida S, Esumi H. Induction of vascular endothelial growth factor by nitric oxide in human glioblastoma and hepatocellular carcinoma cells. Oncogene 1997;15:437-442.

Chwang TL, Fridland A, Avery TL. 2'-*O*-Nitro-1-β-D-arabinofuranosylcytosine. A new derivative of 1-β-D-arabinofuranosylcytosine that resists enzymatic deamination and has antileukemic activity. J Med Chem 1983a;26:280-283.

Chwang TL, Fridland A, Verhoef V. Novel derivatives of 9-β-D-arabinofuranosylpurines that are cytotoxic to variants of human leukemic lymphoblast cells resistant to both 1-β-D-arabinofuranosylcytosine and 9-β-D-arabinofuranosyladenine. Biochem Pharmacol 1983b;32:2643-2646.

Croen KD. Evidence for antiviral effect of nitric oxide. Inhibition of herpes simplex virus type 1 replication. J Clin Invest 1993;91:2446-2452.

Desgranges C, Razaka G, Rabaud M, Bricaud H, Balzarini J, De Clercq E. Phosphorolysis of (*E*)-5-(2-bromovinyl)-2'-deoxyuridine (BVDU) and other 5-substituted-2'-deoxyuridines by purified human thymidine phosphorylase and intact blood platelets. Biochem Pharmacol 1983;32,3583-3590.

Drapier JC, Hibbs JB. Differentiation of murine macrophages to express non-specific cytotoxicity for tumor cells results in l-arginine-dependent inhibition of mitochondrial iron-sulfur enzymes in the macrophage effector cells. J Immunol 1988;140:2829-2838.

Duschinsky R. 3',5'-Di-*O*-nitrothymidine. In Nucleic Acid Chemistry: Improved and New Synthetic Procedures, Methods and Techniques. Townsend LB, Tipson RS (editors). Wiley; New York, 1978, Vol 1, pp 295-297.

Ellman GL. A calorimetric method for determining low concentrations of mercaptans. Arch Biochem Biophys 1958;74,443-450.

Esteban-Gamboa A, Balzarini J, Esnouf R, De Clercq E, Camarasa MJ, Perez-Perez MJ. Design, synthesis, and enzymatic evaluation of multisubstrate analogue inhibitors of *Escherichia coli* thymidine phosphorylase. J Med Chem 2000;43,971-983.

Evelo CTA, Versteegh JFM, Blaauboer BJ. Kinetics of the formation and secretion of the aniline metabolite 4-aminophenol and its conjugates by isolated rat hepatocytes. Xenobiotica 1984;14,409-416.

Fiorucci S, Antonelli E, Morelli O, Mencarelli A, Casini A, Mello T, Palazzetti B, Tallet D, del Soldato P, Morelli A. NCX-1000, a NO-releasing derivative of ursodeoxycholic acid, selectively delivers NO to the liver and protects against development of portal hypertension. Proc Natl Acad Sci USA 2001;10:10.

Forrester K, Ambs S, Lupold SE, Kapust RB, Spillare EA, Weinberg WC, Felley-Bosco E, Wang XW, Geller DA, Tzeng E, Billiar TR, Harris CC. Nitric oxide-induced p53 accumulation and regulation of inducible nitric oxide synthase expression by wild-type p53. Proc Natl Acad Sci USA 1996;93:2442-2447.

Forstermann U. Biochemistry and molecular biology of nitric oxide synthases. Arzneimittelforschung 1994;44:402-407.

Gasco A, Fruttero R, Sorba G. No-donors: An emerging class of compounds in medicinal chemistry. IL Farmaco 1996;51:617-635.

Gerlowski LE, Jain RK. Physiologically based pharmacokinetic modeling: principles and applications. J Pharm Sci 1983;72:1103-1126.

Gibaldi M. Biopharmaceutics and clinical pharmacokinetics. Lea & Febiger; Philadelphia, 1991. pp. 19-21.

Giziewicz J, Wnuk SF, Robins MJ. Nucleic acid related compounds. 107. Efficient nitration of uracil base and nucleoside derivatives. J Org Chem 1999;64:2149-2151.

Grisham MB, Johnson GG, Lancaster JR. Quantitation of nitrate and nitrite in extracellular fluids. Methods Enzymol 1996;268:237-246.

Hansch C, Elkins D. Partition coefficients and their uses. Chem Rev 1971;71: 525-554.

Harris N, Buller RML, Karupiah G. Gamma interferon-induced, nitric oxide-mediated inhibition of vaccinia virus replication. J Virol 1995;69:910-915.

Hibbs JB, Taintor RR, Vavrin Z, Rachlin EM. Nitric oxide: a cytotoxic activated macrophage effector molecule. Biochem Biophys Res Commun 1988;157:87-94.

Hou YC, Janczuk A, Wang PG. Current trends in the development of nitric oxide donors. Current Pharmaceutical Design 1999;5:417-441.

Huang GF, Torrence PF. Nitration of cytosine, 1-methylcytosine and 2'-deoxycytidine 5'-monophosphate by nitronium tetrafluoroborate in sulfolane. Preparation of 5-nitro-2'-deoxycytidine. J Carbohydrates Nucleosides Nucleotides 1978;5:317-327.

Jaffrey SR, Erdjument-Bromage H, Ferris CD, Tempst P, Snyder SH. Protein S-nitrosylation: A physiological signal for neuronal nitric oxide. Nat Cell Biol 2001;3:193-197.

Jenkins DC, Charles IG, Thomsen LL, Moss DW, Holmes LS, Baylis SA, Rhodes P, Westmore K, Emson PC, Moncada S. Roles of nitric oxide in tumor growth. Proc Natl Acad Sci USA 1995;92:4392-4396.

Khalili P, Naimi E, Knaus EE, Wiebe LI. Pharmacokinetics and metabolism of the novel synthetic *C*-nucleoside, 1-(2-deoxy-β-D-ribofuranosyl)-2,4-difluoro-5-iodobenzene: a potential mimic of 5-iodo-2'-deoxyuridine. Biopharm Drug Dispos 2002;23,105-113.

Komatsu T, Bi Z, Reiss CS. Interferon-γ induced type I nitric oxide synthase activity inhibits viral replication in neurons. J Neuroimmunol 1996;68:101-108.

Kreil TR, Eibl MM. Nitric oxide and viral infection: no antiviral activity against a flavivirus in vitro and evidence for contribution to pathogenesis in experimental infection in vivo. Virology 1996;219:304-306.

Lepoivre M, Chenais B, Yapo A, Lemaire G, Thelander L, Tenu J-P. Alterations of ribonucleotide reductase activity following induction of the nitrite-generating pathway in adenocarcinoma cells. J Biol Chem 1990;265:14143-14149.

Lichtenthaler FW, Muller HJ. 5'-Nitrates of pyrimidine nucleosides: Nitric acid analogs of nucleosides. Angew Chem Int Ed Engl 1973;12:752-753.

Lowenstein CJ, Hill SL, Lafond-walker A, Wu J, Allen G, Landavere M, Rose NR, Herskowitz A. Nitric oxide inhibits viral replication in murine myocarditis. J Clin Invest 1996;97:1837-1843.

Mannick JB. The antiviral role of nitric oxide. Res Immunol 1995;146:693-697.

Mariani G., Cei A, Collecchi P, Baranowska-Kortylewicz J, Van den Abbeele AD, Di Luca L, Di Stefano R, Viacava P, Ferdeghini EM, Di Sacco S, Salvadori PA, Bevilacqua G, Adelstein SJ, Mosca F, Kassis AI. Tumor targeting in vivo and metabolic fate of 5-[iodine-125] iodo-2'-deoxyuridine following intratumoral injection in patients with colorectal cancer. J Nucl Med 1993;34:1175-1183.

Melkova Z, Esteban M. Inhibition of vaccinia virus DNA replication by inducible expression of nitric oxide synthase. J Immunol 1995;155:5711-5718.

Mikami S, Kawashima S, Kanazawa K, Hirata K, Katayama Y, Hotta H, Hayashi Y, Ito H, Yokoyama M. Expression of nitric oxide synthase in a murine model of viral myocarditis induced by coxsackievirus B3. Biochem Biophys Res Commun 1996;220:983-989.

Miles AM, Wink DA, Cook JC, Grisham MB. Determination of nitric oxide using fluorescence spectroscopy. Methods Enzymol 1996;268:105-120.

Moncada S, Higgs A. The L-arginine-nitric oxide pathway. N Engl J Med 1993;329:2002-2012.

Moncada S, Palmer RM, Higgs EA. Biosynthesis of nitric oxide from L-arginine. A pathway for the regulation of cell function and communication. Biochem Pharmacol 1989;38:1709-1715.

Moncada S, Palmer RM, Higgs EA. Nitric oxide: physiology, pathophysiology and pharmacology. Pharm Rev 1991;43:109-142.

Murrel W. Nitro-glycerine as a remedy for angina pectoris. Lancet 1879;1:80-81.

Nagano T, Yoshimura T. Bioimaging of nitric oxide. Chem Rev 2002;102:1235-1269.

Naimi E, Zhou AH, Khalili P, Wiebe LI, Balzarini J, De Cleercq E, Knaus EE. Synthesis of 3'- and 5'-nitrooxy pyrimidine nucleoside nitrate esters: " Nitric oxide donor" agents for evaluation as anticancer and antiviral agents. J Med Chem 2003;46:995-1004.

Narurkar MM, Mitra AK. Synthesis, physiochemical properties, and cytotoxicity of a series of 5'-ester prodrugs of 5-iodo-2'-deoxyuridine. Pharm Res 1988;5:734-737.

Nathan C, Xie QW. Regulation of biosynthesis of nitric oxide. J Biol Chem 1994;269:13725-13728.

Nims RW, Cook JC, Krishna MC, Christodoulou D, Poore CMB, Miles AM, Grisham MB, Wink DA. Colorimetric assays for nitric oxide and nitrogen oxide species formed from nitric oxide stock solutions and donor compounds. Nitric Oxide, Part A: Sources and detection of NO. Methods Enzymol 1996;268:93-105.

Parang K, 1997. Evaluation of myristic acid analogs & 5'-O-ester prodrugs of dThd, AZT & FLT. Ph.D. Thesis, University of Alberta, p.133.

Parker JD, Parker JO. Nitrate therapy for stable angina pectoris. N Engl J Med 1998;338:520-531.

Prusoff WH, Jaffe JJ, Guenther H. Studies in the mouse of the pharmacology of 5-iododeoxyuridine, an analogue of thymidine. Biochem Pharmacol 1960;3:110-121.

Reiss CS, Komatsu T. Does nitric oxide play a critical role in viral infections? J Virol 1998;72:4547-4551.

Rossoni G, Manfredi B, Colonna VD, Bernareggi M, Berti F. The nitroderivative of aspirin, NCX 4016, reduces infarct size caused by myocardial ischemia-reperfusion in the anesthetized rat. J Pharmacol Exp Ther 2001;297:380-387.

Sanders SP, Siekierski ES, Porter JD, Richards SM, Proud D. Nitric oxide inhibits rhinovirus-induced cytokine production and viral replication in a human respiratory epithelial cell line. J Virol 1998;72:934-942.

Santi DV, McHenry CS, Sommer H. Mechanisms of interaction of thymidylate synthetase with 5-fluorodeoxyuridylate. Biochemistry 1974;13:471-481.

Shan RD, Knaus EE. The design of (-)-(*S*)-2-nitrooxyethyl 1,4-dihydro-2,6-dimethyl-3-nitro-4-(2-trifluoromethylphenyl)pyridine-5-carboxylate: A cardioselective positive inotrope derivative of Bay K 8644. Bioorg & Med Chem Letters 1999;9:2613-2614.

Smith DE, Brenner DE, Knusten CA, Deremer SJ, Terrio PA, Johnson NJ, Stetson PL, Ensminger WD. Mutual kinetic interaction between 5-fluorouracil and bromodeoxyuridine or iododeoxyuridine in dogs. Drug Metab Dispos 1992; 21:277-283.

Staeheli P. Interferon-inducible proteins and the anti-viral state. Adv Virus Res 1990;38:147-200.

Stamler JS, Singel DJ, Loscalzo J. Biochemistry of nitric oxide and its redox activated forms. Science 1992;258:1898-1902.

Stuehr DJ, Griffith OW. Mammalian nitric oxide synthases. Adv Enzymol Relat Areas Mol Biol 1992;65:287-346.

Stuehr DJ, Nathan CF. Nitric oxide: a macrophage product responsible for cytostasis and respiratory inhibition in tumor cell growth. J Exp Med 1989;169:1543-1555.

Sveinbjornsson B, Olsen R, Seternes OM, Seljelid R. Macrophage cytotoxicity against murine Meth A sarcoma involves nitric-oxide-mediated apoptosis. Biochem Biophys Res Commun 1996;223:643-649.

Szabo' C, Southan GJ, Thiemermann C. Beneficial effects and improved survival in rodent models of septic shock with *S*-methylisothiourea sulfate, a potent and selective inhibitor of inducible nitric oxide synthase. Proc Natl Acad Sci USA 1994;91:12472-12476.

Thomsen LL, Scott JM, Topley P, Knowles RG, Keerie AJ, Frend AJ. Selective inhibition of inducible nitric oxide synthase inhibits tumor growth in vivo: studies with 1400W, a novel inhibitor. Cancer Res 1997;57:3300-3304.

Titheradge MA. The enzymatic measurement of nitrate and nitrite. In: Nitric Oxide Protocols. Titheradge MA (editor). Humana Press; Totawa, NJ, 1998. Vol 100, pp. 83-91.

Vaidyanathan G, Zalutsky MR. Preparation of 5-[^{131}I]iodo- and 5-[^{211}At]astato-1-(2-deoxy-2-fluoro-β-D-arabinofuranosyl)uracil by a halodestannylation reaction. Nucl Med Biol 1998;25:487-496.

Wang PG, Xian M, Tang X, Wu X, Wen Z, Cai T, Janczuk J. Nitric oxide donors: Chemical activities and biological applications. Chem Rev 2002;102: 1091-1134.

Wang ZX, Duan W, Wiebe LI, Balzarini J, De Clercq E, Knaus EE. Synthesis of 1-(2-deoxy-β-D-ribofuranosyl)-2,4-difluoro-5-substituted-benzene thymidine mimics, some related α-anomers, and their evaluation as antiviral and anticancer agents. Nucleosides Nucleotides Nucleic Acids 2001;20:11-40.

Zaragoza C, Ocampo CJ, Saura M, McMillan A, Lowenstein CJ. Nitric oxide inhibition of coxsackievirus replication in vitro. J Clin Invest 1997;100:1760-1767.

5. General discussions and conclusions

The primary objective of this study was to evaluate some of the pharmacokinetic, biochemical, and physiochemical properties of selected 5-substituted derivatives of 1-(2-deoxy-β-D-ribofuranosyl)-2,4-difluorobenzene and 1-(2,3-dideoxy-3-nitrooxy-β-D-ribofuranosyl) uracil. Specifically, 1-(2-deoxy-β-D-ribofuranosyl)-2,4-difluoro-5-iodobenzene (5-IDFPdR) and 1-(2,3-dideoxy-3-nitrooxy-β-D-ribofuranosyl)-5-iodouracil (INUdR), also referred to as 5-iodo-3'-*O*-nitro-2'-deoxyuridine, were studied in vitro and in vivo. The following conclusions can be made based on the results of the studies described in this thesis.

5-IDFPdR, a novel *C*-aryl nucleoside mimic is very lipophilic (log P = 2.9), and very stable in vitro. The high lipophilicity of 5-IDFPdR compared to IUdR (log P = -0.96), would be expected to alter tissue biodistribution, especially through facile diffusion across the blood-brain-barrier (BBB), and into other lipoidal tissues. In contrast to classical 5-substituted-2'-deoxyuridines such as IUdR, which readily undergo deglycosylation and dehalogenation in the presence of pyrimidine phosphorylases, 5-IDFPdR is very stable in plasma/blood and resistant to phosphorolysis by bacterial thymidine phosphorylase.

5-IDFPdR exhibits dose-dependent pharmacokinetics in male Sprague-Dawley rats, especially following oral administration over the dose-range studied. In view of the low renal clearance of 5-IDFPdR, the observed decreased total body clearance of 5-IDFPdR with increasing dose may be explained in part by saturable non-renal metabolism of 5-IDFPdR. As a consequence of dose-dependent kinetics, dosage regimens for 5-IDFPdR would have to be carefully designed to avoid potential unpredictable toxicity and/or lack of pharmacological response associated with the disproportional changes in steady state drug concentrations on changing dose.

Overall, only a fraction of the total administered 5-IDFPdR dose has been accounted for here. In addition to the phase II glucuronide and sulfate conjugates that were found, other metabolic pathways likely contribute to the elimination of 5-IDFPdR and would need to be investigated in future studies. Moreover, studies with radiolabeled 5-IDFPdR would be needed to estimate the bioavailability of 5-IDFPdR and to perform imaging studies that may elucidate the distribution of 5-IDFPdR in the body. Being a very lipophilic nucleoside, 5-IDFPdR may be trapped in, or bound to lipoidal tissues as well as incorporated into DNA.

Since lack of cytotoxicity of 5-IDFPdR and related compounds may be due to their inefficient phosphorylation by cellular nucleoside kinases, it may be possible to transform this class of compounds into a class of effective anticancer/antiviral agents by making their 5'-*cyclo*Sal-pronucleotide derivatives (Meier et al., 1998, 1999a,b). 5'-*cyclo*Sal-pronucleotide derivatization could serve as a useful strategy to overcome a metabolic blockade such as rate-limiting monophosphorylation of the nucleoside mimic 5-IDFPdR.

INUdR, a novel 3'-nitrooxy pyrimidine nucleoside nitrate ester is lipophilic (log P = 1.12) and stable towards phosphorolysis by the thymidine phosphorylase enzyme. Despite its good chemical stability, INUdR is unstable in rat plasma and degrades rapidly and directly to NUdR (deiodinated INUdR). This direct dehalogenation of a halopyrimidine, is unlike the reductive dehalogenation reported for most other nucleosides in which a catabolic breakdown of the nucleoside often precedes the reductive dehalogenation of the nucleobase (Smith et al., 1992). Introduction of a nitrooxy group at the 3'-position of the sugar ring of IUdR does not appear to have any stabilizing effect against its deiodination in plasma. Instead, it seems to introduce a rather unique mechanism for dehalogenation of INUdR, possibly due to some unique steric or electronic effect.

While INUdR did not exhibit any significant cytotoxicity against the various cancer cell lines examined, it did have some antiviral activity against certain viruses, including herpes simplex virus type 1 (KOS), herpes simplex virus type 2 (G), and vaccinia virus (IC_{50} = 48 μg/mL). The antiviral effects of INUdR are likely to be due in part to the release of NO from this compound, since it has been shown that replication of herpes simplex virus type 1 (Croen, 1993) and vaccinia virus (Harris et al., 1995) are inhibited by induction of NO synthase, or by the addition of NO-donors.

The pharmacokinetics of INUdR following single intravenous bolus and oral doses of INUdR (40 mg/kg) to male Sprague-Dawley (SD) rats is characterized by a short elimination half-life ($T_{1/2}$= 0.3 to 0.4 h), a large steady-state volume of distribution (V_{ss} 0.89 L/kg) which may be suggestive of intracellular distribution of INUdR, and a high oral bioavailability (Fa = 0.95). Glucuronide metabolites of INUdR were recovered in both urine and bile samples.

5.1. References

Croen KD. Evidence for antiviral effect of nitric oxide. Inhibition of herpes simplex virus type 1 replication. J Clin Invest 1993;91:2446-2452.

Harris N, Buller RML, Karupiah G. Gamma interferon-induced, nitric oxide-mediated inhibition of vaccinia virus replication. J Virol 1995;69:910-915.

Meier C, Knispel T, De Clercq E, Balzarini J. *Cyclo*Sal-pronucleotides of 2',3'-dideoxyadenosine and 2',3'-didehydroadenosine: Synthesis and antiviral evaluation of a highly efficient nucleotide delivery system. J Med Chem 1999b;42:1604-1614.

Meier C, Knispel T, Marquez VE, Siddiqui MA, De Clercq E, Balzarini J. *Cyclo*Sal-pronucleotides of 2'-fluoro-*ara*- and 2'-fluoro-*ribo*-2',3'-dideoxyadenosine as a strategy to bypass a metabolic blockade. J Med Chem 1999a;42:1615-1624.

Meier C, Lorey M, De Clercq E, Balzarini J. *Cyclo*Sal- 2',3'-dideoxy-2',3'-didehydrothymidine monophosphate (*cyclo*Sal-d4TMP): Synthesis and antiviral evaluation of a new d4TMP delivery system. J Med Chem 1998;41:1417-1427.

Smith DE, Brenner DE, Knusten CA, Deremer SJ, Terrio PA, Johnson NJ, Stetson PL, Ensminger WD. Mutual kinetic interaction between 5-fluorouracil and bromodeoxyuridine or iododeoxyuridine in dogs. Drug Metab Dispos 1992; 21:277-283.

6. Appendix

Synthesis of 3'- and 5'-nitrooxy pyrimidine nucleoside nitrate esters: " Nitric oxide donor" agents for evaluation as anticancer and antiviral agents.

Naimi E, Zhou A, Khalili P, Wiebe LI, Balzarini J, De Clercq E, Knaus EE.

J Med Chem 2003;46:995-1004.

J. Med. Chem. **2003**, *46*, 995–1004

Synthesis of 3′- and 5′-Nitrooxy Pyrimidine Nucleoside Nitrate Esters: "Nitric Oxide Donor" Agents for Evaluation as Anticancer and Antiviral Agents

Ebrahim Naimi,[†] Aihua Zhou,[†] Panteha Khalili,[†] Leonard I. Wiebe,[†] Jan Balzarini,[§] Erik De Clercq,[§] and Edward E. Knaus*,[†]

Faculty of Pharmacy and Pharmaceutical Sciences, University of Alberta, Edmonton, Alberta T6G 2N8, Canada, and Rega Institute for Medical Research, Minderbroedersstraat 10, Leuven B-3000, Belgium

Received July 10, 2002

A group of 3′-*O*-nitro-2′-deoxyuridines, 3′-*O*-nitro-2′-deoxycytidines, and 5′-*O*-nitro-2′-deoxyuridines possessing a variety of substituents (H, Me, F, I) at the C-5 position were synthesized for evaluation as anticancer/antiviral agents that have the ability to concomitantly release cytotoxic nitric oxide (•NO). Although these compounds generally released a greater percent of •NO than the reference drug isosorbide dinitrate upon incubation in the presence of L-cysteine, or serum, their cytotoxicity (CC$_{50}$ = 10^{-3} to 10^{-6} M range) was comparable to 5-iodo-2′-deoxyuridine, but weaker than 5-fluoro-2′-deoxyuridine, against a variety of cancer cell lines. No differences in cytotoxicity against nontransfected (KBALB, 143B), and the corresponding transfected (KBALB–STK, 143B-LTK) cancer cell lines possessing the herpes simplex virus type 1 (HSV-1) thymidine kinase gene (TK$^+$) were observed, indicating that expression of the viral TK enzyme did not provide a gene therapeutic effect. These nitrate esters were inactive antiviral agents except for 5-iodo-3′-*O*-nitro-2′-deoxyuridine that showed modest activity against HSV-1, HSV-2, and vaccinia virus.

Introduction

Since the discovery that nitric oxide (•NO) is biosynthesized in mammalian cells, •NO has become a molecule of immense interest in medical research. In mammalian systems, •NO is synthesized via an enzymatic oxidation of L-arginine by nitric oxide synthase isozymes [neuronal (nNOS), inducible (iNOS), endothelial (eNOS)] that are differentially expressed and play different physiological roles.[1–4] •NO production in response to immune activation, or inflammatory reaction, has been shown to serve as part of the host defense system against cancerous cells, and intracellular microbes and parasites.[5] In this regard activated macrophages, that produce •NO, have been shown to inhibit DNA synthesis in tumor cells.[6] Pretreatment of various cell lines with a •NO-donor led to inhibition of the replication of poliovirus, picornavirus, and rhinovirus.[3] In addition, IFN-γ treated cells produce •NO that inhibits HSV-1 (herpesvirus).[3] Other studies indicate that the antitumor activity of IL-1α may be mediated by the production of •NO from tumor-derived endothelial cells,[7] and that macrophage •NO synthesis delays progression of ultraviolet light-induced murine skin cancer through to an antitumor immune response.[8]

•NO plays an important role in the action of a number of anticancer drugs due to its ability to influence various aspects of tumor biology including modulation of cell growth,[9] apoptosis,[10] differentiation,[11] metastatic capability,[12] and tumor-induced immunosuppression.[13] Thus, adriamycin stimulates •NO production in EMT-6 cells, and in vivo adriamycin inhibits tumorigenesis partially via a •NO-dependent, nonapoptotic mechanism.[14] Several antiviral acyclic nucleotide analogues activate expression of cytokine genes such as TNF-α and IL-10 in macrophages, and IFN-γ in splenocytes, resulting in an enhanced production of •NO.[15] A group of glyco-*S*-nitrosothiols were found to be cytotoxic to DU-145 human prostate cancer cells in vitro.[16] Induction of •NO production by cytokines indicated that high levels of •NO may contribute to the induction of apoptosis and inhibition of pancreatic tumor growth.[17] A correlation exists between the intracellular levels of •NO with the cytotoxicity of hydroxyguanidine in HL60 cells, where a higher toxicity was observed in hypoxic cells relative to oxic cells.[18] The hypoxic cell radiosensitization effects of the •NO-donor Et$_2$N[N(NO)]$^-$ Na$^+$, coupled with the vasodilatory effect of •NO on tumor vasculature, suggest that an agent of this type opens a new avenue in radiation oncology treatment.[19] The rate and extent of •NO release from •NO/nucleophile adducts, which release •NO spontaneously in solution, correlated with inhibition of DNA synthesis in A375 human melanoma cells.[9] Tamoxifen has been shown to induce iNOS, producing •NO that is cytotoxic.[20] •NO-induced apoptosis in macrophages activated with cisplatin and IFN-γ requires activation of an endonuclease.[21] •NO-donor agents have been shown to enhance melphalan cytoxicity in breast cancer MCF-7 cells, possibly by delaying entry into the S-phase and a G2/M block.[22] Using a number of aromatic *N*-nitroso compounds, it was shown that the extent of •NO generation was the reciprocal of ID$_{50}$ growth inhibition (cytotoxicity).[23] These data collectively indicate that •NO exhibits a cytotoxic effect and/or enhances the cytotoxic effect of anticancer drugs. However, there are a few instances where •NO is detrimental to anticancer activity. For example, •NO generated from a •NO-donor drug was shown to prevent

10.1021/jm020299r CCC: $25.00 © 2003 American Chemical Society
Published on Web 02/12/2003

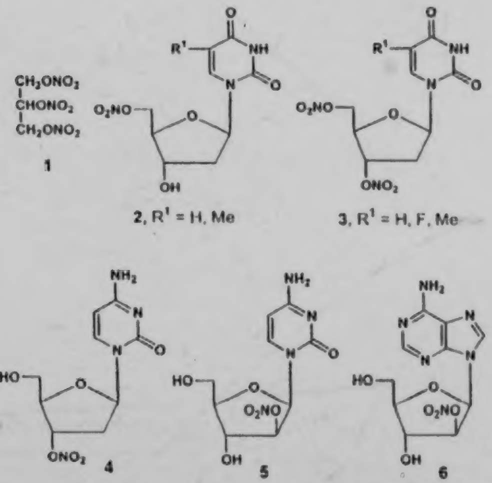

Figure 1. Structures of glycerol trinitrate (**1**), 5′-*O*-nitro-2′-deoxyuridine (**2**), 3′,5′-di-*O*-nitro-2′-deoxyuridine (**3**), 3′-*O*-nitro-2′-deoxycytidine (**4**), nitrara-C (**5**), and nitrara-A (**6**) nitrate esters.

taxol-induced apoptosis, and this was attributed to inhibition of an IL-1 beta converting enzyme-like protease cascade (human neuroblastoma cell line, NB-39-nu).[24] A related study showed that the protective effect of •NO on taxol-induced apoptosis may be partially caused by inhibiting entrance of the cells into the G2/M phase (human leukemia HL-60 cells).[25] These data indicate that the efficacy of an •NO-donor anticancer drug may be dependent upon the specific cell line.

Organic nitrates ($RONO_2$), which are nitric acid esters of mono- or polyhydric alcohols, represent the oldest class of •NO donor compounds that include the classical drug glycerol trinitrate (**1**) that is used to treat angina pectoris.[26] Although some 5′-*O*-nitro-2′-deoxyuridine (**2**),[27,28] 3′,5′-di-*O*-nitro-2′-deoxyuridine (**3**),[29−31] and 3′-*O*-nitro-2′-deoxycytidine (**4**)[32] compounds have been synthesized, no biological data were reported (see structures in Figure 1). On the other hand, the 2′-*O*-nitro derivatives of arabinocytidine (Nitrara-C, **5**), which resists enzymatic deamination, exhibited antileukemic activity in vitro and in vivo.[33] The related 2′-*O*-nitro derivative of arabinoadenine (Nitrara-A, **6**), that is deaminated about 25-fold slower than Ara-A, inhibited the proliferation of human T-lymphoblasts (CCRF−CEM cell line) in vitro.[34] The design of tumor selective •NO-donor/nucleoside hybrid drugs, that release both cytotoxic •NO and a nucleoside drug in a controlled fashion, constitutes an attractive method to develop a novel class of double-barreled anticancer drugs. The nucleoside component of these hybrid drugs, as the 5′-monophosphate, could act as an irreversible inhibitor of thymidylate synthase (TS), whereas the 5′-triphosphate could serve as an unnatural substrate for, or inhibitor of, DNA polymerase to elicit a cytotoxic anticancer/antiviral effect. Accordingly, we now report the syntheses, in vitro •NO release data, and anticancer and antiviral activities, for a group of 3′-*O*-nitro-2′-deoxyuridines (**10a**−**d**), 3′-*O*-nitro-2′-deoxycytidines (**13a**−**c**), and 5′-*O*-nitro-2′-deoxyuridines (**15a**−**c**).

Scheme 1[a]

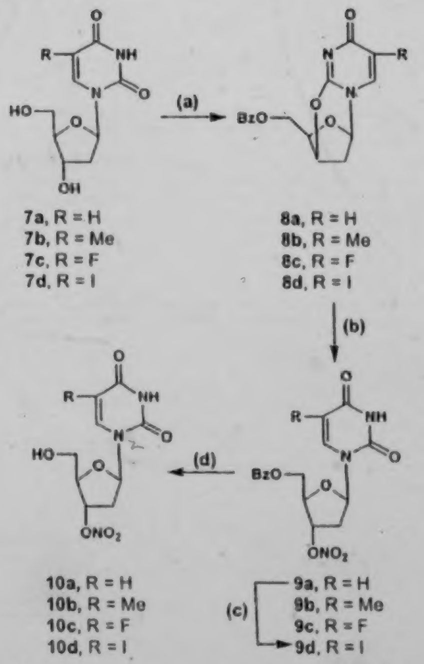

[a] Reagents and conditions: (a) C_6H_5COOH, Ph_3P, DIAD, DMF, 25 °C; (b) NH_4NO_3, DMF, 110 °C; (c) ICl, NaN_3, MeCN, 0 °C → 25 °C; (d) NaOMe, MeOH, 25 °C.

Chemistry

A group of 2,3′-anhydro-5′-*O*-benzoyl-2′-deoxyuridines **8a**−**d** possessing a variety of C-5 substituents (R = H, Me, F, I) were prepared from the 2′-deoxyuridine precursors **7a**−**d** by a one-pot tandem Mitsunobu reaction,[35,36] using triphenylphosphine, diisopropyl azodicarboxylate, and benzoic acid in 81%, 74%, 90%, and 82% yield, respectively. Ring opening of the 2,3′-anhydro derivatives **8a**−**d** proceeded readily upon reaction with ammonium nitrate (NH_4NO_3) in dimethyl formamide to form the respective 3′-*O*-nitrate esters **9a**−**d** in 31%, 34%, 50%, and 2.8% yield, respectively. Since conversion of the 5-iodo compound **8d** to **9d** was low (2.8% yield) in this reaction, compound **9d** was prepared by iodination of **9a** using iodine monochloride (ICl) and sodium azide (NaN_3) in acetonitrile[37] in 82.5% yield (see Scheme 1). Deprotection of compounds **9a**−**d** using NaOMe in MeOH afforded the target 5-substituted-3′-*O*-nitro-2′-deoxyuridines **10a**−**d** in 91−95% yield.

The configuration at the C-3′ carbon, and the rotamer orientation of the uracil (**10a**) and thymine (**10b**) ring, was analyzed by nuclear Overhauser enhancement (NOE) ^{1}H NMR difference spectroscopy (Figure 2). Selective irradiation of the H-3′ signal resulted in an enhancement of the arabino (up) H-2′ signal of **10a** (2.2%), and of **10b** (1.9%), indicating that the C-3′ nitrooxy substituent is in the ribo (down) position. No NOE effect was observed between H-3′ and either H-2′ or H-1′ of **10a**,**b**. The observation that selective irradiation of the H-4′ signal resulted in enhancement of the H-1′ signal of **10a** (3.1%), and of **10b** (2.5%), indicates

169

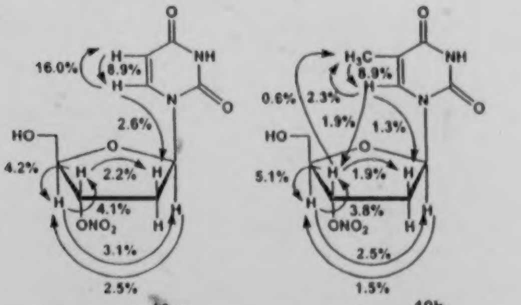

10a **10b**

Figure 2. Some NOE measurements to determine the rotameric orientation of the uracil base moiety, and the conformation of the nitrooxy substituent, for the 3′-*O*-nitro-2′-deoxyuridine compounds **10a**,**b** in DMSO-d_6 at 22 °C.

that these two hydrogen atoms are on the same face of the sugar moiety which is indicative of the β-configuration.[38] Selective irradiation of the H-6 signal of **10a** produced an enhancement of the arabino (up) H-2′ signal (2.6%), whereas a similar irradiation for **10b** showed enhancement for the arabino H-2′ (1.3%), and the H-3′ (1.9%), signals. These NOE data indicate the C-6 hydrogen of the uracil moiety of **10a**, or the thymine moiety of **10b**, is oriented in the direction of the sugar ring.

A related group of 3′-*O*-nitro-2′-deoxycytidines **13a–c** having a C-5 hydrogen, methyl, or iodo substituent were prepared using the three-step reaction sequence illustrated in Scheme 2. Thus, reaction of the 5′-*O*-benzoyl-3′-*O*-nitro-2′-deoxyuridines **9a**,**b** with 1,2,4-triazole and 4-chlorophenyl dichlorophosphate in pyridine[39-41] afforded the corresponding 4-(1,2,4-triazolo) derivatives **11a** and **11b** in 79 and 71% yield, respectively. Subsequent treatment of **11a**, or **11b**, with aqueous ammonia in dioxane[39-41] yielded the 2′-deoxycytidine compound **12a** (49%), or **12b** (36%), which on deprotection with NaOMe in MeOH to remove the 5′-*O*-benzoyl moiety, afforded the target 3′-*O*-nitro-2′-deoxycytidine **13a** (95%), or 5-methyl-3′-*O*-nitro-2′-deoxycytidine **13b** (94%), respectively. Iodination of **13a** with iodic acid and iodine[42,43] yielded 5-iodo-3′-*O*-nitro-2′-deoxycytidine **13c** (56%). The procedure described above for the synthesis of **13a** is superior to the reported method involving nitration of 2′-deoxycytidine 5′-*O*-monophosphate using nitronium tetrafluoroborate, which gave a mixture of the 5′-*O*-monophosphates of 5-nitro-3′-*O*-nitro-2′-deoxycytidine, 5-nitro-2′-deoxycytidine, and 3′-*O*-nitro-2′-deoxycytidine in a ratio of 12:1:3 that were subsequently dephosphorylated by the action of alkaline phosphatase to the free nucleosides.[32]

The 5′-*O*-nitro-2′-deoxyuridines **15a–c** possessing a C-5 H, Me, or I substituent were also prepared (see Scheme 3). Accordingly, nucleophilic displacement of the 5′-*O*-tosylate moiety in **14a**, or **14b**, using $LiNO_3$ in DMF at 110 °C, afforded the respective 5′-*O*-nitro product **15a** (73%), or **15b** (71%). This synthesis of **15a** was superior to nitration of 2′-deoxyuridine with 90% nitric acid at −70 °C which gave a mixture of **15a** (20%) and 3′,5′-di-*O*-nitro-2′-deoxyuridine (13%).[27] Synthesis of **15b** by displacement of the 5′-*O*-tosylate moiety in **14b**, was equally effective to a reported method involving displacement of either a 5′-*O*-P(=S)OEt$_3$, or 5′-I, substituent using $AgNO_3$.[28] Electrophilic iodination of **15a** using ICl and NaN_3 in MeCN gave the 5-iodo product **15c** (65%).

Scheme 2[a]

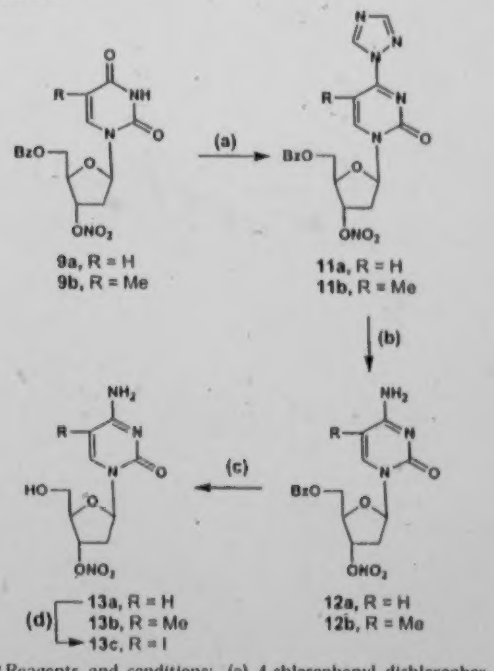

[a] Reagents and conditions: (a) 4-chlorophenyl dichlorophosphate, 1,2,4-triazole, pyridine, 0 °C → 25 °C; (b) NH_4OH, dioxane, 25 °C; (c) NaOMe, MeOH, 25 °C; (d) iodine, iodic acid, acetic acid, H_2O, CCl_4, 25 °C.

Scheme 3[a]

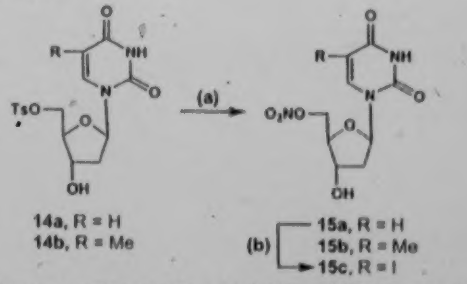

[a] Reagents and conditions: (a) $LiNO_3$, DMF, 100–110 °C, overnight; (b) ICl, NaN_3, MeCN, 0 °C → 25 °C, 48 h.

Results and Discussion

Organic nitrate esters are generally stable in neutral or mild acidic aqueous solution, but nucleophilic hydrolysis to an alcohol and nitrate occur under strongly alkaline conditions. •NO release from organic nitrates may occur as a result of either nonenzymatic or enzymatic biotransformation that proceeds via a three-electron reduction. Accordingly, cellular thiols may play a role in the nonenzymatic production of •NO from glycerol trinitrate (**1**, GTN) whereas, a NADPH-depend-

Table 1. In Vitro Percent Nitric Oxide Release for 3′-*O*-Nitro-2′-deoxyuridines (**10a**–**d**), 3′-*O*-Nitro-2′-deoxycytidines (**13a**–**c**), and 5′-*O*-nitro-2′-deoxyuridines (**15a**–**c**)

	% NO release[a] (18 mM L-cysteine)		% NO release[b] (serum)	
compd	1 hour	16 hours	1 hour	16 hours
10a	4.9 ± 0.0	51.0 ± 0.1	7.7 ± 0.7	9.0 ± 1.5
10b	4.9 ± 0.1	53.6 ± 0.7	7.4 ± 0.9	7.4 ± 0.3
10c	0.0 ± 0.0	3.8 ± 0.1	4.0 ± 0.9	6.6 ± 0.7
10d	3.9 ± 0.1	37.6 ± 0.1	12.3 ± 1.1	13.2 ± 0.3
13a	1.5 ± 0.0	17.1 ± 0.2	18.8 ± 0.9	20.2 ± 0.9
13b	3.8 ± 0.0	50.3 ± 0.7	47.1 ± 3.1	59.5 ± 1.5
13c	4.0 ± 0.1	47.2 ± 0.0	12.5 ± 0.5	17.6 ± 1.7
15a	5.4 ± 0.1	59.9 ± 1.7	2.9 ± 0.8	4.4 ± 1.0
15b	5.0 ± 0.0	59.8 ± 0.2	3.6 ± 0.4	4.8 ± 1.1
15c	3.7 ± 0.1	36.4 ± 0.4	3.9 ± 0.5	4.7 ± 1.0
ISDN[c]	3.5 ± 0.2	24.0 ± 0.2	1.9 ± 0.1	2.6 ± 0.6

[a] The percent nitric oxide released from the test compound was determined as the percent of nitrite (NO_2^-) produced in the presence of L-cysteine (18 mM) as quantitated using the Griess reagent (±SD, $n = 3$). [b] The percent nitric oxide released from the test compound was determined as the percent of nitrite (NO_2^-) produced in the presence of serum as quantitated using the Griess reagent (±SD, $n = 3$). [c] ISDN = isosorbide dinitrate (ISDN possesses two ONO_2 groups which may release •NO, whereas compounds **10**, **13**, and **15** possess only one ONO_2 group that may release •NO).

ent cytochrome P450 pathway and specific isozymes of the glutathione-*S*-transferase group are thought to be operative in the biotransformation/bioactivation of organic nitrates.[26] Although the sole product from reaction of •NO with oxygen in water is nitrite, •NO reacts rapidly with superoxide anion to initially produce a cytotoxic peroxynitrite anion ($ONOO^-$) species that can damage DNA.[5]

The percentages of •NO released, quantitated as nitrite (NO_2^-) using the Griess reaction,[44] upon incubation of the 3′-*O*-nitro derivatives of 2′-deoxyuridine (**10a**–**d**) and 2′-deoxycytidine (**13a**–**c**), and the 5′-*O*-nitro derivatives of 2′-deoxyuridine (**15a**–**c**) in the presence of 18 mM L-cysteine or serum are listed in Table 1. All three groups of compounds (**10**, **13**, **15**) that possess a single ONO_2 moiety, with the exception of 5-fluoro-3′-*O*-nitro-2′-deoxyuridine (**10c**), exhibited comparable or in most instances superior nitric oxide release (1.5–5.4% range at 1 h, and 17.1–59.9% range at 16 h) upon incubation in the presence of L-cysteine compared to the reference drug isosorbide dinitrate (3.5 and 24% release at 1 h and 16 h) that contains two ONO_2 moieties. These results are consistent with the observation that thiols enhance in vitro release of •NO in aqueous buffer solution for •NO-donor compounds although intact cells and tissues show that conversion of organic nitrate esters ($RONO_2$) to •NO is not free-thiol dependent.[45] In contrast, release of •NO from **10**, **13**, and **15** was negligible in the absence of L-cysteine (<0.05% at 1 h and <1.0% at 16 h). A similar study to determine the release of •NO upon incubation in the presence of serum showed that 3′-*O*-nitro-2′-deoxycytidine compounds (**13**) generally provided a greater percent •NO release than the related compounds **10** and **15**. The unusually high release of •NO from 5-methyl-3′-*O*-nitro-2′-deoxycytidine (**13b**, 47.1%) upon incubation with serum at 1 h, relative to that in the presence of 18 mM L-cysteine (3.8% release), indicates that •NO must be released from **13b** by a thiol-independent mechanism in serum. Compounds **10a**–**d**, **13a**–**c**, and **15a**–**c** all exhibited a greater release of •NO in the presence of serum (2.9–47.1% range at 1 h, and 4.4–59.5% range at 16 h) than the reference drug isosorbide dinitrate (1.9% at 1 h and 2.6% at 16 h).

Compounds **10a**–**d**, **13a**–**c**, **15a**–**c**, and the reference compounds 5-iodo-2′-deoxyuridine (IUDR), 5-fluoro-2′-deoxyuridine (FUDR), and thymidine, were evaluated for their tumor cell cytotoxicity using the MTT cytotoxicity assay[46] (see data in Table 2). These 3′- and 5′-*O*-nitro pyrimidine nucleosides exhibited comparable cytotoxicity (CC$_{50}$ = 10^{-3} to 10^{-6} M range) to 5-iodo-2′-deoxyuridine, but weak cytotoxicity in comparison to 5-fluoro-2′-deoxyuridine, against KBALB, KBALB–STK, 143B, 143B-LTK, and EMT-6. 5-Fluoro-3′-*O*-nitro-2′-deoxyuridine (**10c**) was the most cytotoxic compound against this group of cancer cell lines (CC$_{50}$ = 10^{-6} M range). Elaboration of the 3′-OH group of IUDR to a 3′-*O*-NO_2 group (**10d**) decreased cytotoxicity by 2.5- to 26-fold in all cell lines except for EMT-6 cells where cytotoxicity was enhanced by about 6-fold. The position of the *O*-NO_2 substituent was not a determinant of anticancer activity, since 5-iodo-3′-*O*-nitro-2′-deoxyuridine (**10d**) and 5-iodo-5′-*O*-nitro-2′-deoxyuridine (**15c**) were approximately equipotent. The observation that compounds **10c**–**d** and **13c** exhibited similar cytotoxicity against nontransfected (KBALB, 143B), and the corresponding transfected (KBALB–STK, 143B-LTK) cancer cell lines possessing the herpes simplex virus type 1 (HSV-1) thymidine kinase gene (TK$^+$) indicates that expression of the viral TK enzyme did not provide a gene therapeutic effect. This observation was also made for **10a** and **10b** that did not show increased cytostatic activity in murine mammary (FM3A) and human osteosarcoma cells transfected with the HSV-1 TK gene when compared with their parental counterparts (data not shown). The •NO drug ISDN exhibited comparable cytotoxicity (CC$_{50}$ = 10^{-4} M range) against all cell lines tested (Table 2).

Compounds **10a**–**d** were evaluated for their antiviral activity in a wide variety of assay systems.[47] Antiviral activities against herpes simplex virus type 1 (KOS), herpes simplex virus type 2 (G), thymidine kinase-deficient (TK$^-$) herpes simplex virus type 1 (KOS, ACV^r), vaccinia virus, and vesicular stomatitis virus in E$_6$SM cells were determined. These compounds were generally inactive or exhibited negligible activity in these antiviral assay systems (at concentrations up to 400 μg/mL). 5-Iodo-3′-*O*-nitro-2′-deoxyuridine (**10d**) showed some inhibitory activity against HSV-1 (KOS), HSV-2 (G), and vaccinia virus (IC$_{50}$ = 48 μg/mL), relative to the reference drug (*E*)-5-(2-iodovinyl)-2′-deoxyuridine (IC$_{50}$ = 0.0051, 80.0, and 2.3 μg/mL, respectively). In addition, compounds **10a**–**d** did not reduce cytopathicity induced by parainfluenza-3 virus, reovirus-1, Sindbis virus, Coxsakie B4 virus, or Punta Toro virus in Vero cell cultures (IC$_{50}$ > 80 μg/mL), or respiratory syncytial virus in HeLa cell cultures (IC$_{50}$ > 80 μg/mL).

The modest anticancer, and near absence of antiviral, efficacy for this novel class of •NO-donor nucleosides could be due to a number of factors. For example, it is possible that the sugar moiety does not undergo phosphorylation by thymidine kinase (TK) to the 5′-mono-

Table 2. In Vitro Cell Cytotoxicity for 3′-*O*-Nitro-2′-deoxyuridines (**10a–d**), 3′-*O*-Nitro-2′-deoxycytidines (**13a–c**), and 5′-*O*-Nitro-2′-deoxyuridines (**15a–c**)

	cellular toxicity (CC_{50}, M) toward various cell lines[a]				
compd	KBALB[b]	KBALB–STK[c]	143-B[d]	143B-LTK[c]	EMT-6[e]
10a	-	-	-	8.5×10^{-4}	
10b	1.0×10^{-3}	7.0×10^{-3}	-	-	-
10c	8.0×10^{-6}	3.5×10^{-6}	2.4×10^{-8}	7.4×10^{-5}	6.2×10^{-6}
10d	2.4×10^{-4}	2.6×10^{-4}	5.8×10^{-4}	4.1×10^{-4}	2.3×10^{-5}
13a	-	-	-	2.0×10^{-4}	-
13b	-	-	-	1.0×10^{-3}	-
13c	1.0×10^{-3}	2.5×10^{-4}	2.0×10^{-4}	2.0×10^{-4}	3.4×10^{-4}
15a	1.0×10^{-3}			-	
15b	-	3.0×10^{-4}	-	-	
15c	3.4×10^{-4}	2.5×10^{-4}	3.4×10^{-4}	2.1×10^{-5}	-
IUDR[f]	9.7×10^{-5}	1.0×10^{-5}	7.0×10^{-3}	7.4×10^{-3}	3.8×10^{-4}
FUDR[g]	6.0×10^{-11}	8.8×10^{-11}	9.0×10^{-5}	1.0×10^{-4}	9.0×10^{-12}
thymidine	9.5×10^{-5}	1.0×10^{-4}	-	-	1.3×10^{-4}
ISDN[h]	9.7×10^{-4}	6.5×10^{-4}	6.0×10^{-4}	7.0×10^{-4}	-

[a] The molar concentration of the test compound that killed 50% of the cells (or 50% cell survival) upon incubation for 3–5 days at 37 °C in a humidified atmosphere of 95% air and 5% CO_2 (mean value, $n = 6$) was determined using the 3-(4,5-dimethyl-2-thiazolyl)-2,5-diphenyl-2*H*-tetrazolium bromide (MTT) assay. [b] Transformed fibroblast sarcoma cell line. [c] These cells were transfected by, and expressed, the herpes simplex virus type 1 thymidine kinase (HSV-1 TK) gene. [d] Human osteosarcoma cell line. [e] Mouse mammary carcinoma cell line. [f] IUDR = 5-iodo-2′-deoxyuridine. [g] FUDR = 5-fluoro-2′-deoxyuridine. [h] ISDN = isosorbide dinitrate.

phosphate (5′-MP). Support for this explanation is based on the observations that there are generally negligible differences in anticancer/antiviral activities between nontransfected (KBALB, 143B) and viral TK-transfected (KBALB–STK, 143B-LTK) cell lines. Alternatively, this group of nucleoside nitrate esters may be devoid of anticancer/antiviral activity due to the fact that they are not inhibitors of thymidylate synthase (TS). Credence for this possibility is based on the belief that the anticancer activity exhibited by 5-fluoro-2′-deoxyuridine is primarily due to inhibition of DNA biosynthesis by blocking TS, the enzyme which catalyzes the methylation of 2′-deoxyuridine-5′-monophosphate to 2′-deoxythymidine-5′-monophosphate.[48,49] Furthermore, inhibition of TS is the mechanism by which certain nucleosides such as (*E*)-5-(2-iodovinyl)-2′-deoxyuridine and 5-(1-azidovinyl)-2′-deoxyuridine seem to exhibit their cytostatic effect.[50]

Conclusions

A group of nitric oxide donor 3′-*O*-nitro derivatives of 2′-deoxyuridine (**10**) and 2′-deoxycytidine (**13**), and 5′-*O*-nitro-2′-deoxyuridines (**15**), were designed to investigate the concept whether the concomitant release of cytotoxic nitric oxide may enhance the anticancer/antiviral efficacy of pyrimidine nucleosides. This group of compounds generally exhibits comparable and in most instances superior nitric oxide release, upon incubation with phosphate buffer containing 18 mM L-cysteine or in the presence of serum, compared to the reference drug isosorbide dinitrate. This group of 3′- and 5′-*O*-nitrate esters exhibit comparable in vitro cytotoxicity to 5-iodo-2′-deoxyuridine, but weaker cytotoxicity than 5-fluoro-2′-deoxyuridine, in a variety of cancer cell lines. These nitrate esters were devoid of antiviral activity except for 5-iodo-3′-*O*-nitro-2′-deoxyuridine, which showed marginal activity against HSV-1, HSV-2 and vaccinia virus in cell cultures.

Experimental Section

General. Melting points were determined with a Thomas-Hoover capillary apparatus and are uncorrected. Nuclear magnetic resonance (^{1}H NMR, ^{13}C NMR) spectra were recorded on a Bruker AM-300 spectrometer. Proton chemical shifts (δ) are given relative to internal TMS (δ 0), and the assignment of exchangeable protons (N*H*, O*H*) was confirmed by addition of D_2O. The nuclear Overhauser enhancement (NOE) studies were performed under steady-state conditions using the Bruker NOE DIFF.AU software program (signal:noise ratio of 136 for a single pulse). DMSO-d_6 was dried using molecular sieves (type 3A, 1.6-mm pellets) and degassed by passage of dry argon gas at 22 °C just prior to use. Molecular tumbling time was not altered. ^{13}C NMR spectra were acquired using the *J* modulated spin–echo technique where methyl and methine carbon resonances appear as positive peaks, methylene and quaternary carbon resonances appear as negative peaks, and carbon chemical shifts (δ) are given relative to $CDCl_3$ (δ 77). Elemental analyses were performed by the MicroAnalysis Service Laboratory, Department of Chemistry, University of Alberta, and the results were within ±0.4% of theoretical values for all elements listed. Silica gel 60A (Silicycle Co., 230–400 mesh) was used for all flash column chromatography separations. 5′-*O*-Tosyl-2′-deoxyuridine (**14a**)[51] and 5′-*O*-tosyl-2′-deoxythymidine (**14b**)[52] were prepared according to literature procedures. All other reagents were purchased from Aldrich Chemical (Milwaukee, WI).

General Method for the Preparation of 5-Substituted-2,3′-anhydro-5′-*O*-benzoyl-2′-deoxyuridines (8a–d). A solution containing either **7a**, **7b**, **7c**, or **7d** (65.7 mmol) and triphenylphosphine (Ph_3P, 25.9 g, 98.6 mmol) in DMF (90 mL) was prepared, a solution comprised of diisopropyl azodicarboxylate (DIAD, 19.5 mL, 98.6 mmol) and benzoic acid (12.1 g, 98.6 mmol) in DMF (40 mL) was added dropwise with stirring at 25 °C, and the reaction was allowed to proceed for 30 min at 25 °C. An additional aliquot of Ph_3P (98.6 mmol) and DIAD (98.6 mmol) was added, the reaction was allowed to proceed for 1 h, Et_2O (400 mL) was added, and the mixture was stirred for 10 min at 25 °C. The resulting suspension was cooled to ice-bath temperature, and the white crystalline precipitate was collected by filtration and washed with cold Et_2O to give the respective product **8a**, **8b**, **8c**, or **8d**. Physical and spectral data for **8a–d** are listed below.

2,3′-Anhydro-5′-*O*-benzoyl-2′-deoxyuridine (8a). White solid; yield, 81%; mp 225–226 °C; ^{1}H NMR (DMSO-d_6): δ 7.93 (d, J = 7.8 Hz, 2H, *o*-benzoyl hydrogens), 7.66 (d, J = 7.5 Hz, 1H, H-6), 7.63–7.68 (m, 1H, *p*-benzoyl hydrogen), 7.47–7.52 (m, 2H, *m*-benzoyl hydrogens), 5.97 (d, J = 3.3 Hz, 1H, H-1′), 5.78 (d, J = 7.5 Hz, 1H, H-5), 5.45 (br s, 1H, H-3′), 4.50–4.60 (m, 2H, H-5′), 4.37 (ddd, J = 11.7, 6.3 Hz, 1H, H-4′), 2.52–2.88 (m, 2H, H-2′); ^{13}C NMR (DMSO-d_6): δ 170.05, 165.14, 153.50, 140.57, 133.34, 129.06, 128.92, 128.55, 107.88, 86.94, 81.86, 77.28, 62.48, 32.68. Anal. ($C_{16}H_{14}N_2O_5$) C, H, N.

2,3′-Anhydro-5′-*O*-benzoyl-2′-deoxythymidine (8b). White solid; yield, 74%; mp 245–246 °C; ^{1}H NMR (DMSO-d_6): δ 7.90 (dd, *J* = 6.9, 1.2 Hz, 2H, *o*-benzoyl hydrogens), 7.63–7.68 (m, 1H, *p*-benzoyl hydrogen), 7.57 (s, 1H, H-6) 7.46–7.57 (m, 2H, *m*-benzoyl hydrogens), 5.90 (d, *J* = 3.6 Hz, 1H, H-1′), 5.42 (br s, 1H, H-3′), 4.50–4.61 (m, 2H, H-5′), 4.36 (dd, *J* = 11.7, 5.4 Hz, 1H, H-4′), 2.53–2.88 (m, 2H, H-2′), 1.72 (s, 3H, CH_3); ^{13}C NMR (DMSO-d_6): δ 170.63, 165.14, 153.13, 136.32, 133.30, 129.04, 128.70, 128.37, 116.00, 86.81, 81.80, 77.07, 62.30, 32.71, 12.85. Anal. ($C_{17}H_{16}N_2O_5$) C, H, N.

5-Fluoro-2,3′-anhydro-5′-*O*-benzoyl-2′-deoxyuridine (8c). White solid; yield, 90%; mp 235–236 °C; ^{1}H NMR (DMSO-d_6): δ 8.10 (d, *J* = 5.4 Hz, 1H, H-6), 7.89–7.91 (m, 2H, *o*-benzoyl hydrogens), 7.62–7.68 (m, 1H, *p*-benzoyl hydrogen), 7.46–7.51 (m, 2H, *m*-benzoyl hydrogens), 5.92 (d, *J* = 3.9 Hz, 1H, H-1′), 5.48 (br s, 1H, H-3′), 4.54–4.65 (m, 2H, H-5′), 4.43 (dd, *J* = 11.7, 6.3 Hz, 1H, H-4′), 2.67–2.71 (m, 1H, H-2′α), 2.56 (dt, *J* = 13.5, 2.7 Hz, 1H, H-2′β); ^{13}C NMR (DMSO-d_6): δ 165.11 (CO_2), 162.16 (d, J_{CCF} = 16.5 Hz, C-4 *C*O), 151.22 (*C*-2), 144.31 (d, J_{CF} = 248.3 Hz, *C*-5), 133.32, 128.99 and 128.51 (phenyl *C*H), 128.90 (phenyl *C*-1), 125.34 (d, J_{CCF} = 33.0 Hz, *C*-6), 87.45 (*C*-1′), 82.11 (*C*-3′), 77.70 (*C*-4′), 62.21 (*C*-5′), 32.46 (*C*-2′). Anal. ($C_{16}H_{13}FN_2O_5$) C, H, N.

5-Iodo-2,3′-anhydro-5′-*O*-benzoyl-2′-deoxyuridine (8d). White solid; yield, 82%; mp 224–225 °C; ^{1}H NMR (DMSO-d_6): δ 8.30 (s, 1H, H-6), 7.86–7.94 (m, 2H, *o*-benzoyl hydrogens), 7.60–7.67 (m, 1H, *p*-benzoyl hydrogen), 7.46–7.51 (m, 2H, *m*-benzoyl hydrogens), 5.98 (d, *J* = 3.6 Hz, 1H, H-1′), 5.46 (br s, 1H, H-3′), 4.54–4.61 (m, 2H, H-5′), 4.42 (ddd, *J* = 11.7, 6.3, 5.4 Hz, 1H, H-4′), 2.55–2.88 (m, 2H, H-2′); ^{13}C NMR (DMSO-d_6): δ 166.57, 165.14, 153.80, 145.05, 133.34, 128.99, 128.88, 128.55, 87.15, 81.99, 80.68, 77.64, 62.16, 32.48. Anal. ($C_{16}H_{13}IN_2O_5$) C, H, N.

General Method for the Preparation of 5-Substituted-3′-*O*-nitro-5′-O-benzoyl-2′-deoxyuridines (9a–d). A mixture containing either **8a**, **8b**, **8c**, or **8d** (26.1 mmol) and NH_4NO_3 (31.3 g, 391.5 mmol) in dry DMF (120 mL) was stirred at 110–120 °C for 12 h under argon. The solvent was removed in vacuo, and the residue was purified via silica gel flash column chromatography using hexanes–EtOAc (1:3, 1:2, 1:7 or 1:1, v/v, respectively) as eluent to give the corresponding product **9a**, **9b**, **9c**, or **9d**. Physical and spectral data for **9a–d** are listed below.

3′-*O*-Nitro-5′-*O*-benzoyl-2′-deoxyuridine (9a). White crystals (CH_2Cl_2–hexane); yield, 31%; mp 168–170 °C; ^{1}H NMR (DMSO-d_6): δ 11.43 (s, 1H, N*H*), 7.99 (d, *J* = 7.8 Hz, 2H, *o*-benzoyl hydrogens), 7.67 (d, *J* = 7.8 Hz, 1H, H-6), 7.65–7.70 (m, 1H, *p*-benzoyl hydrogen), 7.52–7.57 (m, 2H, *m*-benzoyl hydrogens), 6.13 (dd, *J* = 7.8, 6.3 Hz, 1H, H-1′), 5.76 (dd, *J* = 5.4, 1.2 Hz, 1H, H-3′), 5.60 (d, *J* = 7.8 Hz, 1H, H-5), 4.48–4.61 (m, 3H, H-4′, H-5′), 2.56–2.74 (m, 2H, H-2′); ^{13}C NMR (DMSO-d_6): δ 165.32, 162.77, 150.15, 140.44, 133.48, 129.15, 129.06, 128.72, 102.06, 84.78, 83.29, 79.17, 64.04, 34.24. Anal. ($C_{16}H_{15}N_3O_8$) C, H, N.

3′-*O*-Nitro-5′-*O*-benzoyl-2′-deoxythymidine (9b). White crystals (CH_2Cl_2–hexane); yield, 34%; mp 109–110 °C; ^{1}H NMR (DMSO-d_6): δ 11.40 (s, 1H, N*H*), 8.02 (dd, *J* = 8.4, 1.5 Hz, 2H, *o*-benzoyl hydrogens), 7.66–7.71 (m, 1H, *p*-benzoyl hydrogen), 7.52–7.57 (m, 2H, *m*-benzoyl hydrogens), 7.44 (s, 1H, H-6), 6.17 (dd, *J* = 8.4, 6.9 Hz, 1H, H-1′), 5.80 (br d, *J* = 6.6 Hz, 1H, H-3′), 4.62 (dt, *J* = 7.8, 2.1 Hz, 1H, H-4′), 4.49–4.57 (m, 2H, H-5′), 2.57–2.72 (m, 2H, H-2′), 1.59 (s, 3H, CH_3); ^{13}C NMR (DMSO-d_6): δ 165.30, 163.35, 150.16, 135.43, 133.49, 129.14, 129.06, 128.74, 109.89, 83.99, 83.32, 78.97, 64.03, 34.21, 11.79. Anal. ($C_{17}H_{17}N_3O_8$) C, H, N.

5-Fluoro-3′-*O*-nitro-5′-*O*-benzoyl-2′-deoxyuridine (9c). White crystals (EtOAc–hexane); yield, 50%; mp 168–170 °C; ^{1}H NMR (DMSO-d_6): δ 11.15 (br s, 1H, N*H*), 7.86 (dd, *J* = 8.4, 1.5 Hz, 2H, *o*-benzoyl hydrogens), 7.76 (d, *J* = 6.0 Hz, 1H, H-6), 7.63–7.68 (m, 1H, *p*-benzoyl hydrogen), 7.47–7.52 (m, 2H, *m*-benzoyl hydrogen), 6.55 (d, *J* = 3.3 Hz, 1H, H-1′), 5.46 (br d, *J* = 1.5 Hz, 1H, H-3′), 4.52–4.62 (m, 2H, H-5′), 4.43 (dd, *J* = 11.7, 6.0 Hz, 1H, H-4′), 2.56–2.63 (m, 2H, H-2′); ^{13}C NMR (DMSO-d_6): δ 165.11 (CO_2), 153.34 (d, J_{CCF} = 26.4 Hz, C-4 *C*=O), 149.82 (d, *J* = 12.8 Hz, C-2 *C*=O), 145.28 (d, J_{CF} = 242.8 Hz, C-5), 136.47 (d, J_{CCF} = 25.3 Hz, C-6), 133.36, 129.02, 128.53 and 128.38 (phenyl carbons), 82.61 (C-1′), 78.92 (C-3′), 77.57 (C-4′), 62.16 (C-5′), 31.75 (C-2′). Anal. ($C_{16}H_{14}FN_3O_8$) C, H, N.

5-Iodo-3′-*O*-nitro-5′-*O*-benzoyl-2′-deoxyuridine (9d). Method A: White foam; yield, 2.8%; mp 85–86 °C; ^{1}H NMR ($CDCl_3$): δ 9.40 (s, 1H, N*H*), 8.02–8.11 (m, 2H, *o*-benzoyl hydrogens), 7.89 (s, 1H, H-6), 7.60–7.70 (m, 1H, *p*-benzoyl hydrogens), 7.43–7.52 (m, 2H, *m*-benzoyl hydrogens), 6.21 (dd, *J* = 6.6, 5.7 Hz, 1H, H-1′), 5.64 (d, *J* = 6.6 Hz, 1H, H-3′), 4.68–4.76 (m, 2H, H-5′), 4.58 (br s, 1H, H-4′), 2.81 (dd, *J* = 14.4, 5.1 Hz, 1H, H-2′α), 2.37 (ddd, *J* = 14.7, 7.5, 7.2 Hz, 1H, H-2′β); ^{13}C NMR ($CDCl_3$): δ 165.87, 159.53, 149.47, 143.43, 133.84, 129.60, 128.87, 128.81, 85.92, 82.60, 81.52, 69.03, 63.91, 36.97. Anal. ($C_{16}H_{14}IN_3O_8$) C, H, N.

Method B: A mixture of **9a** (1.0 g, 2.65 mmol) and NaN_3 (0.69 g, 10.6 mmol) in dry MeCN (50 mL) was cooled in an ice-bath, a solution of ICl (1.07 g, 6.6 mmol) in MeCN (5 mL) was added dropwise during 5 min, and the reaction was allowed to proceed at 25 °C for 48 h with stirring under an argon atmosphere. Removal of the solvent in vacuo gave a residue that was purified via flash silica gel column chromatography using hexanes–EtOAc (1:1, v/v) as eluent to afford **9d** (1.1 g, 82.5%) as a white foam, which was identical (mp, ^{1}H NMR) to **9d** described above under Method A.

General Method for the Preparation of 5-Substituted-3′-*O*-nitro-2′-deoxyuridines (10a–d). A solution of NaOMe in MeOH (12.75 mL of 0.5 M) was added to either **9a**, **9b**, **9c**, or **9d** (3.18 mmol) and the reaction was allowed to proceed at 25 °C for 1 h with stirring. The reaction was quenched by addition of NH_4Cl (0.5 g), and the solvent was removed in vacuo. Purification of the residue by flash silica gel column chromatography using MeOH–CH_2Cl_2 (1:9, v/v) as eluent yielded the respective product **10a**, **10b**, **10c**, or **10d**. Physical and spectral data for **10a–d** are listed below.

3′-*O*-Nitro-2′-deoxyuridine (10a) was obtained directly as white crystals; yield, 91%; mp 188–190 °C; ^{1}H NMR (DMSO-d_6): δ 11.35 (br s, 1H, N*H*), 7.88 (d, *J* = 8.4 Hz, 1H, H-6), 6.13 (dd, *J* = 8.7, 5.7 Hz, 1H, H-1′), 5.67 (d, *J* = 8.4 Hz, 1H, H-5), 5.58 (d, *J* = 6.0 Hz, 1H, H-3′), 5.25 (br s, 1H, 5′-O*H*), 4.21 (d, *J* = 1.8 Hz, 1H, H-4′), 3.60–3.74 (m, 2H, H-5′), 2.45–2.56 (m, 1H, H2′α), 2.40 (ddd, *J* = 14.7, 8.7, 6.3 Hz, 1H, H-2′β); ^{13}C NMR (DMSO-d_6): δ 162.86, 150.25, 140.12, 102.13, 84.59, 83.84, 82.46, 61.26, 35.23. Anal. ($C_9H_{11}N_3O_7$) C, H, N.

3′-*O*-Nitro-2′-deoxythymidine (10b). White crystals (CH_2Cl_2–hexane); yield, 92%; mp 137–139 °C; ^{1}H NMR (DMSO-d_6): δ 11.36 (s, 1H, N*H*), 7.72 (s, 1H, H-6), 6.14 (dd, *J* = 8.4, 6.0 Hz, 1H, H-1′), 5.59 (d, *J* = 5.7 Hz, 1H, H-3′), 5.31 (t, *J* = 5.4 Hz, 1H, 5′-O*H*), 4.18 (d, *J* = 1.8 Hz, 1H, H-4′), 3.67 (dd, *J* = 5.1, 3.3 Hz, 2H, H-5′), 2.37–2.52 (m, 2H, H-2′), 1.78 (s, 3H, CH_3); ^{13}C NMR (DMSO-d_6): δ 163.50 (C-4 *C*=O), 150.31 (C-2 *C*=O), 135.66 (C-6), 109.76 (C-5), 84.54 (C-1′), 83.45 (C-3′), 82.23 (C-4′), 61.28 (C-5′), 34.91 (C-2′), 12.24 (CH_3). Anal. ($C_{10}H_{13}N_3O_7$) C, H, N.

5-Fluoro-3′-*O*-nitro-2′-deoxyuridine (10c) was obtained directly as white crystals; yield, 95%; mp 195–197 °C; ^{1}H NMR (DMSO-d_6): δ 11.20 (br s, 1H, N*H*), 7.76 (d, *J* = 6.0 Hz, 1H, H-6), 6.49 (d, *J* = 2.7 Hz, 1H, H-1′), 5.28 (d, *J* = 1.2 Hz, 1H, H-3′), 5.02 (br s, 1H, 5′-O*H*), 4.20 (dt, *J* = 6.3, 2.4 Hz, 1H, H-4′), 3.42–3.58 (m, 2H, H-5′), 2.45–2.56 (m, 2H, H-2′); ^{13}C NMR (DMSO-d_6): δ 153.31 (d, J_{CCF} = 26.4 Hz, C-4 *C*=O), 150.12 (C-2 *C*=O), 145.17 (d, J_{CF} = 241.7 Hz, C-5), 136.04 (d, J_{CCF} = 29.7 Hz, C-6), 85.85 (C-1′), 78.62 (C-3′), 77.26 (C-4′), 59.28 (C-5′), 31.68 (C-2′). Anal. ($C_9H_{10}FN_3O_7$) C, H, N.

5-Iodo-3′-*O*-nitro-2′-deoxyuridine (10d) was obtained directly as white crystals; yield, 92%; mp 170–172 °C; ^{1}H NMR (DMSO-d_6): δ 11.74 (s, 1H, N*H*), 8.36 (s, 1H, H-6), 6.09 (dd, *J* = 8.4, 6.0 Hz, 1H, H-1′), 5.59 (d, *J* = 5.7 Hz, 1H, H-3′), 5.40 (t, *J* = 5.1 Hz, 1H, 5′-O*H*), 4.23 (br d, *J* = 1.8 Hz, 1H, H-4′), 3.62–3.80 (m, 2H, H-5′), 2.40–2.56 (m, 2H, H-2′); ^{13}C NMR (DMSO-d_6): δ 160.13, 149.87, 144.51, 84.34, 84.18, 82.69, 69.76, 61.10, 35.54. Anal. ($C_9H_{10}IN_3O_7$) C, H, N.

General Method for the Preparation of 5-Substituted-4-(1,2,4-triazolo)-4-deoxy-3′-*O*-nitro-5′-*O*-

benzoyl-2′-deoxyuridine (11a,b). 4-Chlorophenyl dichlorophosphate (0.88 mL, 5.32 mmol), and then 1,2,4-triazole (0.74 g, 10.64 mmol), was added to a solution of either **9a** or **9b** (5.32 mmol) in pyridine (20 mL) at 0 °C with stirring. The reaction was allowed to proceed at 25 °C for 4 days with stirring, and the solvent was removed in vacuo. The residue was dissolved in CH_2Cl_2 (200 mL), this solution was washed with water (2 × 50 mL) and aqueous $NaHCO_3$ (50 mL), the organic fraction was dried (Na_2SO_4), and the solvent was removed in vacuo. Purification of the residue by flash silica gel column chromatography using hexanes−EtOAc (1:3 and 1:5, v/v, respectively) gave the respective product **11a** or **11b**. Physical and spectral data for **11a,b** are listed below.

4-(1,2,4-Triazolo)-4-deoxy-3′-*O*-nitro-5′-*O*-benzoyl-2′-deoxyuridine (11a) was obtained directly as white crystals that were washed with cold ether: yield, 79%; mp 85−87 °C; ^{1}H NMR ($CDCl_3$): δ 9.20 (s, 1H, triazole hydrogen), 8.23 (d, J = 7.2 Hz, 1H, H-6), 8.09 (s, 1H, triazole hydrogen), 7.89 (dd, J = 8.7, 1.2 Hz, 2H, *o*-benzoyl hydrogens), 7.49−7.58 (m, 1H, *p*-benzoyl hydrogen), 7.32−7.42 (m, 2H, *m*-benzoyl hydrogens), 6.94 (d, J = 7.2 Hz, 1H, H-5), 6.20 (dd, J = 7.5, 5.7 Hz, 1H, H-1′), 5.65 (d, J = 6.9 Hz, 1H, H-3′), 4.81 (dd, J = 12.0, 3.3 Hz, 1H, H-5′a), 4.72 (dd, J = 5.1, 3.0 Hz, 1H, H-4′), 4.66 (dd, J = 12.0, 3.6 Hz, 1H, H-5′b), 3.18 (ddd, J = 15.3, 7.2, 1.5 Hz, 1H, H-2′α), 2.33−2.43 (m, 1H, H-2′β); ^{13}C NMR ($CDCl_3$): δ 165.72 (CO_2), 159.42 (C-2 *C*=O), 153.88 (C-4), 145.19 (C-6), 143.18 (phenyl C-1), 133.78, 129.34, 128.77 and 128.68 (phenyl and triazole *C*H), 94.74 (C-5), 88.47 (C-1′), 82.78 (C-3′), 82.46 (C-4′), 63.85 (C-5′), 38.01 (C-2′). Anal. ($C_{18}H_{16}N_6O_7$) C, H, N.

4-(1,2,4-Triazolo)-4-deoxy-3′-*O*-nitro-5′-*O*-benzoyl-2′-deoxythymidine (11b). White foam; yield, 71%; mp 59−60 °C; ^{1}H NMR (DMSO-d_6): δ 9.29 (s, 1H, triazole hydrogen), 8.35 (s, 1H, triazole hydrogen), 8.24 (s, 1H, H-6), 7.89 (dd, J = 8.4, 1.5 Hz, 2H, *o*-benzoyl hydrogens), 7.57−7.62 (m, 1H, *p*-benzoyl hydrogen), 7.43−7.48 (m, 2H, *m*-benzoyl hydrogens), 6.15 (dd, J = 7.2, 6.6 Hz, 1H, H-1′), 5.85 (dd, J = 4.8, 2.1 Hz, 1H, H-3′), 4.83 (br dd, J = 6.3, 4.2 Hz, 1H, H-4′), 4.73 (dd, J = 12.3, 3.9 Hz, 1H, H-5′a), 4.60 (dd, J = 12.3, 4.5 Hz, 1H, H-5′b), 2.91 (ddd, J = 15.3, 6.6, 1.5 Hz, 1H, H-2′α), 2.68−2.80 (m, 1H, H-2′β), 2.10 (s, 3H, CH_3); ^{13}C NMR (DMSO-d_6): δ 165.24, 157.85, 152.71, 147.35, 147.29, 133.39, 129.08, 128.96, 128.92, 128.58, 104.66, 87.76, 83.64, 80.95, 64.14, 36.32, 15.76. Anal. ($C_{19}H_{18}N_6O_7$) C, H, N.

General Method for the Preparation of 5-Substituted-3′-*O*-nitro-5′-*O*-benzoyl-2′-deoxycytidines (12a,b). A solution of either **11a** or **11b** (3.74 mmol) in NH_4OH/dioxane (1:3, v/v, 80 mL) was stirred at 25 °C for 5 h prior to removal of the solvent in vacuo. The residue was purified via flash silica gel column chromatography using MeOH:CH_2Cl_2 (1:9, v/v) as eluent to give the respective products **12a** and **12b**. Physical and spectral data for **12a,b** are listed below.

3′-*O*-Nitro-5′-*O*-benzoyl-2′-deoxycytidine (12a) was obtained directly as white crystals, which were washed with cold ether: yield, 49%; mp 139−141 °C; ^{1}H NMR (DMSO-d_6): δ 7.98 (dd, J = 8.4, 1.2 Hz, 2H, *o*-benzoyl hydrogens), 7.68 (ddt, J = 14.7, 7.5, 1.2 Hz, 1H, *p*-benzoyl hydrogen), 7.62 (d, J = 7.8 Hz, 1H, H-6), 7.51−7.56 (m, 2H, *m*-benzoyl hydrogens), 7.23 (s, 2H, NH_2), 6.13 (dd, J = 7.8, 6.0 Hz, 1H, H-1′), 5.77 (d, J = 4.8 Hz, 1H, H-3′), 5.68 (d, J = 7.8 Hz, 1H, H-5), 4.51−4.60 (m, 3H, H-4′, H-5′), 2.52−2.61 (m, 2H, H-2′); ^{13}C NMR (DMSO-d_6): δ 165.80, 165.43, 165.24 and 154.57 (quaternary carbons), 140.68 (C-6), 133.34, 129.05, and 128.60 (phenyl *C*H), 94.30 (C-5), 85.60 (C-1′), 83.77 (C-3′), 79.21 (C-4′), 64.19 (C-5′), 35.04 (C-2′). Anal. ($C_{16}H_{16}N_4O_7$) C, H, N.

5-Methyl-3′-*O*-nitro-5′-*O*-benzoyl-2′-deoxycytidine (12b) was obtained directly as white crystals, which were washed with cold ether; yield, 36%; mp 158−160 °C; ^{1}H NMR (DMSO-d_6): δ 8.15 (d, J = 8.1 Hz, 2H, *o*-benzoyl hydrogens), 7.76−7.85 (m, 1H, *p*-benzoyl hydrogen), 7.59−7.71 (m, 2H, *m*-benzoyl hydrogens), 7.55 (br s, 1H, NHa), 7.49 (s, 1H, H-6), 7.00 (br s, 1H, NHb), 6.32 (dd, J = 8.1, 6.0 Hz, 1H, H-1′), 5.90−5.96 (m, 1H, H-3′), 4.63−4.79 (m, 3H, H-4′, H-5′), 2.60−2.70 (m, 2H, H-2′), 1.77 (s, 3H, CH_3); ^{13}C NMR (DMSO-d_6): δ 165.30, 165.22, 165.16, 154.66, 137.54, 133.48, 129.06, 128.73, 101.81, 84.98, 83.87, 79.08, 64.22, 35.04, 12.90. Anal. ($C_{17}H_{18}N_4O_7$) C, H, N.

General Method for the Preparation of 5-Substituted-3′-*O*-nitro-2′-deoxycytidines (13a,b). A solution of NaOMe in MeOH (3.7 mL of 0.5 M) was added to either **12a** or **12b** (0.93 mmol), the mixture was stirred at 25 °C for 15 min, and the solvent was removed in vacuo. Purification of the residue by flash silica gel column chromatography using MeOH:CH_2Cl_2 (1:4, v/v) as eluent afforded the respective products **13a** and **13b**. Physical and spectral data for **13a,b** are listed below.

3′-*O*-Nitro-2′-deoxycytidine (13a). White foam; yield, 95%; mp 65−66 °C (lit.[32] mp 177−178 °C); ^{1}H NMR (DMSO-d_6): δ 7.80 (d, J = 7.8 Hz, 1H, H-6), 7.20 and 7.26 (two s, 1H each, NH_2), 6.14 (dd, J = 8.7, 5.4 Hz, 1H, H-1′), 5.76 (d, J = 7.8 Hz, 1H, H-5), 5.59 (d, J = 6.0 Hz, 1H, H-3′), 5.25 (t, J = 5.4 Hz, 1H, 5′-OH), 4.19 (br d, J = 1.8 Hz, 1H, H-4′), 3.62−3.66 (m, 2H, H-5′), 2.45−2.52 (m, 1H, H-2′α), 2.29 (ddd, J = 14.7, 6.0, 2.7 Hz, 1H, H-2′β); ^{13}C NMR (DMSO-d_6): δ 163.67, 152.34, 141.70, 94.37, 85.02, 84.80, 82.78, 61.09, 35.88. Anal. ($C_9H_{12}N_4O_6$) C, H, N.

5-Methyl-3′-*O*-nitro-2′-deoxycytidine (13b). Colorless oil, which was crystallized from EtOAc−hexane to give white crystals; yield, 94%; mp 141−143 °C; ^{1}H NMR (DMSO-d_6): δ 7.62 (s, 1H, H-6), 7.35 and 6.90 (two s, 1H each, NH_2), 6.14 (dd, J = 9.0, 5.7 Hz, 1H, H-1′), 5.57 (d, J = 5.1 Hz, 1H, H-3′), 5.35 (br s, 1H, 5′-OH), 4.16 (d, J = 2.1 Hz, 1H, H-4′), 3.60−3.70 (m, 2H, H-5′), 2.41−2.49 (m, 1H, H-2′α), 2.25−2.36 (m, 1H, H-2′β), 1.84 (s, 3H, CH_3); ^{13}C NMR (DMSO-d_6): δ 165.40 (C-2 *C*=O), 155.10 (C-4), 138.12 (C-6), 101.96 (C-5), 84.88 and 84.79 (C-1′ and C-3′), 82.36 (C-4′), 61.45 (C-5′), 35.70 (C-2′), 13.30 (CH_3). Anal. ($C_{10}H_{14}N_4O_6$) C, H, N.

5-Iodo-3′-*O*-nitro-2′-deoxycytidine (13c). A mixture of **13a** (0.144 g, 0.53 mmol), iodine (0.135 g, 0.53 mmol), and iodic acid (0.093 g, 0.53 mmol) in acetic acid, H_2O, and CCl_4 (8:3:2, v/v/v, 26 mL) was stirred at 25 °C for 14 h. Removal of the solvents in vacuo, coevaporation of toluene (2 × 20 mL) from the residue, dissolution of the residue in CH_2Cl_2 (100 mL), filtration, washing with aqueous $NaHCO_3$ (50 mL), and drying the organic fraction (Na_2SO_4) were carried out consecutively. The solvent was removed in vacuo to give a residue that was purified via flash silica gel column chromatography using MeOH:CH_2Cl_2 (1:9, v/v) as eluent to afford **13c** (0.118 g, 56%) as a white foam: mp 81−82 °C; ^{1}H NMR (DMSO-d_6): δ 8.23 (s, 1H, H-6), 7.95 and 6.75 (two br s, 1H each, NH_2), 6.09 (dd, J = 8.7, 5.7 Hz, 1H, H-1′), 5.59 (d, J = 6.0 Hz, 1H, H-3′), 5.36 (t, J = 5.4 Hz, 1H, 5′-OH), 4.20−4.28 (m, 1H, H-4′), 3.62−3.76 (m, 2H, H-5′), 2.49−2.56 (m, 1H, H-2′α), 2.36 (ddd, J = 15.0, 8.4, 6.6 Hz, 1H, H-2′β); ^{13}C NMR (DMSO-d_6): δ 163.58, 153.61, 147.07, 85.11, 84.83, 82.63, 61.13, 57.04 (C-5), 36.10. Anal. ($C_9H_{11}IN_4O_6$) C, H, N.

General Method for the Preparation of 5-Substituted-5′-*O*-nitro-2′-deoxyuridines (15a,b). A mixture of either **14a** or **14b** (6.54 mmol) and $LiNO_3$ (4.48 g, 65 mmol) in dry DMF (30 mL) was stirred at 100 °C for 14 h under argon. Removal of the solvent in vacuo gave a residue, toluene (20 mL) was added, and the solvent was removed in vacuo. Purification of the residue via flash silica gel column chromatography using a gradient of 5% → 10% MeOH in CH_2Cl_2 as eluent gave a pale yellow oil which was recrystallized from MeOH to yield the respective product **15a** or **15b**. Physical and spectral data for **15a,b** are listed below.

5′-*O*-Nitro-2′-deoxyuridine (15a). Yield, 73%; mp 170−172 °C (lit.[27] mp 175 °C); ^{1}H NMR (DMSO-d_6): δ 11.34 (s, 1H, NH), 7.65 (d, J = 8.1 Hz, 1H, H-6), 6.16 (dd, J = 7.2, 6.6 Hz, 1H, H-1′), 5.65 (d, J = 8.1 Hz, 1H, H-5), 5.53 (d, J = 3.9 Hz, 1H, 3′-OH), 4.79 (dd, J = 11.4, 3.6 Hz, 1H, H-5′a), 4.66 (dd, J = 11.4, 6.9 Hz, 1H, H-5′b), 4.20−4.27 (m, 1H, H-3′), 3.95−4.00 (m, 1H, H-4′), 2.09−2.28 (m, 2H, H-2′); ^{13}C NMR (DMSO-d_6) δ 162.81, 150.19, 140.65, 101.98, 84.59, 81.76, 73.05 (C-5′), 70.10, 38.19. Anal. ($C_9H_{11}N_3O_7$) C, H, N.

5′-*O*-Nitro-2′-deoxythymidine (15b). Yield, 71%; mp 183−185 °C (lit.[28] mp 189 °C); ^{1}H NMR (DMSO-d_6): δ 11.32 (s, 1H, NH), 7.46 (s, 1H, H-6), 6.19 (t, J = 6.9 Hz, 1H, H-1′), 5.51 (d, J = 3.3 Hz, 1H, 3′-OH), 4.81 (dd, J = 11.4, 3.9 Hz, 1H, H-5′a), 4.69 (dd, J = 11.4, 6.6 Hz, 1H, H-5′b), 4.28–4.30 (m, 1H, H-3′), 3.96 (ddd, J = 6.6, 3.9, 3.6 Hz, 1H, H-4′), 2.25 (ddd, J = 14.1, 7.2, 6.9 Hz, 1H, H-2′α), 2.11 (ddd, J = 14.1, 6.3, 3.9 Hz, 1H, H-2′β), 1.78 (s, 3H, CH_3); ^{13}C NMR (DMSO-d_6): δ 163.50, 150.28, 135.99, 109.79, 84.08, 81.69, 73.07 (C-5′), 70.26, 38.08, 12.07. Anal. ($C_{10}H_{13}N_3O_7$) C, H, N.

5-Iodo-5′-*O*-nitro-2′-deoxyuridine (15c). A mixture of **15a** (0.2 g, 0.74 mmol) and NaN_3 (0.19 g, 2.94 mmol) in dry MeCN (20 mL) was cooled in an ice-bath. A solution of ICl (0.36 g, 2.2 mmol) in MeCN (3 mL) was added dropwise during 5 min, and the reaction was allowed to proceed at 25 °C for 48 h with stirring under argon. The solvent was removed in vacuo and the residue was purified via silica gel flash column chromatography using a gradient of 5% → 10% MeOH in CH_2Cl_2 as eluent to give **15c** (0.19 g, 65%) as white crystals: mp 181–183 °C; ^{1}H NMR (DMSO-d_6): δ 11.80 (s, 1H, NH), 8.10 (s, 1H, H-6), 6.18 (dd, J = 6.9, 3.9 Hz, 1H, H-1′), 5.59 (d, J = 4.2 Hz, 1H, 3′-OH), 4.75–4.94 (m, 2H, H-5′), 4.33–4.37 (m, 1H, H-3′), 4.06 (ddd, J = 6.9, 6.6, 3.6 Hz, 1H, H-4′), 2.40 (ddd, J = 14.1, 7.2, 6.9 Hz, 1H, H-2′α), 2.19 (ddd, J = 14.1, 6.6, 3.9 Hz, 1H, H-2′β); ^{13}C NMR (DMSO-d_6): δ 160.21(C-4 C=O), 149.86 (C-2 C=O), 144.80 (C-6), 85.18 (C-1′), 82.08 (C-3′), 72.85 (C-5′), 70.13 (C-4′), 69.78 (C-5), 38.32. Anal. ($C_9H_{10}IN_3O_7$) C, H, N.

In Vitro Nitric Oxide Release Assays. 1. Incubation With 18 mM L-cysteine in Phosphate Buffer (pH 7.4). In vitro nitric oxide release was assayed using a modification of the previously reported procedure.[14] Briefly, a solution of the test compound (1 mL of a 2 mM solution in 0.1 M phosphate buffer (pH 7.4) was mixed thoroughly with a freshly prepared solution of L-cysteine (1 mL of a 36 mM solution in 0.1 M phosphate buffer, pH 7.4), and the mixture was incubated at 37 °C, for 1 and 16 h in the absence of air. After exposure to air for 10 min at 25 °C, an aliquot of the Griess reagent (1 mL) [freshly prepared by mixing equal volumes of 1.0% sulfanilamide (prepared and stored in aqueous 5% phosphoric acid) and 0.1% *N*-naphthylethylenediamine dihydrochloride in water] was added to an equal volume (1 mL) of each test compound's incubation solution with mixing. After 10 min had elapsed, absorbance was measured at 540 nm using a Philips PU 8740 UV/VIS scanning spectrophotometer. Solutions of 0–60 μM sodium nitrite were used to prepare a nitrite absorbance versus concentration curve under the same experimental conditions. The percent nitric oxide released (quantitated as nitrite ion) was calculated (±SEM, n = 3) from the standard nitrite versus concentration curve.

2. Incubation with Phosphate Buffer (pH 7.4). This assay was performed as described under procedure 1 above, except that a solution of the test compound (2 mL of a 1 mM solution in 0.1 M phosphate buffer pH 7.4) was used, and no L-cysteine was added.

3. Incubation with Rat Serum. Nitric oxide release was measured by modification of the reported procedure for in vivo serum samples.[51] Briefly, rat serum was prepared by filtration with a Millipore UL trafree-15 centrifugal filter. Stock solutions of test compounds (1×10^{-2} M) were prepared, and 10 μL of each test compound solution was mixed with filtered serum (90 μL), which corresponds to the reaction sample. Each reaction sample was incubated for either 1 h or 16h at 37 °C in the presence of 0.2 U/mL Aspergillus nitrate reductase, 50 mM HEPES buffer, 5 μM FAD, and 0.1 mM NADPH to provide a total volume of 500 μL that was comprised of the following composition for the blank and the reaction sample (in brackets), respectively: water 300 μL (290 μL), 1 M HEPES 25 μL (25 μL), serum 90 μL (100 μL), 0.1 mM FAD 25 μL (25 μL), 1 mM NADPH 50 μL (50 μL), 10U/mL Nase 10 μL (10 μL). Following the incubation, 5 μL of lactate dehydrogenase (1500 U/mL) and 50 μL of 100 mM pyruvic acid were added to each tube to oxidize any unreacted NADPH, and samples were incubated for 10 min. Greiss reagent (550 μL) was then added to each tube, the mixture was allowed to stand at 25 °C for 10 min, absorbance for each sample was determined at 540 nm, and % nitric oxide release was calculated as indicated under Procedure 1 described above.

In Vitro Cell Cytotoxicity (MTT assay). KBALB, KBALB–STK, human 143B, and human 143B-LTK cells were cultured in complete DMEM medium supplemented with 10% fetal bovine serum (FBS), and EMT-6 cells were cultured in complete WAYMOUTH medium in 12.5% FBS. Exponentially growing cells were trypsinized, centrifuged, and resuspended in growth medium, and the cell number was readjusted to 8 × 10^3 cells/mL. Cells were seeded into 96-well plates at 8 × 10^2 cells/well and incubated at 37 °C in a humidified 5% CO_2 atmosphere for 24 h.

The test compound was dissolved in DMEM medium, and 100 μL of this solution was added to cells in 96-well plates to produce the preselected test compound concentration. DMEM medium (100 μL) was added to control wells. The plates were incubated for 3 days at 37 °C in a humidified atmosphere consisting of 95% air and 5% CO_2. At the end of the incubation, 3-(4,5-dimethyl-2-thiazolyl)-2,5-diphenyl-2*H*-tetrazolium bromide (MTT, Sigma) was dissolved in phosphate-buffered saline (PBS) to produce a concentration of 5 mg/mL, filtered through a 0.45 μm membrane filter, and diluted (1:5) with prewarmed DMEM medium. An aliquot of this solution (50 μL) was added to each well, and the plates were incubated at 37 °C for 4 h. The medium was removed from the wells, dimethyl sulfoxide (150 μL) was added to each well, and the plates were placed on a shaker for 15 min to dissolve the formazan crystals. The absorbance at 540 nm (A_{540}) was measured immediately in each well using a scanning multiwell spectrophotometer (ELISA reader). A_{540} values, corrected for the absorbance in medium blanks, reflected the concentration of viable cells. The CC_{50} values reported refer to the test drug concentrations that reduced the A_{540} to 50% of the control value (mean value, n = 6). This assay,[16] which depends on the metabolic reduction of MTT to colored formazan, measures cytostatic and cytotoxic effects of the test drug.

Antiviral Activity Assays. The antiviral assays were based on an inhibition of virus-induced cytopathicity in either E_6SM, HeLa or Vero cell cultures, following previously established procedures.[17] Herpes simplex virus type 1 (HSV-1) (KOS), HSV-2 (G), vaccinia virus, vesicular stomatitis virus (VSV), and the thymidine kinase-deficient HSV-1 TK KOS (ACV^r) strains were propagated in E_6SM cell cultures, parainfluenza-3 virus, reovirus-1, Sindbis virus, Coxsackie B4 virus and Punta Toro virus in Vero cell cultures, and respiratory syncytial virus in HeLa cell cultures. Briefly, confluent cell cultures in microtiter plates were exposed to 100 $CCID_{50}$ of virus, 1 $CCID_{50}$ being the virus dose required to infect 50% of the cell cultures. After a 1 h virus adsorption period, residual virus was removed, and the cell cultures were incubated in the presence of varying concentrations (400, 100, etc., μg/mL) of the test compounds. Viral cytopathicity was recorded as soon as it reached completion in the control virus-infected cell cultures.

Acknowledgment. We are grateful to the Alberta Cancer Board (Grant No. RI-124) for financial support of this research. The experiments done at the Rega Institute were supported by the Fonds voor Wetenschappelijk Onderzoek (FWO)-Vlaanderen Krediet no. 9.0104.98, the Geconcerteerde Onderzoeksacties (GOA)-Vlaamse Gemeenschap contract no. 2000/12 and the Belgian Federation Against Cancer (to J. B.). We thank Ann Absillis, Anita Camps, Frieda De Meyer, Lizette van Berckelaer, Lies Vandenheurck, and Anita Van Lierde for excellent technical assistance.

References

(1) Fukuto, J. M.; Komori, Y. The enzymology and manipulation of nitric oxide synthase. *Annu. Rep. Med. Chem.* **1994**, *29*, 83–92.
(2) MacDonald, J. E. Nitric oxide synthase inhibitors. *Annu. Rep. Med. Chem.* **1996**, *31*, 221–230.
(3) Reiss, C. S.; Komatsu, T. Does nitric oxide play a critical role in viral infections? *J. Virol.* **1998**, *72*, 4547–4551, and references therein.

(4) Butler, A. R.; Williams, D. L. H. The physiological role of nitric oxide. *Chem. Soc. Rev.* **1993**, *22*, 233–241.

(5) Kerwin, J. F.; Lancaster, J. R.; Feldman, P. L. Nitric oxide: A new paradigm for second messengers. *J. Med. Chem.* **1995**, *38*, 4343–4362.

(6) Lepoivre, M.; Fieschi, F.; Coves, J.; Thelander, L.; Fontecave, M. Inactivation of ribonucleotide reductase by nitric oxide. *Biochem. Biophys. Res. Commun.* **1991**, *179*, 442–448.

(7) Chang, M. J.; Modzelewski, R. A.; Russell, D. M.; Johnson, C. S. Interleukin 1 alpha and gamma interferon induction of nitric oxide production from murine tumor derived endothelial cells. *Cancer Res.* **1996**, *56*, 886–891.

(8) Yim, C. Y.; Bastian, N. R.; Smith, J. C.; Hibbs, J. B.; Samlowshi, W. E. Macrophage nitric oxide synthesis delays progression of ultraviolet light-induced murine skin cancers. *Cancer Res.* **1993**, *53*, 5507–5511.

(9) Maragos, C. M.; Wang, J. M.; Hrabie, J. A.; Oppenheim, J. J.; Keefer, L. K. Nitric oxide/nucleophile complexes inhibit the in vitro proliferation of A375 melanoma cells via nitric oxide release. *Cancer Res.* **1993**, *53*, 564–568.

(10) Kitajima, I.; Kawahara, K.; Nakajima, T.; Soejima, Y.; Matsuyama, T.; Maruyama, I. Nitric oxide mediated apoptosis in murine mastocytoma. *Biochem. Biophys. Res. Commun.* **1994**, *204*, 244–251.

(11) Magrinat, G.; Mason, S. N.; Shami, P. J.; Weinberg, J. B. Nitric oxide modulation of human leukemic cell differentiation and gene expression. *Blood* **1992**, *80*, 1880–1884.

(12) Dong, Z.; Staroselsky, A.; Qi, X.; Xie, K.; Fidler, I. J. Inverse correlation between expression of inducible nitric oxide synthase activity and production of metastasis in K 1735 murine melanoma cells. *Cancer Res.* **1994**, *54*, 789–793.

(13) DiNapoli, M. R.; Calderon, C. L.; Lopez, D. M. The altered tumoricidal capacity of macrophages isolated from tumor bearing mice is related to reduced expression of the inducible nitric oxide gene. *J. Exp. Med.* **1996**, *183*, 1323–1329.

(14) Lind, D. S.; Kontaridis, M. I.; Edwards, P. D.; Josephs, M. D.; Moldawer, L. L.; Copeland E. M. Nitric oxide contributes to adriamycin's antitumor effect. *J. Surg. Res.* **1997**, *69*, 283–287.

(15) Zidek, Z.; Frankova, D.; Holý, A. Stimulation of cytokine and nitric oxide production by acyclic nucleoside phosphonates. *Nucleosides Nucleotides* **1999**, *18*, 959–961.

(16) Hou, Y.; Wang, J.; Andreanà, P. R.; Cantauria, G.; Tarasia, S.; Sharp, L.; Braunschweiger, P. G.; Wang, P. G. Targeting nitric oxide to cancer cells: Cytotoxicity studies of glyco S nitrosothiols. *Bioorg. Med. Chem. Lett.* **1999**, *9*, 2255–2258.

(17) Hajri, A.; Metzger, E.; Vallat, F.; Coffy, S.; Flatter, E.; Evrard, S.; Marescaux, J., Aprahamian, M. Role of nitric oxide in pancreatic tumour growth: In vivo and in vitro studies. *Br. J. Cancer* **1998**, *78*, 841–849.

(18) Everett, S. A.; Smith, K. A.; Patel, K. B.; Dennis, M. F.; Stratford, M. R. L.; Wardman, P. Nitric oxide involvement in the toxicity of hydroxyguanidine in leukaemia HL60 cells. *Br. J. Cancer* **1996**, *74* (*Suppl. XXVII*), S172–S176.

(19) Mitchell, J. B.; Wink, D. A.; DeGraff, W.; Gamson, J.; Keefer, L. K.; Krishna, M. C. Hypoxic mammalian cell radiosensitization by nitric oxide. *Cancer Res.* **1993**, *53*, 5845–5848.

(20) Loo, S. A.; Lesoon Wood, L. A.; Cooney, R. V. Effects of tamoxifen on nitric oxide synthesis and neoplastic transformation in C3H 1051/2 fibroblasts. *Cancer Lett.* **1998**, *122*, 67–75.

(21) Ranjan, P.; Sodhi, A.; Singh, S. M. Murine peritoneal macrophages treated with cisplatin and interferon gamma undergo NO mediated apoptosis via activation of an endonuclease. *Anti Cancer Drugs* **1998**, *9*, 333–341.

(22) Cook, J. A.; Krishna, M. C.; Pacelli, R.; DeGraff, W.; Liebmann, J.; Mitchell, J. B.; Wink, D. A. Nitric oxide enhancement of melphalan induced cytotoxicity. *Br. J. Cancer* **1997**, *76*, 325–334.

(23) Tanno, M.; Sueyoshi, S.; Miyata, N.; Umehara, K. Characterization of the cytotoxic activity of nitric oxide generating *N* nitroso compounds. *Chem. Pharm. Bull.* **1997**, *45*, 595–598.

(24) Ogura, T.; DeGeorge, G.; Tatemichi, M.; Esumi, H. Suppression of anti microtubule agent induced apoptosis by nitric oxide: Possible mechanism of a new drug resistance. *Jpn. J. Cancer Res.* **1998**, *89*, 199–205.

(25) Pae, H.O.; Yoo, J. C.; Choi, B. M.; Kang, C. L.; Kim, J. D.; Chung, H. T. Apoptotic cell death induced by taxol is inhibited by nitric oxide in human leukemia HL 60 cells. *Immunopharmacol. Immunotoxicol.* **1999**, *21*, 667–682.

(26) For an excellent review see: Wang, P. G.; Xian, M.; Tang, X.; Wu, X.; Wen, Z.; Cai, T.; Janczuk, J. Nitric oxide donors: Chemical activities and biological applications. *Chem. Rev.* **2002**, *102*, 1091–1134; and references therein.

(27) Lichtenthaler, F. W.; Muller, H. J. 5′ Nitrates of pyrimidine nucleosides: Nitric acid analogues of nucleosides. *Angew. Chem., Int. Ed. Engl.* **1973**, *12*, 752–753.

(28) Schwandt, I.; Teichmann, H.; Hilgetag, G.; Kowallik, G.; Langen, P. Konkurrenz bei der durch silber ionen assistierten phosphorylierug. Darstellung von thymidin-5′-nitrat. *Z. Chem.* **1968**, *8*, 177–178.

(29) Duschinsky, R.; Eppenberger, U. Nitric acid esters of pyrimidine nucleosides. *Tetrahedron Lett.* **1967**, 5103–5108.

(30) Duschinsky, R. 3′,5′-Di-*O*-nitrothymidine. In *Nucleic Acid Chemistry: Improved and New Synthetic Procedures, Methods and Techniques*; Townsend, L. B.; Tipson, R. S. Eds.; Wiley: New York, 1978; Vol. 1, pp 295–297.

(31) Giziewicz, J.; Wruk, S. F.; Robins, M. J. Nucleic acid related compounds. 107. Efficient nitration of uracil base and nucleoside derivatives. *J. Org. Chem.* **1999**, *64*, 2149–2151.

(32) Huang, G. F.; Torrence, P. F. Nitration of cytosine, 1 methyl cytosine and 2′ deoxycytidine 5′ monophosphate by nitronium tetrafluoroborate in sulfolane. Preparation of 5-nitro-2′ deoxycytidine. *J. Carbohydrates Nucleosides Nucleotides* **1978**, *5*, 317–327.

(33) Chwang, T. L.; Fridland, A.; Avery, T. L. 2′ *O* Nitro 1 β D arabinofuranosylcytosine. A new derivative of 1 β D arabinofuranosylcytosine that resists enzymatic deamination and has antileukemic activity. *J. Med. Chem.* **1983**, *26*, 280–283.

(34) Chwang, T. L.; Fridland, A.; Verhoef, V. Novel derivatives of 9 β D arabinofuranosylpurines that are cytotoxic to variants of human leukemia lymphoblast cells resistant to both 1-β-D arabinofuranosylcytosine and 9 β-D arabinofuranosyladenine. *Biochem. Pharmacol.* **1983**, *32*, 2643–2646.

(35) Czernecki, S.; Valery, J. M. One step conversion of thymidine into 2,3′-anhydro derivatives. *J. Chem. Soc., Chem. Commun.* **1990**, 801–802.

(36) Becouarn, S.; Czernecki, S.; Valery, J. M. Efficient transformation of thymidine into 2′,3′ didehydro 2′,3′ dideoxy thymidine (D4T) involving opening of a 2, 3′ anhydro derivative by phenylselenol. *Nucleosides Nucleotides* **1995**, *14*, 1227–1232.

(37) Kumar, R.; Wiebe, L. I.; Knaus, E. E. A mild and efficient methodology for synthesis of 5-halogeno uracil nucleosides that occurs via a 5 halogeno 6 azido 5,6 dihydro intermediate. *Can. J. Chem.* **1994**, *72*, 2005–2010.

(38) Walker, J. A.; Chen, J. J.; Hinkley, J. M.; Wise, D. S.; Townsend, L. B. Novel 2′ deoxy pyrazine *C* nucleosides synthesized via palladium catalyzed cross couplings. *Nucleosides Nucleotides* **1997**, *16*, 1999–2012.

(39) Sung, W. L. Chemical conversion of thymidine into 5 methyl-2′-deoxycytidine. *J. Chem. Soc., Chem. Commun.* **1981**, 1089.

(40) Huang, J. T.; Chen, L. C.; Wang, L.; Kim, M. H.; Warshaw, J. A.; Armstrong, D.; Zhu, Q. Y.; Chou, T. C.; Watanabe, K. A.; Adamic, J. M.; Su, T. L.; Fox, J. J.; Polsky, B.; Baron, P. a.; Gold, J. W. M.; Hardy, W. D.; Zuckerman, E. Fluorinated sugar analogues of potential anti HIV 1 nucleosides. *J. Med. Chem.* **1991**, *34*, 1640–1646.

(41) Kozlov, I. A.; Orgel, L. E. The synthesis of 2′ deoxy L cytidine 3′ phosphate. *Nucleosides Nucleotides* **1998**, *17*, 2249–2254.

(42) Irani, R. J.; Santa Lucia, J., Jr. The synthesis of 5 iodocytidine phosphoramidite for heavy atom derivatization of RNA. *Tetrahedron Lett.* **1999**, *40*, 8961–8964.

(43) Bobek, M.; Kavai, I.; Sharma, R. A.; Grill, S.; Dutschman, G.; Cheng, Y. C. Acetylenic nucleosides. 4. 1-β-D-Arabinofuranosyl 5 ethynylcytosine. Improved synthesis and evaluation of biochemical and antiviral properties. *J. Med. Chem.* **1987**, *30*, 2154–2157.

(44) Sako, M.; Oda, S.; Ohara, S.; Hirota, K.; Maki, Y. Facile synthesis and NO generating property of 4*H* [1,2,5]oxadiazolo[3,4 *d*]pyrimidine 5,7 dione 1 oxides. *J. Org. Chem.* **1998**, *63*, 6947–6951.

(45) Gasco, A.; Fruttero, R.; Sorba, G. NO Donors: An emerging class of compounds in medicinal chemistry. *Il Farmaco* **1996**, *51*, 617–635.

(46) Alley, M. C.; Scudiero, D. A.; Monks, A.; Hursey, M. L.; Czerwinski, M. J.; Fine, D. L.; Abbott, B. J.; Mayo, J. G.; Shoemaker, R. H.; Boyd, M. R. Feasibility of drug screening with panels of human tumor cell lines using a microculture tetrazolium assay. *Cancer Res.* **1988**, *48*, 589–601.

(47) De Clercq, E. In vitro detection of antiviral activity. In vitro and ex vivo test systems to rationalize drug design and delivery. In *Minutes of a European Symposium*; Crommelin, D.; Couvreur, P.; Duchêne, D., Eds.; Editions de Santé: Paris, 1994; pp 108–125.

(48) Langenbach, R. J.; Danenberg, P. V.; Heidelberger, C. Thymidylate synthetase: Mechanisms of inhibition by 5-fluoro-2′ deoxyuridylate. *Biochem. Biophys. Res. Commun.* **1972**, *48*, 1565–1571.

(49) Santi, D. V.; McHenry, C. S.; Sommer, H. Mechanisms of interaction of thymidylate synthetase with 5 fluorodeoxyuridylate. *Biochemistry* **1974**, *13*, 471–481.

(50) Balzarini, J.; Andrei, G.; Kumar, R.; Knaus, E. E.; Wiebe, L. I.; De Clercq, E. The cytostatic activity of 5-(1-azidovinyl)-2′-deoxyuridine (AzVDU) against herpes simplex virus thymidine kinase gene-transfected FM3A cells is due to inhibition of thymidylate synthase and enhanced by UV light ($\lambda = 254$ nm) exposure. *FEBS Lett.* **1995**, *373*, 41–44; and references therein.

(51) Henn, T. F. G.; Garnett, M. C.; Chhabra, S. R.; Bycroft, B. W.; Baldwin, R. W. Synthesis of 2′-deoxyuridine and 5-fluoro-2′-deoxyuridine derivatives and evaluation in antibody targeting studies. *J. Med. Chem.* **1993**, *36*, 1570–1579.

(52) Idziak, I.; Just, G. J.; Damha, M. J.; Giannaris, P. A. Synthesis and hybridization properties of amide-linked thymidine dimers incorporated into oligodeoxynucleotides. *Tetrahedron Lett.* **1993**, *34*, 5417–5420.

(53) Grisham, M. B.; Johnson, G. G. [23] Quantitation of nitrate and nitrite in extracellular fluids. *Methods Enzymol.* **1996**, *268*, 237–246.

JM020299R